

Poly(vinyl alcohol)-based hydrogels for joint prosthesis

Ana Carolina da Cruz Quartin Borges

Thesis to obtain the Master of Science Degree in
Biomedical Engineering

Supervisors

Prof. Ana Paula Valagão Amadeu do Serro

Prof. Rogério Anacleto Cordeiro Colaço

Examination Committee

Chairperson: Prof. José Paulo Sequeira Farinha

Supervisor: Prof. Ana Paula Valagão Amadeu do Serro

Members of the Committee: Prof. Célio Gabriel Figueiredo Pina

ACKNOWLEDGEMENTS

I would like to thank my supervisors Prof. Ana Paula Serro and Prof. Rogério Colaço for their guidance, expertise and assistance throughout this project. In particular, I would like to praise Professor Ana Paula for her steadfast support, efficiency and availability and Professor Rogério for the invaluable help and resourcefulness, especially during the mechanical tests.

I would also like to thank Professor Célio Pina for going out of his way to transport the machinery and teaching me the software that made the compression test results herein discussed possible.

Finishing this thesis would have been much more difficult without the help of everyone else in the laboratory. Sofia, Diana, Ana Catarina and Ana, thank you for taking the time to teach me, for keeping me company through arduous, time-consuming tasks, for the comic relief, for lending me your knowledge when I wasn't sure how to move forward and for always answering all my questions.

A very special thank you to Ruza who, for the past few years, has made my never-ending hours at the desk much easier to face.

Thank you to Isabel and José António as well, who were present and supportive way beyond expectations during my childhood, and continue to shape my future even now.

My last and most heartfelt thank you goes to Maria Rosa and João Pedro, Maria and Sara, and David. I don't have the artistry to express the impact you've had in my life in the way you deserve. Truthfully, I have everything to thank you for, and there is no one in this world I would rather share this milestone with.

RESUMO (PORTUGUÊS)

A cartilagem é um tecido especializado, responsável pela mediação do contacto entre ossos em superfícies com movimento relativo. A sua matriz extracelular densa, rica em condrócitos e várias moléculas, permite uma ligeira cedência a cargas externas e providencia uma superfície lubrificada que diminui a fricção. Doenças da articulação como osteoartrite ou artrite reumatóide afectam vários milhões de pessoas em todo o mundo, e o seu impacto deverá continuar a aumentar com o envelhecimento da população e o aumento da obesidade. O melhor tratamento disponível actualmente para doença articular severa é a substituição total. Esta envolve o uso de ligas metálicas biocompatíveis que articulam contra outro metal, cerâmica ou revestimentos de polietileno. Estes materiais apresentam algumas limitações, nomeadamente a blindagem do tecido ósseo relativamente à aplicação de forças, que pode resultar em osteoporose, desgaste conducente a detritos imunogénicos e eventual luxação e fractura. O projecto biomecânico destes implantes assenta sobre interacções “hard-on-hard” e “hard-on-soft”. Este tipo de projecto dos actuais implantes não mimetiza as interacções “soft-on-soft” que ocorrem na cartilagem natural. Hidrogéis, nomeadamente os hidrogéis à base de polivinil alcóol (PVA), têm sido estudados e mencionados como uma alternativa possível para os materiais usados em próteses de anca e joelho devido à sua biocompatibilidade, capacidade de intumescimento e comportamento tribológico.

Neste trabalho, foram investigadas diferentes formulações de hidrogéis de PVA em termos das suas propriedades físicas (intumescimento, molhabilidade, comportamento termotrópico) e mecânicas (módulo de Young, tenacidade, tensão de ruptura e extensão nominal máxima) visando a sua possível aplicação em próteses de substituição total da anca ou joelho e os resultados foram comparados com a cartilagem natural e outros hidrogéis de PVA na literatura. Observou-se que o intumescimento e o comportamento termotrópico dos materiais foi bastante semelhante ao encontrado na literatura. Observou-se também que, mecanicamente, hidrogéis de maior peso molecular apresentam características comparáveis com as das cartilagens naturais. Contudo, todos os géis estudados apresentam uma maior resistência à compressão que tracção, ao contrário do comportamento típico da cartilagem, que é mais resistente à tracção.

Palavras-chave: hidrogéis de PVA, cartilagem articular, propriedades mecânicas, propriedades termotrópicas, intumescimento, molhabilidade

ABSTRACT (INGLÊS)

Cartilage is a specialized tissue responsible for mediating contact between bones on surfaces with relative movement. Its dense extracellular matrix, rich in chondrocytes and various molecules, allows a slight yield to external loads and provides a lubricated surface that lowers friction. Joint diseases such as osteoarthritis or rheumatoid arthritis affect several million people around the world, and their impact is expected to continue to increase with aging populations and rising obesity. The best treatment currently available for severe joint disease is total replacement. This involves the use of biocompatible metal alloys that articulate against other metals, ceramic or polyethylene coatings. These materials present some limitations, namely the shielding of the bone with regard to the application of forces, which can result in osteoporosis, wear leading to immunogenic debris and eventual dislocation and fracture. The biomechanical design of these implants relies on "hard-on-hard" and "hard-on-soft" interactions. This type of design does not mimic the soft-on-soft interactions that occur in natural cartilage. Hydrogels, namely polyvinyl alcohol-based hydrogels (PVA), have been studied and mentioned as a possible alternative for materials used in hip and knee prostheses because of their biocompatibility, swelling ability and tribological behavior.

In this work, different formulations of PVA hydrogels were investigated in terms of their physical properties (swelling, wettability, thermotropic behavior) and mechanical properties (Young's modulus, toughness, ultimate tensile strength and maximum strain). Total replacement of the hip or knee and the results were compared with the natural cartilage and other PVA hydrogels in the literature. It was observed that the swelling and thermotropic behavior of the materials was very similar to those found in the literature. It has also been observed that, mechanically, higher molecular weight hydrogels have characteristics comparable to those of natural cartilages. However, all the gels studied have a higher compressive strength than traction, as opposed to the typical cartilage behavior, which is more resistant to compression.

Keywords: PVA hydrogels, articular cartilage replacement, mechanical properties, thermotropic properties, swelling, wettability

TABLE OF CONTENTS

ACKNOWLEDGEMENTS.....	II
RESUMO (PORTUGUÊS)	III
ABSTRACT (INGLÊS).....	IV
TABLE OF CONTENTS	V
LIST OF FIGURES.....	VII
LIST OF TABLES.....	IX
ACRONYMS	X
1. INTRODUCTION	1
2. STATE OF THE ART	3
2.1. ARTICULAR CARTILAGE IN THE HUMAN BODY	3
2.2. ANATOMY AND PHYSIOLOGY OF THE CARTILAGE.....	3
2.2.1. COMPOSITION.....	3
2.2.2. ARCHITECTURE	4
2.2.3. METABOLISM.....	5
2.3. PROPERTIES OF NATURAL CARTILAGE	6
2.3.1. PHYSICAL PROPERTIES	6
2.3.1.1. SWELLING BEHAVIOUR	6
2.3.1.2. WETTABILITY	7
2.3.2. MECHANICAL PROPERTIES.....	9
2.4. JOINT PATHOLOGIES AND RISK FACTORS	11
2.4.1. INFLAMMATORY PATHWAY TO ARTHRITIS.....	11
2.4.2. NON-INFLAMMATORY PATHWAY TO ARTHRITIS	12
2.5. CURRENT THERAPEUTIC SOLUTIONS.....	14
2.5.1. BEST AVAILABLE PROSTHESIS TECHNOLOGY IN THE PRESENT.....	14
2.6. NEW THERAPEUTIC SOLUTIONS.....	16
2.6.1. POLY(VINYL ALCOHOL) HYDROGELS FOR ARTIFICIAL CARTILAGE.....	19
3. MATERIALS AND METHODS	22
3.1. PREPARATION OF PVA HYDROGELS.....	22
3.2. SAMPLES CHARACTERIZATION	23
3.2.1. SWELLING BEHAVIOUR	23
3.2.2. WETTABILITY	24
3.2.3. THERMOTROPIC BEHAVIOUR.....	26

3.2.4. MECHANICAL PROPERTIES	28
4. RESULTS AND DISCUSSION	33
4.1. OPTIMIZATION OF THE HYDROGEL PREPARATION PROTOCOL	33
4.2. SAMPLES CHARACTERIZATION	39
4.2.1. PHYSICAL PROPERTIES	39
4.2.1.1. SWELLING BEHAVIOUR	39
4.2.1.2. WETTABILITY	43
4.2.2. MECHANICAL PROPERTIES	46
4.2.3. THERMOTROPIC BEHAVIOUR	52
5. CONCLUSIONS	58
6. FUTURE WORK	61
7. REFERENCES	62
8. ANNEXES	78

LIST OF FIGURES

FIGURE 1: DIAGRAM OF THE ORGANIZATION OF CARTILAGE. A) CELLULAR ORGANIZATION; B) COLLAGEN FIBER ARCHITECTURE ³⁵	5
FIGURE 2: VARIATION IN WATER CONTENT AS A FUNCTION OF DEPTH IN POST-MORTEM AND OA CARTILAGE. ⁴⁶	7
FIGURE 3: VARIATION OF THE FRICTION COEFFICIENT AND THE CONTACT ANGLE IN CARTILAGE. ⁴⁸ ARTICULAR SURFACE CONTACT ANGLE ($^{\circ}$) OF NORMAL CARTILAGE: 103 $^{\circ}$ POINT M; BOVINE PATELLA 100.1 $^{\circ}$ POINT L; HUMAN KNEE 79.7 $^{\circ}$ POINT K; HIP 76.3 $^{\circ}$ POINT J. ⁵⁰ ARTHRITIC SURFACE: CARTILAGE 65 $^{\circ}$ POINT G; BOVINE PATELLA 70 $^{\circ}$ POINT I; HUMAN KNEE 63 $^{\circ}$ POINT H; HIP 56.3 $^{\circ}$ POINT F. ⁵⁰ DELIPIDIZED CARTILAGE BOVINE KNEE SURFACE WETTABILITY CONTACT ANGLE ($^{\circ}$) AFTER: 1 MIN 71 $^{\circ}$ POINT A; 3 MIN 56 $^{\circ}$ POINT B; AND 21 MIN 39 $^{\circ}$ POINT C. NORMAL BOVINE KNEE CONTACT ANGLE ($^{\circ}$) WAS 93 $^{\circ}$ POINT D; AND 98 POINT E.	7
FIGURE 4: THE WETTABILITY CONTACT ANGLE OF SALINE DROPS ON CARTILAGE SAMPLES AS A FUNCTION OF AIR-DRYING TIME (1) JOINT WAS OPENED AND AIR-DRIED, (2) JOINT WAS DABBED IN SALINE 60 MIN AND AIR-DRIED. ⁴⁸	8
FIGURE 5: DIAGRAM OF COMPARISON BETWEEN THE HEALTHY KNEE JOINT AND A JOINT WITH RHEUMATOID ARTHRITIS.....	12
FIGURE 6: COMPARISON BETWEEN A HEALTHY KNEE AND AN OSTEOARTHRITIC KNEE. A) DIAGRAM; B) X-RAY IMAGE. ⁹⁹	13
FIGURE 7: COMPARISON BETWEEN A HEALTHY HIP AND AN ARTHRITIC HIP. A) DIAGRAM; B) X-RAY IMAGE. ¹⁰⁰	13
FIGURE 8: THE BASIC COMPONENTS OF THE DESIGN OF A HIP PROTHESIS.	15
FIGURE 9: DIAGRAM OF THE VARIATION IN COMPOSITION OF THE PRODUCED PVA HYDROGELS.	22
FIGURE 10: THREE-PHASE SYSTEM DIAGRAM FOR THE DETERMINATION OF THE CONTACT ANGLE.	24
FIGURE 11. - AN EXAMPLE OF A CAPTIVE BUBBLE OF AIR IN A LIQUID ENVIRONMENT AND THE MEASURED CONTACT ANGLE. ²³¹	25
FIGURE 12: TEST SET-UP FOR THE MEASUREMENT OF THE CONTACT ANGLE OF A CAPTIVE BUBBLE OF AIR AGAINST PVA-H.	26
FIGURE 13: DSC SET-UP.	27
FIGURE 14: A TYPICAL STRESS-STRAIN CURVE OF AN ELASTIC MATERIAL.....	29
FIGURE 15: A TYPICAL STRESS-STRAIN CURVE OF A VISCOELASTIC MATERIAL.....	30
FIGURE 16: SCHEMATIC OF THE APPEARANCE OF THE CUSTOM-MADE PUNCH.	30
FIGURE 17: TEST SET-UP FOR TENSILE TESTING.....	31
FIGURE 18: TEST SET-UP FOR COMPRESSIVE TESTING.	32
FIGURE 19: PARTIALLY DESINTEGRATED FT GEL.	35
FIGURE 20: STRIATIONS ON THE GEL UPON	35
FIGURE 21: EFFECTS OF VACUUM ON THE GELATION OF PVA.....	36
FIGURE 22. SEMI IRREVERSIBLE CONTRACTURE OF THICK PVA HYDROGELS.	36
FIGURE 23: THIN PVA HYDROGELS: UP AND SIDE VIEWS.....	36
FIGURE 24: THICK PVA HYDROGEL.....	37
FIGURE 25: TYPICAL %SR PROFILE FOR PVA HYDROGELS DISPLAYING AN OVERSHOOTING PHENOMENON AT THE 30-MINUTE MARK.	39
FIGURE 26: QUALITATIVE SUMMARY OF THE TRENDS OF THE %SR OF PVA AS A FUNCTION OF ADDITIVES AND MOLECULAR WEIGHT.	40
FIGURE 27: QUALITATIVE SUMMARY OF THE TRENDS OF THE %EWC OF PVA AS A FUNCTION OF ADDITIVES AND MOLECULAR WEIGHT.	41
FIGURE 28: QUALITATIVE SUMMARY OF THE TRENDS OF THE CONTACT ANGLE OF PVA AS A FUNCTION OF ADDITIVES AND MOLECULAR WEIGHT.	43
FIGURE 29: PICTURE OF MEASURED CAPTIVE AIR BUBBLE ANGLE.....	44
FIGURE 30: MEASUREMENT OF THE CONTACT ANGLES USING THE CAPTIVE BUBBLE METHOD IN PVA-H.....	45
FIGURE 31: SEM IMAGES SHOWING THE SURFACE TOPOGRAPHY OF A) A CD IRRADIATED PVA BLEND HYDROGEL ²⁶⁷ B) A FT PVA HYDROGEL ²⁶⁸	46
FIGURE 32: ILLUSTRATIVE EXAMPLE OF THE TENSILE STRESS-STRAIN CURVES OF PVA-H.	47
FIGURE 33: ILLUSTRATIVE EXAMPLE OF COMPRESSIVE STRESS-STRAIN CURVES OF PVA-H.....	47
FIGURE 34: MEASUREMENT OF THE COMPRESSIVE YM OF A PVA HYDROGEL USING STRESS-STRAIN CURVES. THE YELLOW LINE REPRESENTS THE MEASURED CURVE, THE GREEN LINE REPRESENTS THE PORTION OF THE CURVE USED TO CALCULATE THE YM AND THE DOTTED LINE CORRESPONDS TO ITS LINEAR ADJUSTMENT.	48
FIGURE 35: MEASUREMENT OF THE TENSILE YM OF A PVA HYDROGEL USING STRESS-STRAIN CURVES. THE YELLOW LINE REPRESENTS THE MEASURED CURVE, THE GREEN LINE REPRESENTS THE PORTION OF THE CURVE USED TO CALCULATE THE YM AND THE DOTTED LINE CORRESPONDS TO ITS LINEAR ADJUSTMENT.	48
FIGURE 36: MEASUREMENT OF UTS AND MAXIMUM STRAIN RATE OF A PVA HYDROGEL. X-AXIS: MAXIMUM STRAIN RATE (30.441% IN THIS CASE); Y-AXIS: UTS (0.51 MPa IN THIS CASE).....	49
FIGURE 37: STRESS-STRAIN CURVE OF PVA H + PVP HYDROGEL SAMPLE SHOWING PLASTIC DEFORMATION UPON UNLOADING.....	52
FIGURE 38: ENTHALPY OF FUSION OF PVA HYDROGELS UNDER DRY CONDITIONS.	54
FIGURE 39: PEAK TEMPERATURE OF PVA HYDROGELS UNDER DRY CONDITIONS.....	54

FIGURE 40: DSC CURVES OF DRY SAMPLES (EACH CURVE REPRESENTS A DIFFERENT TEST). A) PVA M; B) PVA M + PVP; C) PVA M + PVP + G; D) PVA H; E) PVA H + PVP; F) PVA H + PVP + G.....	55
FIGURE 41: DSC CURVES OF HYDRATED SAMPLES (EACH CURVE REPRESENTS A DIFFERENT TEST). A) PVA M; B) PVA M + PVP; C) PVA M + PVP + G; D) PVA H; E) PVA H + PVP; F) PVA H + PVP + G	56
FIGURE 42: ENTHALPY OF FUSION OF PVA HYDROGELS UNDER HYDRATED CONDITIONS.	57
FIGURE 43: VISUAL REPRESENTATION OF THE PEAK TEMPERATURE OF PVA HYDROGELS UNDER HYDRATED CONDITIONS.....	57
FIGURE 44: SR PROFILE OF PVA L.	78
FIGURE 45: SR PROFILE OF PVA L + PVP.	78
FIGURE 46: SR PROFILE OF PVA L + PVP + G.....	79
FIGURE 47: SR PROFILE OF PVA M.....	79
FIGURE 48: SR PROFILE OF PVA M + PVP.....	80
FIGURE 49: SR PROFILE OF PVA M + PVP + G.....	80
FIGURE 50: SR PROFILE OF PVA H.	81
FIGURE 51: SR PROFILE OF PVA H + PVP.....	81
FIGURE 52: SR PROFILE OF PVA H + PVP + G.....	82
FIGURE 53: VISUAL REPRESENTATION OF THE AVERAGE %SR OF PVA HYDROGELS.....	82
FIGURE 54: VISUAL REPRESENTATION OF THE AVERAGE %EWC OF PVA HYDROGELS.	83
FIGURE 55: TENSILE STRESS-STRAIN CURVES OF PVA L.....	83
FIGURE 56: TENSILE STRESS-STRAIN CURVES OF PVA L + PVP.	84
FIGURE 57: TENSILE STRESS-STRAIN CURVES OF PVA L + PVP + G.	84
FIGURE 58: TENSILE STRESS-STRAIN CURVES OF PVA M.	85
FIGURE 59: TENSILE STRESS-STRAIN CURVES OF PVA M + PVP.	85
FIGURE 60: TENSILE STRESS-STRAIN CURVES OF PVA M + PVP + G.	86
FIGURE 61: TENSILE STRESS-STRAIN CURVES OF PVA H.	86
FIGURE 62: TENSILE STRESS-STRAIN CURVES OF PVA H + PVP.	87
FIGURE 63: TENSILE STRESS-STRAIN CURVES OF PVA H + PVP + G.	87
FIGURE 64: COMPRESSIVE (UNCONFINED) STRESS-STRAIN CURVES OF PVA HYDROGELS. THE STARTING POINT OF THE CURVES HAS BEEN ALTERED TO MAKE IT EASIER TO COMPARE REPETITIONS OF THE SAME FORMULATION.	88

LIST OF TABLES

TABLE 1: CONTACT ANGLE IN DIFFERENT AIR-DRIED ARTICULAR CARTILAGE SURFACES. ^{48,50,55,56}	8
TABLE 2: SUMMARY OF MECHANICAL PROPERTIES OF NATIVE CARTILAGE.....	10
TABLE 3: YM AND UTS OF MATERIALS USED IN JOINT REPAIR. ^{122,123}	15
TABLE 4: SUMMARY OF MATERIALS WITH POTENTIAL APPLICATIONS IN CARTILAGE REPAIR OR REPLACEMENT. ¹⁵⁷	18
TABLE 5: PVA POWDERS USED AND SOME OF THEIR CHARACTERISTICS.	22
TABLE 6: SUMMARY OF TESTED PROTOCOLS USED FOR THE PRODUCTION OF PVA HYDROGELS AND THEIR RESULTS.....	33
TABLE 7: AVERAGE SWELLING RATIO (%) AND EQUILIBRIUM WATER CONTENT (%) FOR THE TESTED GELS.	40
TABLE 8: SUMMARY AND COMPARISON OF MEASURED CONTACT ANGLE IN PVA-H VS THE LITERATURE. ^{48,50,55,56}	44
TABLE 9: SUMMARY OF THE MECHANICAL PROPERTIES OF NATURAL CARTILAGE, PVA IN THE LITERATURE AND PVA IN THE SCOPE OF THIS WORK. NOTE: IN SAMPLES WHERE FRACTURED TOUGHNESS IS DEFINED AS A MINIMUM VALUE, THE PRESENTED VALUE WAS MEASURED AT A STRAIN RATE OF 3. COMPRESSIVE TOUGHNESS WAS MEASURED AT A STRESS LEVEL OF 500kPA.	50
TABLE 10: TOUGHNESS PROPERTIES UNDER TENSION AND COMPRESSION FOR PVA-H AT A STRESS LEVEL OF 500kPA.	52
TABLE 11: THERMOTROPIC BEHAVIOUR (T _m , ENTHALPY OF FUSION, DEGREE OF CRYSTALLINITY) OF THE PVA HYDROGELS UNDER DRY CONDITIONS. (* A PVA PRODUCT BY KURARAY)	53
TABLE 12: THERMOTROPIC BEHAVIOUR (T _m , ENTHALPY OF FUSION AND PERCENTAGE OF FREE AND LOOSELY BOUND WATER) OF THE PVA HYDROGELS UNDER HYDRATED CONDITIONS.....	57
TABLE 13: QUALITATIVE COMPARISON OF PVA HYDROGELS.	60

ACRONYMS

DD: Deionized and distilled

DSC: Differential scanning calorimetry

ECM: Extra-cellular matrix

EWC: Equilibrium water content

G: Glyoxal

GAG: Glycosaminoglycan

HA: Hyaluronic acid

MS: Maximum Strain

MSC: Mesenchymal stem cell

MSR: Maximum Strain Rate

OA: Osteoarthritis

PCL: Polycaprolactone

PE: Polyethylene

PEG: Polyethylene glycol

PG: Proteoglycan

PGA: Polyglycolide

PLA: Poly(lactic acid)

PLGA: Poly(lactic-co-glycolic acid)

PMMA: Poly(methyl methacrylate)

PNiPAAm: Poly(N-isopropylacrylamide)

PRP: Platelet-rich plasma

PU: Polyurethane

PVA H: High molecular weight poly(vinyl alcohol hydrogel)

PVA L: Low molecular weight poly(vinyl alcohol hydrogel)

PVA M: Medium molecular weight poly(vinyl alcohol hydrogel)

PVA: Poly(vinyl alcohol)

PVA-H: Poly(vinyl alcohol) hydrogel

PVP: Polyvinylpyrrolidone

RA: Rheumatoid arthritis

RM: Regenerative Medicine

SR: Swelling Ratio

STZ: Superficial tangential zone

TEC: Tissue Engineered Construct

Tg: Glass transition temperature

THA: Total hip Arthroplasty

TKA: Total knee Arthroplasty

Tm: Melting temperature

TSA: Total shoulder arthroplasty

UHMWPE: Ultra high molecular weight polyethylene

UTS: Ultimate Tensile Strength

WC: Water content

YM: Young's modulus

1. INTRODUCTION

Cartilage is an avascular, specialized connective tissue composed of a dense extracellular matrix which houses chondrocytes and a variety of molecules, with a very low capacity for intrinsic healing and repair. Joint pathologies such as osteoarthritis (OA) and rheumatoid arthritis (RA) are leading causes of disability worldwide, which affect articular cartilage.^{1,2} The degeneration of joint tissue gives rise to painful symptoms, which can ultimately lead to loss of joint function. This effect is particularly pronounced in the overweight and the elderly – both increasing trends in the world's demographics.³

Various approaches have been pursued in order to relieve symptoms and mitigate the impact of disease, from the use of pharmaceuticals to surgery, all of which have advantages and limitations. Total arthroplasties, indicated for the advanced state of disease, are widely recognized as the most successful treatment for very extreme cases of cartilage degeneration.⁴⁻⁷ Currently, the most widespread implant designs articulate a metallic alloy piece against a ultra-high molecular weight polyethylene (UHMWPE), a ceramic lining or metal. Despite its success rates, several concerns remain, the most frequent being wear of the polyethylene lining (45%), followed by inflammation (26%) and aseptic loosening (17%), which ultimately lead to implant failure.⁸ This may be partly explained by the very design of current implants on the market, which have hard-on-soft (UHMWPE) or hard-on-hard (ceramic or metal-on-metal) articulation surfaces which do not mimic the soft-on-soft contact seen in Nature.

In the natural joint, all articulating bones are lined with cartilage, creating a soft-on-soft interaction interface. When compressed, the structure of the tissue allows it to yield slightly and release synovial fluid, which provides superior lubrication, lessens the impact of loads and, as consequence, prevents wear. Prostheses on the market fall into one of two categories, none of which correspond to the native case: hard-on-soft and hard-on-hard. The present-day clinical practice resorts to very different articulation dynamics, which could explain the diminished properties of man-made constructs and prosthesis failure.

Hence, there is a gap in the market for effective cartilage substitutes that mimic the natural joint. By investigating new, synthetic cartilage substitute materials, it may be possible to extend the lifetime of contemporary constructs, decrease symptom relapse and reduce costs and the need for revision surgery.

Several hydrogels have gained attention in this field due to being biocompatible and their ability to retain a high water content. Of these, PVA hydrogels has become an attractive material for cartilage replacement applications. PVA is biocompatible and presents good swelling properties.⁹ The characteristics of the resulting hydrogel may also be tailored by adjusting the production method^{10,11} or by combining PVA with other compounds to produce a more suitable and stable material.¹²⁻¹⁴ Furthermore, there are already some clinical applications of PVA, such as surgical sponges, contact lenses and hydrophilic coating for catheters.⁹

The motivation for this work stems from a variety of circumstances. All in all, the prevalence and burden of disease for types of arthritis is a major hindrance for the quality of life of a large portion of the world's

population, and only expected to worsen. Cartilage has a very slow turnover and as a result, it is difficult to replace by natural means.¹⁵ Some solutions for localized injuries have been proposed, albeit with limited application. Furthermore, many hypotheses have been studied to increase implant longevity, but none have been implemented as of yet. As so, new, improved biomimetic materials for cartilage replacement is a very relevant topic with significant potential in biomedical applications. Hydrogels, and particularly PVA, seem to hold promise for addressing joint-related issues. Research in this field may one day uncover an optimal solution that increases quality of life and minimizes patient dissatisfaction.

The objective of this work is to create a protocol for the production of (nine) PVA-based hydrogels and perform their characterization, where the variables in the formulation are the molecular weight of the PVA (Low, Medium, High) and the presence (or absence) of other compounds in the solution (pure PVA; PVA and PVP; PVA, PVP and glyoxal). All the manufactured gels have been characterized regarding their swelling behaviour, wettability, thermotropic behaviour and mechanical properties. In the end, the material best suited for cartilage replacement in total replacement implants was chosen.

In the first chapter of this thesis, the theme is presented and the goals of this work are defined. The second chapter addresses the State of the Art, comprising information on cartilage anatomy and properties, joint pathologies and risk factors, current therapeutic solutions for severe joint degeneration and new therapeutic solutions, such as PVA hydrogels. The third chapter refers to the Materials and Methods, where the experimental procedures for the preparation of the hydrogels and the analytical methods used for the characterization of their properties are further explained. The fourth chapter, Results and Discussion, presents the data collected from the experimental part of the work, its analysis and its contextualization in regard to the literature. In the fifth chapter, Conclusions, a summary of the knowledge gathered from this work is presented, followed by the sixth chapter, where Future Work is addressed.

2. STATE OF THE ART

2.1. ARTICULAR CARTILAGE IN THE HUMAN BODY

The structural integrity of human bodies depends on bone, muscle and cartilage. Bone is rigid, working as a supportive framework for the body, while muscle is flexible and stretchable. Cartilage is somewhere in between, hard enough to provide some support and structure but also a much larger degree of compliance than bone. Therefore, it can play a role in areas where some structure is paramount but fewer constraints are a must. For instance, the cartilage at the end of the human ribcage bones facilitates the expansion and contraction of the thorax in respiration.

Articular cartilage is a highly specialized connective tissue which covers the surface of the joints. Functionally, articular cartilage is an important mediator of bone-to-bone contact in areas designed for movement. Taking the gait cycle as a relevant example in the scope of this dissertation, without it, the extremities of the bones about which movement occurs would be unprotected. Their ends would be subjected to hard-on-hard interactions which, in turn, would increase friction and wear on the surface, ultimately compromising integrity and function. The unique blend of properties cartilage possesses enables it to mitigate the effects of external loads by yielding slightly and to facilitate articulation by providing a lubricated surface that lowers friction.

2.2. ANATOMY AND PHYSIOLOGY OF THE CARTILAGE

2.2.1. COMPOSITION

Cartilage is composed of a dense extracellular matrix, rich in water, proteoglycans, collagens, chondrocytes and low amounts of non-collagenous proteins and glycoproteins. Each component serves a different purpose in the overall system, a topic which is briefly elaborated below.

65% to 85% of the wet weight of articular cartilage is water, which makes it the most prevalent component of the joint. The percentage of water varies from 85% at the superficial zone to 65% in the deep zone.¹⁶ In the tissue, it plays a role in the lubrication of the entire structure and nutrient transport (to chondrocytes). Approximately 30% of this water occupies the intrafibrillar space within the collagen network.^{17,18} There, it exists in the form of a gel. By doing so, upon the application of a compressive force, its motion along the matrix becomes more restricted. This creates a pressure gradient and flow resistance that allows a certain amount of water to remain within the tissue and cushion the impact of significant loads.^{19,20}

About 60% of the dry weight of cartilage is collagen, which makes it the most abundant macromolecule in the joint.²¹ 90% to 95% of that amount is type II collagen²², that creates a fibril network with proteoglycans (PG) aggregates. Other collagens present in much minor amounts, e.g. such as types I, IV, V, VI, IX and XI help to stabilize this network²². Collagens are composed of 3 polypeptide α -chains, where amino acid residues can be found, namely proline, hydroxylsine and glycine. Proline undergoes hydroxylation, forming hydroxyproline. The presence of hydroxyproline and hydroxylsine helps form hydrogen bonds along the molecule, providing structure. Additionally, α -chains are left handed helices

that organize in a triple, right-handed helix structure. By arranging in this manner, the end structure is more extendable than the α -chain, and confers desirable tensile and shear properties to the cartilage.²³

The second largest group of macromolecules in the extracellular matrix (ECM) of cartilage are proteoglycans (30% of its dry weight²⁴). Generally speaking, PG consist of multiple chains of glycosaminoglycans (GAG) that establish sulfide bonds with hyaluronic acid. The most important PG is aggrecan, which forms aggregates with hyaluronan and is responsible for the osmotic properties of cartilage.²⁵ Other PG such as decorin, fibromodulin and biglycan interact with the fibrinous structures formed by collagen.²⁶

Chondrocytes are the only cells found in the cartilage tissue (2% of the total volume²⁷). Their function is to establish a specialized microenvironment in their immediate vicinity and stimulate the development, maintenance and repair of the ECM²⁷. Because these cells are derived from mesenchymal stem cells (MSC), they have limited replication potential. Hence, cartilage has a low capacity for intrinsic healing and repair. Chondrocytes populate all the layers of the joint tissue, but their morphology, size and number vary according to the zone. For instance, in the deep zone chondrocytes are larger, rounder and more scattered than in the superficial zone. While these cells do not typically display direct signal transduction between them, they do respond to a plethora of stimuli, such as mechanical loads, hydrostatic forces, and growth factors.²⁸

Lastly, several non-collagenous proteins and glycoproteins have been identified in articular cartilage, although their function is not entirely characterized. Evidence points to the likelihood of them playing a role in maintaining the integrity of the ECM.²⁶

2.2.2. ARCHITECTURE

Even though the composition is generally the same in qualitative terms, different zones and regions display different densities and configurations of their components. Articular joints are heterogeneous, tissues, with composition and structure that vary with depth (Fig. 1). Four zones can be discerned in this stratified tissue: the superficial zone, the middle zone, the deep zone and the calcified zone²⁹. In each zone, 3 regions can be identified: the pericellular matrix, the territorial matrix, and the interterritorial matrix. As a result, this tissue exhibits mechanical anisotropy and non-linearity.

The superficial zone is a thin layer (10% to 20% of total cartilage thickness), with a large amount of flat chondrocytes and a dense network of type II and type IX collagen fibers arranged parallel to the articular surface^{29,30}. The superficial zone has direct contact with synovial fluid, and is responsible for protecting the deeper layers from shear, tensile and compressive stresses³¹.

Anatomically and functionally, the middle zone it is a transitional zone (40% to 60% of total thickness) between the superficial and the deep zones. The collagen fibrils are thicker and aligned obliquely for a smooth transition to the deep zone configuration³⁰. In the matrix, fewer, rounder chondrocytes and proteoglycans can be found²⁹. This layer helps to mitigate the effect of compressive forces.

In contrast with the superficial zone, the collagen fibrils, which are thickest in the deep zone (30% of total thickness), align perpendicularly to the articular surface. Similarly to other zones, chondrocytes and proteoglycans can be identified. Chondrocytes arrange in columns and proteoglycans are at their highest concentration in the deep zone, which allow this zone to resist the highest resistance to compression³². Because it is one of the densest layers, it is less permeable and has the lowest water concentration.

The calcified zone is nearly void of cellular content and almost entirely made up of an extension of the deep zone calcified collagen fibers. In this layer, the cartilage is secured to the subchondral bone²⁹.

As previously referred, each zone can be further divided into 3 discernible regions, the first one being the pericellular matrix. This layer is where proteoglycans, glycoproteins and noncollagenous proteins tend to gather, completely surrounding the cell membrane of the chondrocytes. Studies suggest it may have an important part in the initiation of signal transduction within cartilage³³

The territorial region is adjacent to the pericellular matrix and presents a high content in collagen fibrils. Evidence suggests that it may play a role in the protection of chondrocytes against biomechanical stresses, as well as in the maintenance of cartilage architecture and its ability to resist significant loads.²⁶

The interterritorial region is made up of randomly orientated collagen fibers, arranged differently according to the zone, and a high content of proteoglycans. This regions is the largest contributor to the biomechanical properties inherent to cartilage.³⁴

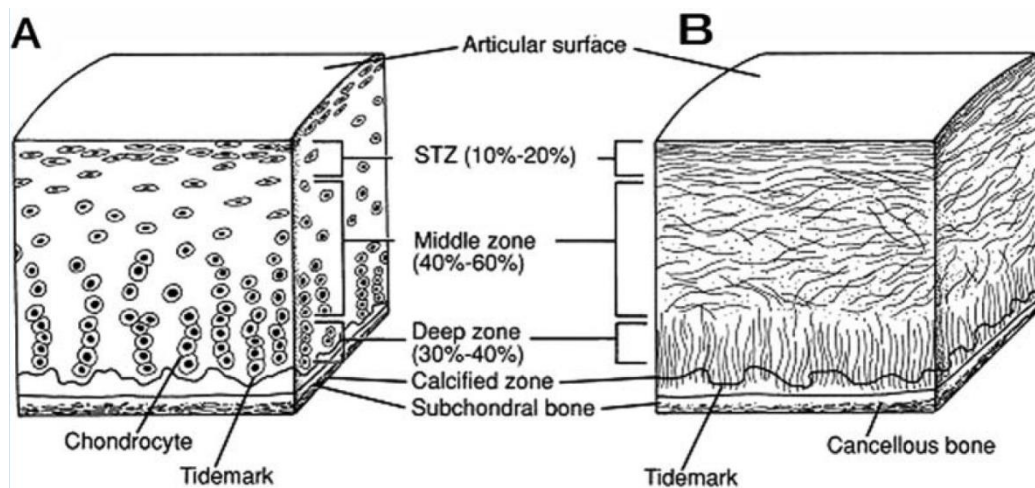


Figure 1: Diagram of the organization of cartilage. a) cellular organization; b) collagen fiber architecture³⁵

2.2.3. METABOLISM

Chondrocytes produce various matrix components, according to external mechanical and chemical stimuli. Proinflammatory cytokines like interleukin-1 and tumor necrosis factor are some of the products

of its metabolism, which are involved in the turnover of the ECM.³⁶ Proteoglycans are also produced in chondrocytes through a metabolism regulated by several regulatory peptides and growth factors.

Since cartilage is not vascularized, chondrocytes depend mainly on anaerobic metabolism and get their nutrients through diffusion from the synovial fluid into the matrix. The ECM has an average pore size of 6.0 nm^{15,20,34} and filters molecules according to charge, size and configuration. A variety of proteinases are involved in the renewal of cartilaginous ECM. Collagenase degrades collagen fibrils; gelatinase breaks down collagen types II, IV, V, VII, X, and XI as well as fibronectin and elastin^{37,38}; stromelysin and cathepsins act on the proteoglycan aggrecan, which is associated with the osmotic properties of cartilage.

Joint diseases are commonly triggered by physiological imbalances in the turnover of the microenvironment mediated by chondrocytes. These extreme changes in metabolism are often at the root of joint conditions such as osteoarthritis. It is important to note that despite its ability to withstand a harsh biomechanical environment, cartilage has a slow turnover, making it extremely difficult to recover from serious injury. Based on the synthetic rate of hydroxyproline, the complete turnover of the human femoral head cartilage should be approximately 400 years.¹⁵

2.3. PROPERTIES OF NATURAL CARTILAGE

2.3.1. PHYSICAL PROPERTIES

2.3.1.1. SWELLING BEHAVIOUR

As previously discussed in Section 2.2.1., the water phase of articular cartilage represents 65-85% of its wet weight. Due to the structural differences in its zones, the lowest water content (WC) is observed in the deeper layer, while more superficial areas are more hydrated.^{39,40} The most abundant components of the ECM are collagens and proteoglycans. The latter contain GAGs, which are negatively charged, due to the presence of sulfate and carboxyl groups, and are hydrophilic. As a result, the ECM displays a tendency to swell in the presence of water. Swelling significantly affects the mechanical behaviour of cartilage, since it enhances the pressure gradient that helps it resist strong loads.⁴¹

The literature reports that, for older or diseased cartilage tissue, the swelling capacity tends to increase by about 30%.⁴²⁻⁴⁶ A compromised joint has a more fragile structure that can no longer restrict motion in the same manner as healthy joints, allowing a higher degree of rearrangement to accommodate for the entry of fluid. In other words, the joint becomes incapable of resisting swelling pressures.

Fig. 2 shows the experimental result of an independent study, where post-mortem cartilage presented a maximum of approximately 75% WC at the surface, which slowly decreases with depth until it reaches 64% in the deep zone. Osteoarthritic (OA) cartilage has a higher swelling capacity, and presents a surplus hydration occurs mostly in the middle zone, where there is a higher density of proteoglycans.⁴⁶

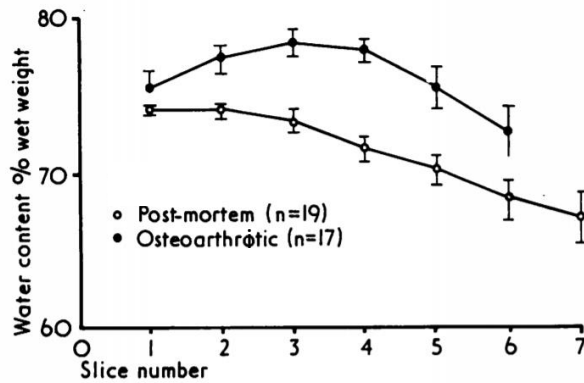


Figure 2: Variation in water content as a function of depth in post-mortem and OA cartilage. ⁴⁶

2.3.1.2. WETTABILITY

Cartilage-cartilage interactions occur within a thick (>0.1 μ m) separation layer with liposomes, lamellar phospholipids, hyaluronate and lubricin.⁴⁷ Moreover, the phosphate groups in phospholipids are negatively charged, which creates a repulsion between adjacent layers and further facilitates slippage. The wettability reflects the structure and composition of materials, and can be correlated to friction. Generally speaking, in cartilage, published results show that the lower the wettability, the higher its capacity to maintain lubrication and, therefore, the lower is the friction (Fig.3).⁴⁸⁻⁵⁰ It is noteworthy to point out these results were obtained using the sessile drop method.

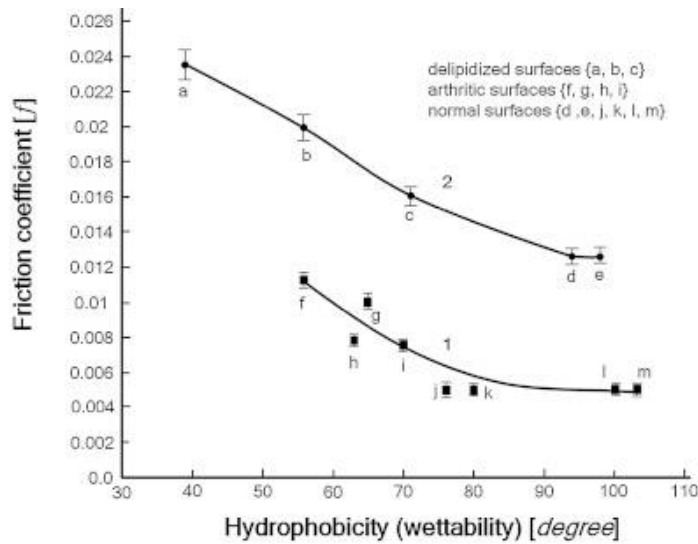


Figure 3: Variation of the friction coefficient and the contact angle in cartilage. ⁴⁸ Articular surface contact angle ($^{\circ}$) of normal cartilage: 103 $^{\circ}$ point m; bovine patella 100.1 $^{\circ}$ point l; human knee 79.7 $^{\circ}$ point k; hip 76.3 $^{\circ}$ point j. ⁵⁰ Arthritic surface: cartilage 65 $^{\circ}$ point g; bovine patella 70 $^{\circ}$ point i; human knee 63 $^{\circ}$ point h; hip 56.3 $^{\circ}$ point f. ⁵⁰ Delipidized cartilage bovine knee wettability contact angle ($^{\circ}$) after: 1 min 71 $^{\circ}$ point a; 3 min 56 $^{\circ}$ point b; and 21 min 39 $^{\circ}$ point c. Normal bovine knee contact angle ($^{\circ}$) was 93 $^{\circ}$ point d; and 98 point e.

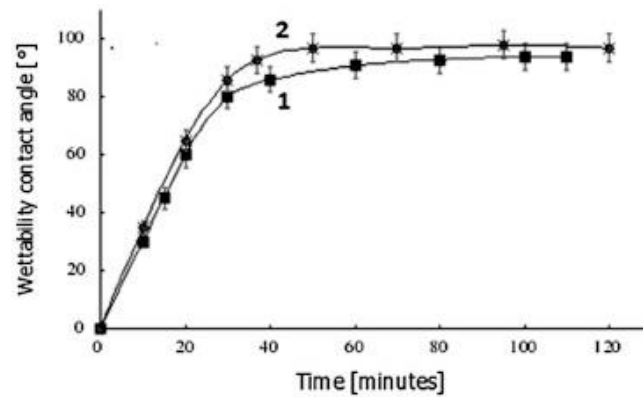


Figure 4: The wettability contact angle of saline drops on cartilage samples as a function of air-drying time (1) joint was opened and air-dried, (2) joint was dabbed in saline 60 min and air-dried.⁴⁸

Cartilage has been observed to modify its wettability according to the environment surrounding it. The pH of the environment surrounding the natural joint is approximately 7.⁵¹ In wet conditions, at this pH level, phosphate groups in the membrane interact with water and enhance adhesion through dipole-dipole attractions.

A study reports that, using the sessile drop method, the joint is highly hydrophilic when completely immersed in synovial fluid (0°), and becomes more hydrophobic as it is left to air-dry over the course of one hour, at which point it stabilizes (~94°) (Fig.4).⁴⁸ Table 1 presents the water contact angle of different types of cartilage after air-drying.

Table 1: Contact angle in different air-dried articular cartilage surfaces.^{48,50,55,56}

Tissue	Contact angle (°)
Normal human AC	94° - 105°
Normal bovine patella	100°
Human knee	80°
Arthritic Knee	63°
Human hip	76°
Arthritic hip	56°

The effect of age and loss of lubrication in cartilage²⁶ should be taken into consideration when talking about cartilage wettability. In fact, diseased cartilage is consistently more hydrophilic than healthy joints, which perfectly reflects the reported increases in swelling capacity in joint disease, since it is associated with the degeneration of the matrix, its inability to resist fluid pressurization and its consequential increase in porosity.

Air-drying interferes with these interactions and causes the loss of charge density of the membrane which, in turn, manifests as surface hydrophobicity or, simply put, a higher contact angle.⁵²⁻⁵⁴ The

literature interprets the transition from hydrophilic to hydrophobic as the effect of the flip-flop movement of the phospholipid layer in the surface. As the surface dries, the bilayer stabilizes with exposed hydrophobic chains⁵³

In the human body, the natural cartilage is continuously exposed to synovial fluid. Under these circumstances, it displays a hydrophilic behaviour with extremely low contact angles. ⁴⁸ The hydrophilic properties have been linked to the presence of GAGs in the ECM.⁵⁷

A thorough literature search revealed no data on the contact angle on hydrated natural cartilage surfaces, which would more accurately mimic the *in vivo* situation. Hence, all the results herein showcased were obtained using a different method than that used for this work, which will be discussed in Sections 3.2.2 and 4.2.1.2..

2.3.2. MECHANICAL PROPERTIES

There are two mechanisms through which cartilage responds to mechanical stresses: deformation of the ECM and resistance to interstitial fluid flow.^{58,59} When the cartilage is subjected to a mechanical force, a pressure gradient is induced in the interstitial fluid, which tends to flow outwards from the point of application of the force, through the pores. The small pore size is a limiting factor in the hydraulic permeability of the tissue (in the superficial layer, hydraulic permeability is low, whereas in the middle and deep zones, it is high).⁶⁰ While this mechanism increases resistance to the water flow, it also contributes to the low coefficient of friction in the joint⁶¹. In addition, GAGs present in the ECM are negatively charged, and attract the bipolar molecules of water. The conjoined action of the hydraulic permeability and electrostatic forces accounts for 95% of the mechanical resistance cartilage is capable of. The remaining 5% correspond to deformation of the ECM. ³⁴

The response of cartilage to mechanical stimuli is time-dependent. For example, creep response after an instantaneous elastic deformation might take up to 1000s to reach a new equilibrium.¹⁹ This can be attributed to the changes in interstitial water flow and ECM deformation induced by mechanical loads, which delay the rate of response. For example, with ECM deformation comes reduction in average pore size, which results in a longer time to reach equilibrium diffusion⁶². In conclusion, the load or displacement applied influences how rapidly the equilibrium state is reached.

Several studies show that many mechanical properties vary according to the joint location^{63,64,65,66}, donor species (human, bovine, murine, etc.)⁶⁷, donor age^{31,68,69} and between articulating surfaces⁷⁰. The YM, for instance, is very susceptible to the anisotropies in the cartilage, changing according to the zone where the test is performed and the orientation of the fibrils in the test specimen. The YM values measured on the middle or deep zone are lower than those measured superficially.³¹ When cartilage is subjected to tensile forces, the collagen fibrils align parallel to the axis of loading and stretch. Hence, the intrinsic stiffness of the collagen fibers found in the joint, their numbers, orientation and degree of cross-linking determine how resistant articular cartilage is against tensile loads, ^{71,31,72} and therefore how high the YM is. The type of test used to ascertain a certain property also influences the results.⁷³

The ultimate tensile strength (UTS) quantifies the maximum stress a material can withstand before necking of the test specimen. Chan et al⁷⁴ and Williamson et al⁷⁰ conducted independent animal studies that revealed a linear relationship between pyridinoline crosslinks and the ultimate tensile strength. They conclude that measuring pyridinoline *in vivo* could potentially be used as an indirect marker of the ultimate tensile strength. Eleswarapu et al⁷⁵ further investigated this matter and concluded that this relationship was also true for many other tissues besides articular cartilage, such as patellar cartilage, medial and lateral menisci and others.

Deformation properties are well characterized for cartilage and related materials, but the same cannot be said of failure properties. Failure can be characterized, for example, in terms of fracture toughness, the amount of energy a material can absorb until rupture⁷⁶ and how it handles crack propagation.⁷⁷ The literature states that the measurement of fracture toughness is complex, due to the anisotropies of the cartilage and the lack of a surface large enough to prevent geometry from influencing the results. Ideally, the fracture properties should at least match those of natural cartilage.⁷⁸

A summary of the mechanical properties of natural cartilage, based on information collected from Little et al.⁷⁹, completed with additional relevant information, can be found in Table. 2.

Table 2: Summary of mechanical properties of native cartilage.

	Description	Value	Testing Method	References
<i>Tensile Young's Modulus</i>	Tensile stiffness of cartilage when subjected to a constant strain rate	4.3 – 25 MPa	Tensile Constant Strain Rate	34,70,80,81
<i>Compressive Young's Modulus</i>	Equilibrium stiffness of the cartilage unconstrained at the sides	0.24 – 1.82 MPa	Confined compression, unconfined compression	34,82–85
<i>Fracture Toughness</i>	The ability of a material to absorb energy and resist fracture	305 – 391 MPa/mm ^{1/2}	Modified single-edge notch test	78
<i>Ultimate Tensile Strength</i>	Maximum that a material can withstand without necking	0.8 – 25 MPa	Tensile Constant Strain Rate	31
<i>Aggregate Modulus</i>	Equilibrium compressive stiffness of cartilage constrained at the sides	0.1 – 2.0	Confined compression, indentation	19,34,82,83
<i>Hydraulic Permeability</i>	Ease by which interstitial water moves through the ECM	10 ⁻¹⁶ – 10 ⁻¹⁵ (m ⁴ /Ns)	Confined compression, unconfined	82,86

			compression, indentation	
<i>Poisson's Ratio</i>	Ratio of lateral strain to strain along the stress direction & a measure of the compressibility of the pores in the ECM	0.06 – 0.3 MPa	Unconfined compression, Indentation	34,65,83,87
<i>Tensile equilibrium modulus</i>	Tensile stiffness of cartilage at the equilibrium	5 – 25 MPa	Tensile stress relaxation	88
<i>Equilibrium shear modulus</i>	Measure of shear stiffness of solid ECM after all viscous ECM effects have subsided	0.05 – 0.4 MPa	Equilibrium shear	89
<i>Complex shear modulus</i>	Apparent stiffness of ECM, which includes both viscous and elastic effects	0.2 – 2.5 MPa	Dynamic shear	63,64,90,91
<i>Shear loss angle</i>	Measurement of how much of the complex shear modulus is caused by viscous effects.	10° - 15°	Dynamic shear	63,87,90,91

2.4. JOINT PATHOLOGIES AND RISK FACTORS

Several diseases and injuries can affect the joint and hinder it from fulfilling its function. They vary in their inflammatory potential, their duration, and severity of symptoms. Typically, conditions can be divided into inflammatory and non-inflammatory.

2.4.1. INFLAMMATORY PATHWAY TO ARTHRITIS

The inflammatory response is a fundamental bodily response tailored for self-defense, classically referred to in the medical community in Latin as “dolor, calor, rubor, tumor”. Or, in other words, pain, localized warmth, redness and swelling. When the inflammatory response is triggered, blood flows into the affected areas, increasing the number of leukocytes at the site. The momentary increase in cellular density as well as the presence of inflammatory substances often cause irritation, wear of the articular cartilage and swelling of the synovium, the thin layer of cells that surround the joints that produce synovial fluid, responsible for joint lubrication. Rheumatoid arthritis, ankylosing spondylitis and psoriatic arthritis are examples of arthritis caused by inflammation.

Rheumatoid arthritis (RA) is the most common inflammatory, systemic autoimmune condition that affects the articular cartilage¹. The synovial membrane becomes swollen and inflamed, which triggers a

damaging cycle of events. Initially, the tendons and ligaments stretch and weaken as a result of the membrane inflammation. The joint then loses its configuration and shape. As the disease progresses, the inflamed membrane invades the cartilage and wears it away, bone erosion occurs and adhesions form in the articular surfaces, which mature into bony connective tissue, ultimately leading to ankylosis. The disease is known to involve cycles of remission and recurrence, but over the course of several years may often result in the complete destruction of cartilage.^{92,93} The symptoms of chronic pain, inflammation, fatigue, loss of joint function, stiffness, reduced motility and further systemic complications ensue.

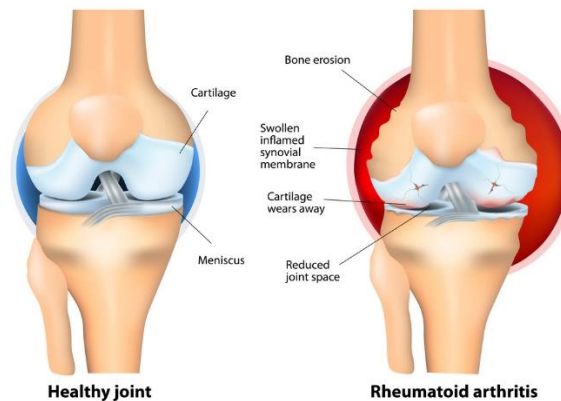


Figure 5: Diagram of comparison between the healthy knee joint and a joint with rheumatoid arthritis.

The disease diagnosis is usually based on patient history and a selection of different exams. However, due to the gradual onset of symptoms, there is often a delay in the detection of the disease.⁹⁴ Annually, in European countries, 20 and 50 new cases per 100,000 people occur.⁹⁵ The management of RA gave rise to annual costs of management of over 45 billion euros in 2008.⁹⁶

The disease can be found in any age group – nevertheless, people over the age of 40 seem to be more susceptible and women are close to three times more likely to develop RA.⁹⁷ Within 2 years of onset of the disease, one third of patients are forced to stop working. 10 years post onset, 30% of patients have severe disability.^{96,97} While in some cases RA is manageable and displays mild symptoms, more severe or untreated cases may shorten life expectancy by 6 to 10 years. The effect is comparable to that of coronary heart disease, stroke and diabetes.⁹⁸

2.4.2. NON-INFLAMMATORY PATHWAY TO ARTHRITIS

Non-inflammatory arthritis is typically known as Osteoarthritis (OA). OA is a progressive disease where cartilage and bone within a joint break down. Typically, the protective cartilage in the joints is exposed to a constant but low level of damage, which the body is able to repair by itself, resulting in no symptoms. However, persistent micro and macro injuries cause cell stress and extracellular matrix degradation, leading to the onset of the disease. Symptoms progress from abnormal metabolism in the joint tissue, followed by cartilage degradation and joint inflammation, bone remodeling and the formation

of spurs. In the more advanced stages of OA, if the cartilage completely disintegrates, bone-on-bone friction occurs. This damage results in a significant amount of pain and swelling, particularly in the weight-bearing joints, that can hinder the patient's capability to utilize them.

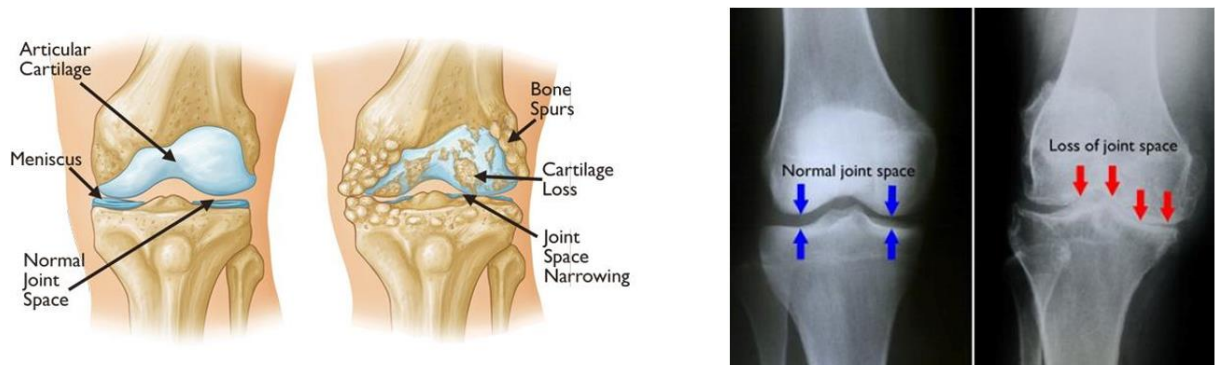


Figure 6: Comparison between a healthy knee and an osteoarthritic knee. a) Diagram; b) X-ray image.⁹⁹

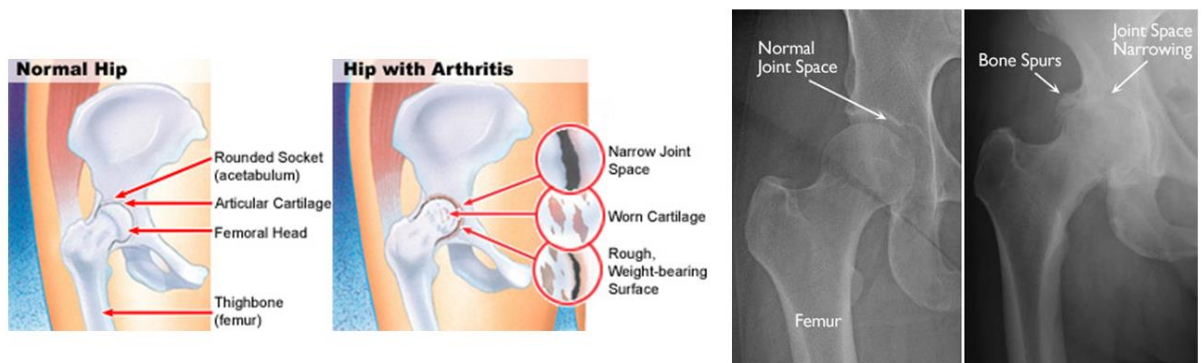


Figure 7: Comparison between a healthy hip and an arthritic hip. a) Diagram; b) X-ray image.¹⁰⁰

The diagnosis of OA is rather straightforward, since imaging techniques allow for an accurate visualization of bone damage, as evidenced in Fig. 6 and 7. The statistics show osteoarthritis is the most prevalent joint disease², with over 40 million registered patients in Europe as of 2003.¹⁰¹ 45% (2008) of the world population is at risk of developing knee OA¹⁰², compared to the 25% (2010) who are likely to suffer from hip OA.¹⁰³ In 2010, OA ranked 11th in the WHO Global Burden of Disease Study as the most common cause of years lived with disability, in contrast with 1990, where it ranked 15th.¹⁰⁴ Segmented by continents, it ranks 6th in East Asia and East Pacific, 10th in North America, 13th in Western Europe and 7th in Eastern Europe. According to the data gathered for a more comprehensive review, on average, the annual economic burden per patient in Europe ranges from 1330€ to 10452€.¹⁰⁵

It has been documented that women suffer from OA more frequently than men^{106,107}, due to reduced volume of cartilage, loss of bone and less developed musculature.¹⁰⁸ Age is also a risk factor, with onset being common between the ages of 40 to 50 years.^{106,107,109,110} Obesity has also been correlated to OA. Research shows that there is a 36% increase in the risk of knee OA for each 5kg of weight gain.¹¹¹ The condition is one of the fastest growing causes for disability and impairment

worldwide, and the trend is expected to increase with aging population and rising levels of obesity. ³ By 2050, OA is expected to impact 130 million individuals worldwide. ¹¹²

Other risk factors at the joint level can also give rise to OA, like trauma or repeated motion which leads to fatigue. In these instances, tears appear in the meniscus as a result of the movement, which in turn initiates internal derangements in the knee that can result in severe OA. The rupture of the anterior crucial ligament leads to an earlier onset of knee disease in 13% of cases, sometimes higher – up to 40% - if the injury is associated with subchondral bone, menisci, damaged cartilage and ligaments, which it often is.¹¹³

2.5. CURRENT THERAPEUTIC SOLUTIONS

Treatment depends on the origin of disease. Regarding RA, specific treatment guidelines are yet to be standardized. Not all countries in Europe, for example, have defined rules for managing the disease.⁹⁷ However, as it is an autoimmune disease, there is no cure, and care is directed towards remission or delaying the progression of the disease. A common, recommended practice for treatment is to initiate pharmacological treatment as soon as the diagnosis is made.⁹⁷ A more comprehensive review on the types of pharmaceuticals that are commonly prescribed can be found elsewhere.¹¹⁴

OA, similarly to RA, has no cure. Thus, long-term management of the disease consists of mitigating or delaying symptoms. Treatment guidelines recommend the use of pain and anti-inflammatory prescription medicine as well as non-pharmacological therapies, exercise and a healthy diet.^{115–118} This therapeutic approach has considerable side effects, is not 100% effective and some countries have restricted regulations that prevent the use of certain drugs.

When damage to the joint is severe, the surgical approach may be indicated. Arthritis affects most notably the hip and the knee. Total knee or hip arthroplasty have been established as one of the most successful treatments for RA and OA, by reducing pain and restoring a degree of motion. Research has shown that 10 years after surgical intervention, the survival rate of the prosthesis stood at about 81-97%.⁴⁻⁷

2.5.1. BEST AVAILABLE PROSTHESIS TECHNOLOGY IN THE PRESENT

Current prostheses are made of a biocompatible, durable, weight-bearing metals. At the contact surfaces of these materials, it is common to add a polyethylene or ceramic lining to the prosthesis, so as to avoid metal-on-metal interactions where wear is easily accelerated. All these materials are much stiffer than cartilage and do not have the same lubrication, deformation and shock absorption properties. Also, the prosthetic materials, conversely to cartilage and bone, are fairly dense and impermeable to water or any other fluid.

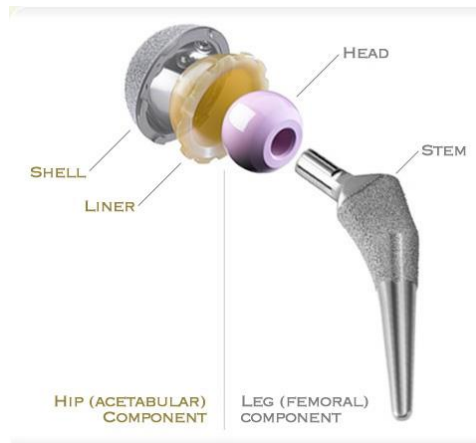


Figure 8: The basic components of the design of a hip prosthesis.

Despite the success of this method of treatment, several concerns remain. In the first 90 days following surgery, patients are vulnerable to complications, from localized deep joint infections to systemic complications like pulmonary embolism and myocardial infarction.¹¹⁹ Age weighs considerably in mortality statistics as well, with patients above 85 years of age six times more likely not to recover than patients 20 years younger.¹²⁰ The most considerable long-term concern, however, is survival of the prosthesis. Revision surgery is often the endpoint after prosthesis failure, but not everyone may be willing or in good enough health to undergo surgery for a second time. As so, a long-lasting prosthesis is a must. Aseptic loosening, fractures, dislocation and osteolysis are common long-term side-effects observed in this clinical profile. A study has found 45% of failures were due to polyethylene wear, while 26% could be attributed to infection and 17% to loosening.⁸

Prostheses, biomechanically speaking, are not a perfect emulation of the native bone and cartilage. All the materials currently used present disadvantages that need to be addressed. The path to an ideal solution should include the conception and design of a cartilage-like material with a very low coefficient of friction that can extend the durability of prostheses.

Table. 3, with information gathered by Beddoes et al¹²¹, compares the properties of materials used for joint treatment.

Table 3: YM and UTS of materials used in joint repair.^{122,123}

Material	Young's Modulus (GPa)	Tensile Strength (MPa)
<i>Cortical bone</i>	17.7	133
<i>Articular cartilage</i>	10.5×10^{-3}	27.5
<i>Co-Cr alloy</i>	210	1085
<i>Zirconia</i>	220	820
<i>Alumina</i>	380	300
<i>PE</i>	0.88	35

The use of ceramics and MoM causes a stress-shielding phenomenon, where the most rigid material – the implant, has a tendency to execute most of the load-bearing. The bone undergoes remodeling and

loses density, sometimes to a point where it no longer has a stable enough structure to support the prosthesis and the implant fails.¹²⁴

All of these materials are subjected to wear from which debris can spread, often triggering an immune response. Such is the case of PE, which releases wear particles that activate the inflammatory pathway and induce osteolysis.^{125–128} MoM implants, especially those made of cobalt chromium, release metal ions upon wear^{129–131}, with toxic¹³² and potentially carcinogenic¹³³ repercussions. Due to safety concerns, various MoM implants have been recalled.^{134,135}

The brittleness of ceramics is their primary disadvantage. Because ceramics have limited deformation under applied stresses, they are more gravely affected by fatigue. Repetition originates small cracks or homogeneities that hamper the material's ability to withstand loads as effectively.¹³⁶ In the worst case scenario, the implant fails upon the break of ceramic bearings.

2.6. NEW THERAPEUTIC SOLUTIONS

Novel approaches to the treatment of OA and RA fall under the fields of Regenerative Medicine (RM) and Tissue Engineered Constructs (TEC). The goal of RM is to restore normal function by replacing, engineering or regenerating native, human biological material. Conceptually, this can be achieved through the stimulation of innate repair mechanisms or by growing tissues and organs for transplantation, when self-repair is impossible. The most promising aspect of RM lies in the use of autologous stem cells and other materials, which nullifies the risk of rejection while perfectly mimicking nature, and provides a solution to the problem of donor shortage for a variety of conditions, not limited to the joint. TECs have a very similar goal to RM, except they rely on the knowledge gathered from different fields including molecular biology, materials science and biomedical engineering and usually contemplate non-autologous options using both natural and synthetic materials. In the past, several solutions have been proposed, from rigid scaffold formation¹³⁷, hydrogels^{12,138,139}, scaffold free options¹⁴⁰ and cell therapies.

Within RM treatments, platelet-rich plasma (PRP) and mesenchymal stem cells (MSC) have been studied. PRP is derived from the patient's blood, which is subjected to centrifugation, allowing the separation of plasma and platelets from the rest of its constituents. This results in a plasma fraction very dense in platelets with applications in cartilage regeneration and neoproliferation.^{141,142}

MSCs have the capacity to differentiate into osteocytes, chondrocytes and adipose tissue. Obtaining these cells poses minimal risks for the patient and, compared to other stem cell types, MSCs can be obtained in larger quantities.¹⁴³ Recent findings suggest autologous MSCs have a natural affinity for the damaged joint tissue, and are capable of aiding in cartilage repair. Not only can they help reduce pain and therefore the need for drugs, but they also secrete anti-inflammatory proteins which reduce stress in their immediate vicinity. By integrating into the tissues, they can simultaneously slow down degeneration and induce healing.

As for TECs, various materials have been used, most notably as hydrogels. Polyethylene glycol (PEG) is one example of such, and it has been proven to be an excellent scaffold for chondrocyte seeding.¹⁴⁴ Scholz et al¹⁴⁵ conducted an animal study in which they attempted to inhibit pathological vascularization of cell seeded PEG/albumin/hyaluronic acid (HA) hydrogels, since blood vessels accelerate hydrogel degeneration. 2 weeks post implantation, no blood vessels were identified and chondrocytes were seen to be functioning normally. Poly(methyl methacrylate) (PMMA) has also been tested as an additive in PEG hydrogels and enhanced mechanical properties were observed. Overall, this outcome was achieved with a high PMMA fraction and crosslink densities and a low molecular weight.¹⁴⁴ In both these studies, the resulting hydrogels were deemed appropriate as cartilage substitutes.

Another material that has gathered attention thus far for cartilage replacement hydrogels is chitosan, a natural material derived from chitin which is biocompatible, biodegradable, nontoxic and available in unlimited supply. Furthermore, chitosan is similar to cartilage in the sense that GAGs and HA are present in both of their matrices.¹⁴⁶ Multiple studies report efficient proliferation of chondrocytes.^{147–149} Cell-seeded chitosan-based hydrogels transplanted by Hao et al¹⁴⁹ succeeded in filling cartilage defects fully after a period of 6 months. Chitosan has also been studied in conjunction with other materials, such as poly(3-caprolactone) (PCL). The concentration of each material has been shown to influence the mechanical properties – 75% chitosan with 25% PCL exhibit good cell adhesion but a 50/50 hydrogel displayed superior mechanical properties.¹⁵⁰ The main issue with chitosan is its inability of forming gels rapidly: if used in the form of an injectable gel, there is a risk that gelation will occur ectopically.¹⁴⁹

Alginate, a natural material derives from algae shows, along with chitosan and PEG, great promise in the field of cartilage repair. It is a natural material derived from algae which, aside from being biocompatible, has been extensively used in additive manufacturing techniques due to its rapid crosslinking.¹⁵¹ Preliminary studies succeeded in bioprinting a 3D porous matrix with 85% cell viability, proliferation and fixation in the matrix, although with subpar mechanical properties compared to natural cartilage¹⁵². Other studies support that alginate can effectively provide an adequate microenvironment for the proliferation of chondrocytes and release of ECM molecules.^{153,154} Markstedt et al¹⁵⁵ reported similar properties with an enhanced compressive modulus, through the addition of cellulose nanofibers to the bioink formulation. Kesti et al¹⁵⁶ conducted an animal study where alginate, gellan and bovine chondrocytes were combined to print 3D scaffolds with desirable mechanical properties and intricate geometries.

Considering the statistics presented in Section 2.3. regarding the major causes of failure of prostheses⁸, a lot of recent research has been directed towards finding new, better articular cartilage substitutes. The materials that have been studied recently fit in one of three categories: natural, synthetic and composites. A summary of some of those materials, can be found in Table 4, based and adapted from

Duarte Campos et al.¹⁵⁷ Most of the literature follows a cell-assisted cartilage repair approach, which should be key to maintain lubrication.

Table 4: Summary of materials with potential applications in cartilage repair or replacement.¹⁵⁷

Material	Type	Advantages	Disadvantages	Reference s
<i>Agarose</i>	Natural	Allows cell differentiation; high GAG/DNA ratio; reparative ability	Difficult migration of cells when polymerized at high concentration; needs to be exposed to mechanical overload	158–165
<i>Alginate</i>	Natural	Allows interaction with cells	Non-ideal mechanical properties	14,153,162,166– 169
<i>Chitosan</i>	Natural	Unlimited resource; high in GAGs and HA	Lacks fast-gelling properties (cannot be applied in situ)	146,147,149,170, 171
<i>Collagen</i>	Natural	Main component of the ECM; good cell adhesion properties; good clinical results with young patients	Needs mechanical stimulation to improve loading capacity; unstable degradation rates	172–183
<i>Fibrin</i>	Natural	Approved by the FDA; stimulates production of GAGs; supports formation of the ECM	Low success rate (depends on cell seeding concentration); unstable degradation rates	165,175,184–186
<i>Hyaluronan</i>	Natural	GAG present in native cartilage; allows interaction with cells; improves expression of collagen type II	Needs growth factors for survival; decreases expression of collagen type I	145,146,167,186– 188
<i>Gellan gum</i>	Natural	Water soluble; good rheological properties	Xenogeneic origin; poor mechanical strength	189
<i>PEG</i>	Synthetic	Allows interaction with chondrocytes; does not support angiogenesis (beneficial for chondrocytes)	Non-ideal strength and compression modulus	30,144,145,158,1 74,190,191
<i>PNiPAAm</i>	Synthetic	Copolymerization possible with AAC; gelling temperature around 37°C; does not support	When polymerized, there is an output of water content; poor mechanical strength	192,193

		angiogenesis; cells keep their phenotype		
<i>PLA</i>	Synthetic	Able to maintain a 3D structure when implanted in vivo; high expression of collagen types I and II; biocompatible	Needs growth factors for cell survival	194,195
<i>PGA</i>	Synthetic	Allows interaction with chondrocytes; tailorable mechanical properties	Mild host immunological response;	153,165,194,196
<i>PLGA</i>	Synthetic	Biocompatible; promotes cell adhesion (beneficial for cartilage regeneration purposes);	Suboptimal mechanical properties for load-bearing applications	175,194,195,197–200
<i>PU</i>	Synthetic	Ease of processing as injectable gel (in situ polymerization); good mechanical properties	Mild host immunological response	201
<i>PVA</i>	Synthetic	Water soluble; excellent adhesion properties; allows interaction with cells	Fixation problems in the non-articulating surface; limitations in mimicking natural cartilage lubrication	12,14,169,183,197,202–204
<i>PVP</i>	Synthetic	Water soluble; good wetting properties; non-toxic in its cross-linked state	Lower thermal stability	205

In the present work, PVA was chosen as a model material for the rubbing surfaces of artificial cartilage.

2.6.1. POLY(VINYL ALCOHOL) HYDROGELS FOR ARTIFICIAL CARTILAGE

PVA is obtained through hydrolysis of polyvinyl acetate. The degree of hydroxylation and polymerization determine the physicochemical and mechanical properties of PVA hydrogels.²⁰⁶ For example, although PVA is known to be soluble in water and form crystals, a highly hydroxylated and polymerized PVA will display these properties to a lesser extent.²⁰⁷ The concentration of PVA also plays a role in the properties of the gel. By manipulating variables such as concentration and molecular weight, it is possible to create a gel with tailored properties that mimic most tissues.

Since PVA is soluble in water, crosslinking, is a crucial step for PVA gel formation. Without a stable structure, the gel is not able to withstand the swelling pressure upon fluid intake and may dissolve.²⁰⁸

Despite being soluble in water, PVA is rather resistant to most organic solvents, which makes it useful for various applications, such as textiles, food packaging, paper products and, more recently, tissue engineering.^{206,207}

PVA is biocompatible, can be sterilized and, like most hydrogels, has good swelling properties. However, its longevity in vivo is compromised by its mechanical characteristics such as the YM, which allows for high swelling ratios, and UTS.

Currently, there are already some clinical applications of PVA, such as surgical sponges, contact lenses and hydrophilic coating for catheters, etc.⁹ For all these reasons, it has become an attractive material for cartilage replacement applications. This application for PVA was first proposed in the literature circa 1970²⁰⁹. PVA is biocompatible, can be sterilized and, like most hydrogels, has good swelling properties. However, its longevity in vivo is compromised by its mechanical characteristics such as the YM, which allows for high swelling ratios, and UTS.

To reinforce its mechanical behaviour, multiple methods can be employed, from altering the preparation of hydrogels to seeking adequate additives that can benefit the overall construct. Freeze-thawing (FT) is a common production method which induces hydrogen bonds between water and the semi-crystalline polymer. Sasada et al¹⁰ were able to increase the mechanical strength of hydrogels from 0.1 – 2.8 MPa²⁰⁹ to around 10 MPa by variation of the FT cycles only.

Swieszkowski et al¹¹ developed a PVA-based cryogel to be used in total shoulder arthroplasty (TSA). Currently PE is used as the bearing surface of the glenoid component. *In silico* replacement with a PVA cryogel predicts a higher contact area between the articulating surfaces and, as consequence, lower wear and higher lubrication. Additionally, they propose that the shock absorbing properties of PVA may mitigate loads at the bone-implant interface which could prevent aseptic loosening. To the best of the author's knowledge, this is the only study that reports PVA as a method to increase the lifetime of total replacement implants.

Alternatively, PVA may also be combined with other materials to produce a more suitable and stable material, according to the application.^{12–14}

Thomas et al²¹⁰ were among those who addressed the suboptimal mechanical properties of PVA-only hydrogels. The introduction of hydrophobic segments within the matrix was found to increase shear, creep and tear strengths without compromising its swelling behaviour and tribological properties.

Bichara et al¹⁴ identified the limitations regarding restoration of craniofacial cartilage using autologous tissue or PE, and developed a chondrocyte-seeded PVA/alginate formulation. A portion of the resulting hydrogels were implanted in nude mice. Others were further cultured in a spinner flask bioreactor for 10 days prior to implantation. Higher levels of GAGs and collagen type II were present in cultured hydrogels, which manifested as a 22% increase in their compressive strength. Alginate was also used by Scholten et al¹⁶⁹. Their construct allowed for cell migration, was capable of releasing biological factors and had similar mechanical properties to those of the joint.

PLGA was used in the form of microspheres as a PVA additive by Charlton et al.¹⁹⁷ The materials were studied as a function of PLGA content, which was expected to help integrate growth factors and chondrocytes. A higher level of PLGA seems to increase hydrogel porosity without strongly affecting the swelling behaviour and the aggregate modulus.

Abedi et al¹⁸³ combined collagen with PVA to facilitate the transplantation of autologous MSCs in rabbits. After 12 weeks, the PVA/collagen/MSC construct had ameliorated chondrocyte morphology, continuous subchondral bone and formation of thicker cartilage VS the control group.

PVP is widely reported in the literature as a good complementary material to PVA.^{12,211,212} It is a synthetic polymer that possesses good biocompatibility and a tissue-like consistency, high elasticity, mechanical strength as well as excellent tribological behaviour.²¹³ PVP and PVA are miscible, due to hydrogen bonds that form between hydroxyl groups in PVA and carbonyl groups in PVP.²¹⁴ These hydrogen bonds improve mechanical properties, hence why a mixture of both may prove advantageous. Ma et al¹² determined that the optimal formulation for a PVA/PVP hydrogel was a 15 wt% solid solute hydrogel with 1% PVP. At 1% PVP, the mechanical and lubrication properties were improved. Also, the 3D structure and water content were found to be similar to articular cartilage.

Another possible approach is to resort to crosslinkers and increase the network density. One example of such is glyoxal, a known antimicrobial dialdehyde that has been found to be biocompatible and is already used in the disinfection of dental equipment and rooms in dental practices equipment²¹⁵. Several studies have been investigated the use of glyoxal as a chemical cross-linker in hydrogels or as injectable materials for biomedical applications^{216–218}, including PVA-based materials²¹⁹. It was reported that glyoxal is able to induce cross-linking in PVA through acetal bonds with hydroxyl groups from PVA and that the presence of a very small quantity of cross-linker can influence the polymer network and affect important properties such as the swelling capacity and the mechanical properties.²¹⁹

Cartiva® by Carticept Medical is a proprietary PVA-based hydrogel that has entered the market in recent years. It exhibits properties close to that of the natural cartilage and has been approved by the FDA.²²⁰ It is a cryogel, which means its production consists of successive freeze-thawing cycles – an effective technique to control the mechanical properties of a hydrogel, as previously mentioned.²²¹ Cartiva® is indicated for osteoarthritis of the big toe in the US, Canada, Brazil and the UK. It is often offered as an alternative to joint fusion, which is known to lead to complications in the long-term as the body adjusts to different load distributions.²²² In Canada, Brazil and the UK, the PVA-based cryogel has also been approved for osteoarthritis at the base of the thumb and for localized knee chondral defects.²²³ A study reports the 5 to 8 year follow up of Cartiva® localized knee implants in patients. While most patients showed improvement of knee function, this product was not completely effective in more advanced osteoarthritis cases which ultimately required TKA.²²⁴ Thus far, no reports of clinically approved hydrogels for TKA or THA implant lining have been released. Hence, there is a gap in the medical market for advanced lining materials for metallic prostheses.

3. MATERIALS AND METHODS

3.1. PREPARATION OF PVA HYDROGELS

In the scope of this thesis, the main objective was to characterize different recipes of PVA hydrogels (PVA-H) as potential cartilage replacement for the rubbing surface of TKA or THA. The variables in study were: molecular weight (**L**ow, **M**edium, **H**igh) and additives (none, PVP, PVP + glyoxal).

A total of nine different PVA hydrogels (PVA-H) were fabricated by cast drying. (Fig. 9). PVA was obtained from different sources as listed in Table 5, PVP-K30 was obtained from BASF SE and 40% w/w aqueous solution of glyoxal was purchased from Alfa Aesar. The nature of the experiments demanded the production of two different thicknesses of gels (approximately 0.5mm for thin gels used for characterization methods that work best with film-like samples and 1.5mm for thick gels, used in mechanical tests).

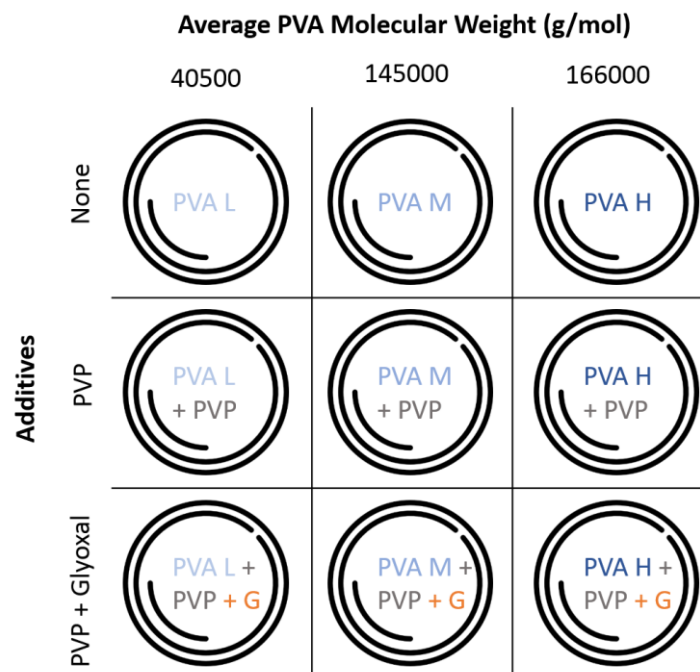


Figure 9: Diagram of the variation in composition of the produced PVA hydrogels.

Table 5: PVA powders used and some of their characteristics.

	Supplier	Mw	Degree of Hydrolysis	Form
PVA L	Sigma Aldrich	31000 - 50000	98-99%	Crystalline powder
PVA M	Kuraray	~ 145000	87-89%	Small crystals
PVA H	Sigma Aldrich	146000 - 186000	99+%	Crystalline powder

The gels were prepared with an initial concentration of PVA of 15 wt% (all varieties listed in Table 5.), following data collected from previous literature^{12,211,225–227}. Nine different solutions were prepared according to Fig. 9, where PVP was used at a concentration of 1%^{12,211,212} of the solid solutes, and glyoxal at 0.02%²²⁸. Glyoxal was introduced as a separate solution combined with chloridic acid (HCl) as a reaction catalyzer.^{219,229}

10 mL (for thin gels) or 75 mL (for thick gels) of PVA solutions were prepared by dissolving the solute in DD water in an oven at 95°C for 24 hours. At the intermediate time 10-15hr the solutions were stirred using the vortex. An additional step was performed whenever air bubbles were still present in the solution after the 24hr period – the solution was subjected to sonication inside a 95°C water bath to keep viscosity at a minimum and allow the release of air bubbles. The solutions were then cast into glass molds (e.g. petri dishes) and placed in a 37°C oven with limited air circulation.

This drying step is crucial for the outcome of the process. If the samples are left to dry under non-controlled conditions, there is a tendency for the formation of stretch marks, which results in a heterogeneous surface and therefore a variable thickness through the sample. On the other hand, vacuum causes a rapid evaporation of water, which boils at the surface of the gel and disrupts the surface.

The thicker gels were still viscous after 24hr and therefore had to be left to dry for an extra day. After the gels partially hardened, ventilation was reintroduced into the system to accelerate the drying process and samples were left at 36°C with air circulation until solvent evaporation was almost complete.

Finally, the gels were washed. The samples were submitted to 24h washing cycles using DD water, until dissolved substances were no longer detected. The water was renewed and analyzed in a Multiskan GO 1.00.40 spectrophotometer after each cycle (start wavelength: 200nm; end wavelength: 700nm). Washing times seemed to be longer in the presence of additives, while the molecular weight of PVA seemed to have no influence over it. Samples were considered clean at absorbance values below 0.1.

3.2. SAMPLES CHARACTERIZATION

3.2.1. SWELLING BEHAVIOUR

When a dry hydrogel is placed in water, the liquid penetrates the matrix and initiates a cycle of expansion of the network. At the equilibrium, where elastic and osmotic forces are balanced, this process stops. Macroscopically, this manifests as an increase in 3D geometry.

When physically cross-linked PVA gels, as those used in this work, are immersed in water, elution also occurs: low-molecular-weight PVA is released into the external medium (water) until an equilibrium state is achieved. This elution behavior is inevitable in PVA cast gels, and depends on the size, number, and distribution of the microcrystallites present in the polymer, characteristics that are determined by the drying conditions of the material, namely temperature and humidity²³⁰.

The test conditions to measure the swelling ratio were thus defined as follows: Pre-washed, hydrated gels were cut into 10mmx5mm strips and dried at 36°C until the mass stabilized. The dry samples were

then placed inside 15ml lab falcons with 2ml of DD water each, shielded from the light. The PVA-H strips were kept at 36°C, a temperature close to that of the human body, and the mass was measured throughout a day until a peak was reached – typically four measurements over the course of 3 hours were sufficient -, and then a week later. The excess moisture in each sample was carefully removed before each weighing. At least 3 repetitions were performed for each formulation.

The percentual swelling ratio, %SR, is defined as follows:

$$\%SR = \frac{w_h - w_d}{w_d} \times 100 \quad (1)$$

Where w_d represents the weight of the dried sample and w_h represents the weight of the hydrated sample.

Knowing the dry and wet weights of the sample, it was also possible to extrapolate what percentage of the wet weight was water.

$$\%EWC = \frac{w_h - w_d}{w_h} * 100 \quad (2)$$

Where w_d represents the weight of the dried sample and w_h represents the weight of the hydrated sample.

3.2.2. WETTABILITY

Wetting is defined as the ability of a liquid droplet to spread over a fluid or solid surface. It is a surface property of materials that depends on the adhesive forces between the liquid and the surface, and the cohesive forces that exist within a liquid. Typically, wettability is measured through the contact angle. With a measured angle below 90°, wettability is considered high, while above 90°, it is considered low (with 0° and 180° corresponding to perfect wettability and perfect non-wettability, respectively).

According to the Young-Dupré Equation, there is a relationship between the contact angle and the surface energies between the phases.

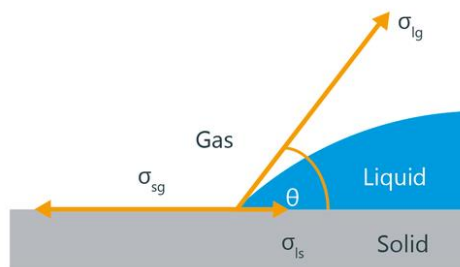


Figure 10: Three-phase system diagram for the determination of the contact angle.

$$\gamma_{sg} = \gamma_{ls} + \gamma_{lg} \times \cos \theta \quad (3)$$

where γ is the surface free energy of the solid, γ_{ls} is the interfacial tension between the liquid and the solid, σ_{lg} is the surface tension of the liquid and θ is the contact angle. The equation applies to three-phase systems in thermodynamic equilibrium, and assumes that the solid phase is smooth and rigid, which is not always the case. In these instances, corrections or other methods may be applied. For the sake of simplicity, however, an approximation to an ideal surface is commonly used.

The contact angle is commonly measured through the sessile drop or the captive bubble method. In the body, cartilage is continuously immersed in synovial fluid, i.e. it is continuously in a hydrated state. To perform the wettability tests in conditions as close to natural as possible, the gel had to be pre-stabilized in water. Therefore, the captive bubble method is the most adequate.

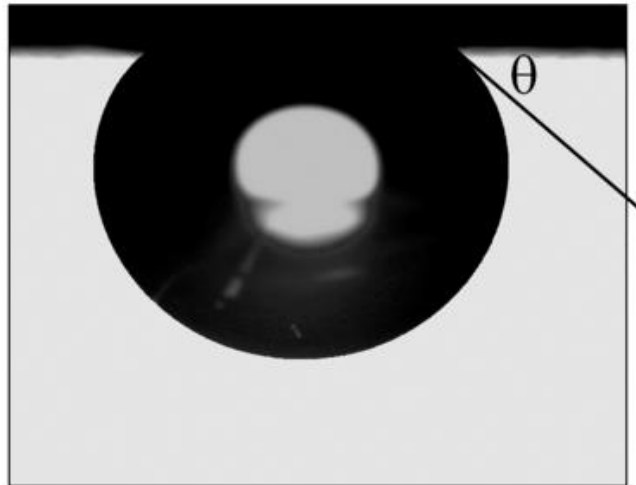


Figure 11. - An example of a captive bubble of air in a liquid environment and the measured contact angle.²³¹

Hence, the wetting properties of the hydrated gel were determined by calculating the contact angle (θ) at the three-phase contact point between the tangent to the contour of a captive bubble (air) and the surface of the sample immersed in DD water. (Fig. 11)

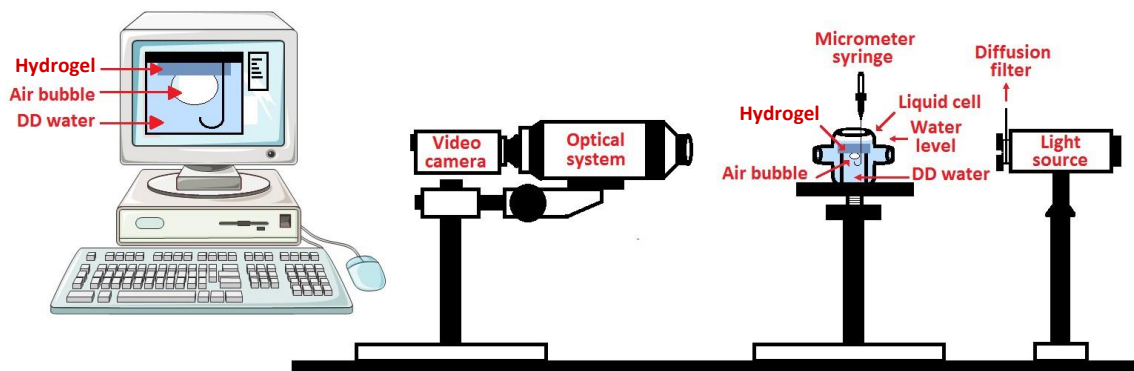


Figure 12: Test set-up for the measurement of the contact angle of a captive bubble of air against PVA-H.

To carry out the captive bubble procedure, a goniometer with a set-up as shown in Fig. 12 was used - A JAI CV-A50 camera, connected to a Data Translation DT3155) frame grabber and supported by a Wild M3Z optical microscope. During 5 minutes, 17 images of a single bubble were acquired. The value of the contact angle was measured on picture 17, when the bubble was stable. 7 to 10 consistent bubbles were done for each hydrogel.

3.2.3. THERMOTROPIC BEHAVIOUR

Differential Scanning Calorimetry (DSC) is used to study the thermal transitions of polymers, such as melting temperature or glass transition. Two crucibles – an empty reference crucible and one with the polymer sample inside – are heated at a constant rate. When the sample undergoes a phase transition, more or less heat will need to flow to it than the reference to maintain both crucibles at the same temperature, depending if the process is endothermic or exothermic

In DSC, the difference in the amount of heat required to increase the temperature of the sample and reference is measured as a function of temperature. A Netzsch DSC 200 F3 Maia machine was used for this purpose. The equipment was controlled with the DSC 200F3 software and the results were analyzed on Proteus Analysis.

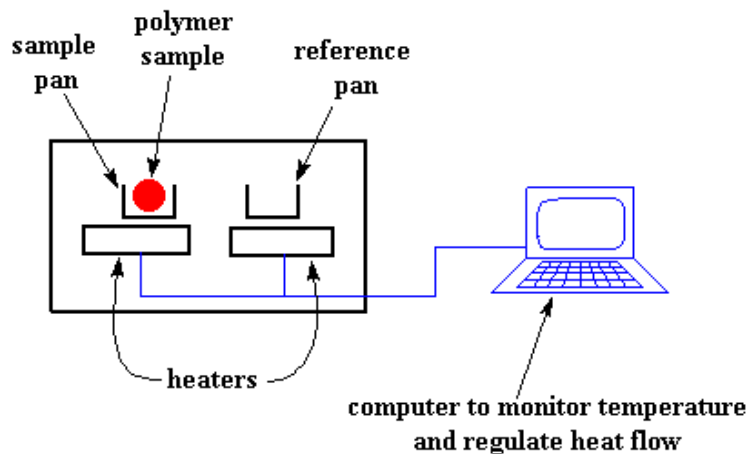


Figure 13: DSC set-up.

The technique was performed in two ways, depending of the state of hydration of the samples. The hydrated samples were subjected to a full heating and cooling cycle, ranging from -35°C to 40°C at a rate of $10^{\circ}\text{C}/\text{min}$. In this test, the intention was to observe the amounts of free and loosely bound water in the samples.

The test was also performed on dry samples. The goal was to detect the glass transition temperature (T_g), the temperature at which the amorphous regions of a polymer transitions from a glassy state to a rubbery one, the melting temperature (T_m), the temperature at which the crystalline portions transition from a solid to a liquid state and the degree of crystallinity of the polymer.

In the literature, T_g of PVA is between $85\text{-}88^{\circ}\text{C}$ ^{232,233,13}, the T_m is at approximately $210\text{-}219^{\circ}\text{C}$ ^{232,13,233} and thermal degradation occurs as a two-step degradation at $300\text{-}450^{\circ}\text{C}$ and $450\text{-}550^{\circ}\text{C}$ ^{13,234}. Based on this information, the dry samples went through one cooling cycle, one heating cycle and one cooling cycle again, from 20°C to 250°C at a rate of $10^{\circ}\text{C}/\text{min}$. The goal was to study the effect of the composition on the thermotropic behaviour of the gels, namely variations in glass transition temperature enthalpy of phase transition.

For the dry test, the samples were previously cut into small pieces, dried at 36°C for 5 days with ventilation and then for an extra 5 days at 36°C with vacuum, totalizing 10 days of total drying time. Samples weighed approximately 3mg each. The equipment is very sensitive to water, rendering inaccurate results if the samples were not conveniently dried. Even at a small size, these ability of these gels to retain water is extremely high which is why vacuum became necessary. After drying them thoroughly, the samples were kept in a desiccator until use.

The degree of crystallinity was calculated as follows:

$$\text{Crystallinity (\%)} = \frac{\Delta H_f}{\Delta H_{f*}} * 100 \quad (4)$$

Where ΔH_f is the specific energy/enthalpy of the sample, and ΔH_{f*} is the enthalpy of pure PVA (138.6 J/g).²³⁵

The percentage of free water in the samples was calculated as follows:

$$\% \text{ Free and loosely bound water} = \frac{\Delta H_f * w_h}{\Delta H_w} \bigg/ \frac{\% EWC * w_h}{100} \quad (5)$$

Where ΔH_f is the specific energy of the sample, w_h is the weight of the hydrated sample, %EWC is the percentual equilibrium water content and ΔH_w is the enthalpy of water (334 J/g)²³⁶

All tests were performed in at least duplicate.

3.2.4. MECHANICAL PROPERTIES

Tensile, compressive and shear testing are typically the methods employed to investigate the mechanical properties of a certain material. In this case, both tensile and compressive tests were conducted.

When a tensile force is applied to a material, it either extends, first reversibly and then irreversibly, or breaks. Because force and extension depend on factors like the dimensions of an object, a single measurement cannot describe all objects made of a certain material. Stress (σ) and strain (ϵ), however, are independent of the 3D dimensions of a material, and are therefore more useful to establish comparisons and to determine characteristic properties of the material. Stress (σ) equals the force (F) per unit of initial cross sectional area A_0 , whereas strain (ϵ) is defined as extension (ΔL) per unit of original length (L_0). The nominal stress and the nominal strain are defined, respectively, as follows.

$$\sigma = \frac{F}{A_0} \quad \epsilon = \frac{\Delta L}{L_0} \quad (6), (7)$$

By plotting the stress against the strain, the characteristic stress-strain curve of the material (called the engineering curve) can be obtained (Fig 14):

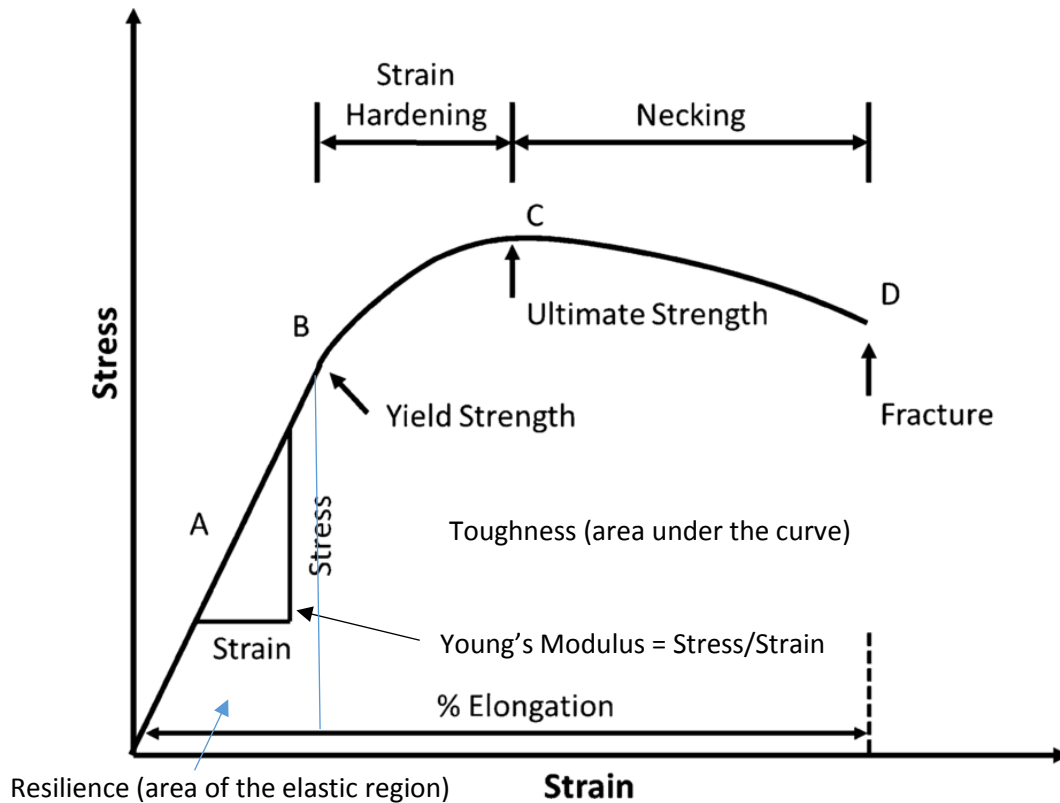


Figure 14: A typical stress-strain curve of an elastic material.

The Young's modulus or modulus of elasticity (E) is the proportionality constant between the stress and strain in the linear region, and serves as a measure of stiffness of the material. It depends on the interatomic forces: the stronger the bond, the higher the value of E is and thus, the higher the stiffness. This property can be calculated using Hooke's Law:

$$E = \frac{\sigma}{\epsilon} \quad (8)$$

where E is the Young's modulus, σ is the stress and ϵ is the strain, as referred above. The Young's modulus was extrapolated from tension and compression stress-strain curves.

The ultimate tensile strength (UTS) is the maximum stress that a material can withstand while subjected to a tensile force. It occurs in the plastic region of a material after the yield point (if it exists), and before the formation of a neck, where strain increases but stress decreases due to the decrease in the cross sectional area. The maximum tensile strain may also be used to specify the failure of a material. Tensile strain capacity is the maximum strain that a solid can withstand without forming a continuous crack. This measurement was based on the data of the tensile test.

Fracture toughness is the energy absorbed by a material before fracture. It can be calculated by integrating the stress-strain curve from the beginning of the test to the moment of rupture. In other words, mathematically, toughness is the area under the entire test curve, but it can be calculated to a given stress or strain level. Toughness is higher in more ductile materials, which can withstand stronger forces and deform more before reaching rupture. In this work it was obtained from the tensile test curves.

Solid objects have an asymmetric equilibrium position at the atomic level that results from the asymmetric form of the Lennard-Jones potential. For this reason, interatomic forces in solid materials resist tensile and compressive forces alike, but there is an overlap in the set of inferable properties of each test. PVA is expected to exhibit a viscoelastic behaviour, which in compression conditions is characterized by an initial, linear stage, where the deformation is reversible (elastic region), a plateau, characterized by entropic changes between entanglements of polymer segments and finally, densification raise, where the non-crystalline segments are arranged orderly and the free volume within the amorphous phase decreases.

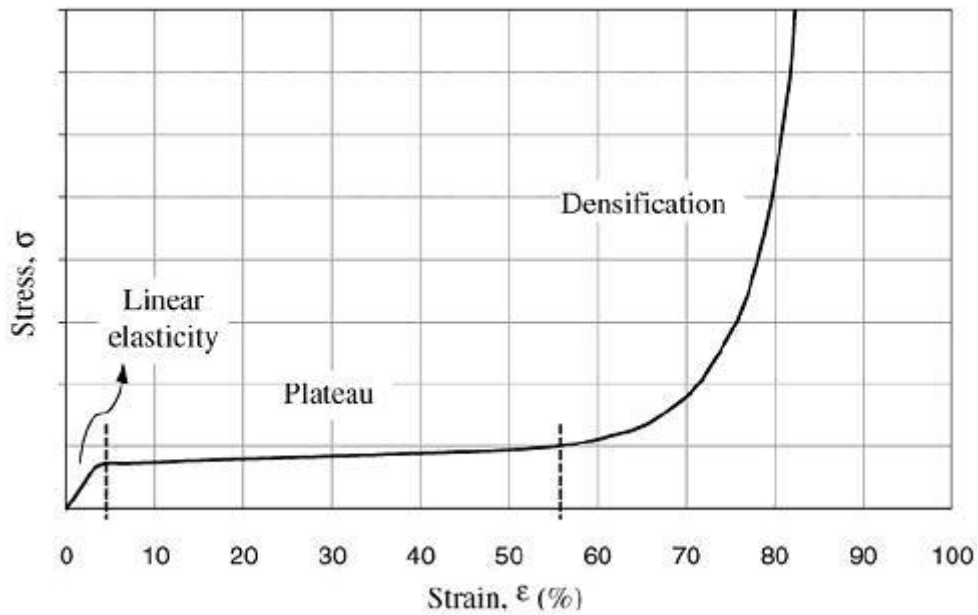


Figure 15: A typical stress-strain curve of a viscoelastic material.

Tensile tests were performed on a TA.XT Express Texture Analyser with miniature tensile (serrated) grips by applying force to the test samples. The most reproducible results were obtained for flat tensile specimens, cut out of the thicker gels using a custom-made punch. (Fig. 16. Dimensions: a gage length of 8mm and 2mm width, a distance of 15mm between shoulders and an 8.5 mm grip section.)

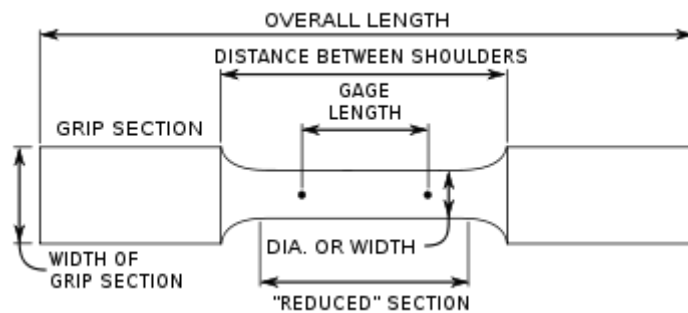


Figure 16: Schematic of the appearance of the custom-made punch.

Miniature tensile grips were attached to a TA.XT express texturometer. The grips were set to a calibration height of 15mm and a maximum displacement of 80mm, at a constant strain rate (1mm/sec). Additionally, sandpaper was glued to the grips, to prevent slippage of the hydrated gels. Stress-strain curves were then obtained, the Young's Modulus was extrapolated from the linear/elastic region of the curves and the ultimate tensile stress and maximum strain rate were measured, as well as the material toughness. A minimum of 3 repetitions per sample were done.



Figure 17: Test set-up for tensile testing.

Unconfined compression tests were performed on 8mm diameter circular PVA-H samples. The test was conducted in a homemade equipment with customized software on LabViewer. To achieve unconfined compression, an indentation attachment was placed on the machine and a small, 10mm diameter circular titanium piece was placed on top of each of the samples. 25N of force were applied to the hydrated hydrogels and the resulting data were analyzed to extrapolate the Young's Modulus and compressive toughness. At least 4 specimens of each sample were tested.



Figure 18: Test set-up for compressive testing.

4. RESULTS AND DISCUSSION

4.1. OPTIMIZATION OF THE HYDROGEL PREPARATION PROTOCOL

The task of producing reproducible and homogeneous PVA-based hydrogels was not simple nor straightforward. The literature presents a wide variety of methodologies, additives, solute concentrations, PVA molecular weight, etc. The compositions chosen for this work were based on studies that determined the optimal concentration of PVA and other compounds¹², without the use of solvents or crosslinkers known to increase toxicity²²¹. Hydrogels containing only PVA (with different molecular weights) were prepared following two distinct methodologies: freeze thawing (FT) and cast drying (CD). The table below summarizes the used conditions for hydrogel production and their outcomes.

Table 6 summarizes the tested methods for hydrogel production and their outcomes.

Table 6: Summary of tested protocols used for the production of PVA hydrogels and their results.

	Process	Method	Result	Observations
#1	FT	Manual dissolution of solutes in DD water at 95°C with magnetic stirrers. Removal of air bubbles with sonication for 5 minutes. Pre-gel solution was poured between two pieces of sylanized glass at the distance of 0.5mm. 3 FT cycles were performed: 1h at -80°C in the freezer, 1h at room temperature.	No gelation	PVA clumps form at the bottom. Dissolution is possible but the solution is too viscous for magnetic stirrers and it is very time-consuming. The sylanized construct traps the water and blocks oxygenation which prevents crystallites from forming within the gel.
#2	FT	Dissolution in oven at 95°C for 24 hours in physiological saline. Removal of air bubbles with sonication for 5 minutes. Pre-gel solution was poured into a glass mold. 5 FT cycles were performed: 16h at -20°C, 8h at room temperature.	Translucent, very soft gel that disintegrates (Fig. 19)	The resulting gel was very fragile and not very easy to manipulate. Swelling tests showed that the mass of the gel decreases over the course of a week.
#3	CD	Dissolution for 20hrs in a flask in an oven at 85°C in DD water. Solution was agitated for 10 minutes after dissolution to release air bubbles. Pre-gel	Transparent, highly striated gel (Fig. 20)	The solution is not completely dissolved, which suggests more time or a higher temperature might be needed.

		<p>solution poured onto glass molds and left to dry at 37°C until evaporation was complete.</p>		<p>Agitation at room temperature is advised against, since the solution cools down, becomes more viscous and starts to solidify. After sonication and reheating, a significant amount of air bubbles formed and were trapped in the viscous liquid.</p> <p>The flask is not the appropriate geometry for such a viscous solution, and as a result a lot of it is lost.</p> <p>As soon as air touches the pre-gel solution, it begins to solidify and striations form along the gel surface.</p>
#4	CD	<p>Variation of #3, where gel was left to dry at room temperature.</p>	<p>Transparent, highly striated gel (Fig. 20)</p>	<p>The harsh thermal transition does not seem to help create a smooth surface for the gel. Striation occurs almost immediately.</p>
#5	CD	<p>Dissolution in oven at 95°C for 20 hours in a falcon. Very gentle agitation and sonication for the removal of air bubbles. Pre-gel solution poured onto glass mold and left to dry inside a weakly sealed vacuum desiccator at room temperature overnight, and then in an oven at 37°C with vacuum.</p>	<p>Transparent, very flat, homogeneous, thin gel – perfect! (Fig. 23)</p>	<p>Vacuum was achieved through a water pump that ran continuously. The huge waste of clean water, the fact that it employs the only water source in the laboratory for extended period of time and limited capacity of production inside the desiccator make this a very impractical and wasteful method, although effective.</p>
#6	CD	<p>Dissolution in oven at 95°C for 20 hours. Pre-gel solution poured into glass mold and left to dry in an oven at 37°C in vacuum.</p>	<p>Air bubbles form and solidify in the gel, rendering a completely unusable surface. (Fig. 21)</p>	<p>Because oxygenation affects the surface of the gel negatively, oxygen deprivation seemed a viable option. Attempt #5 showed promise with vacuum. Later it was observed that the water pump creates a weakly sealed vacuum that likely controls air moisture without being too aggressive, allowing for a slow release of</p>

			remaining air bubbles. When it is moved to a stronger equipment, a lot of the water has already been removed and the gel is partially solidified. The direct transition to a strong vacuum causes sudden evaporation of water, which boils at the surface of the gels. The bubbles are trapped upon gelation.
#7	CD	Dissolution in oven at 95°C for 24 hours. Agitation was performed at the 15 hour mark using the vortex. Pre-gel solution poured into glass mold and left to dry in an oven at 37°C, without vacuum.	Transparent, flat, homogenous thin gel (Fig. 23 and 24) It was hypothesized that by giving the solution more time to rest after agitation, the air bubbles might subside. The dissolution was extended to 24hr to accommodate for this period.



Figure 19: Partially desintegrated FT gel.



Figure 20: Striations on the gel upon rapid cooling and oxygen exposure of the pre-gel solution

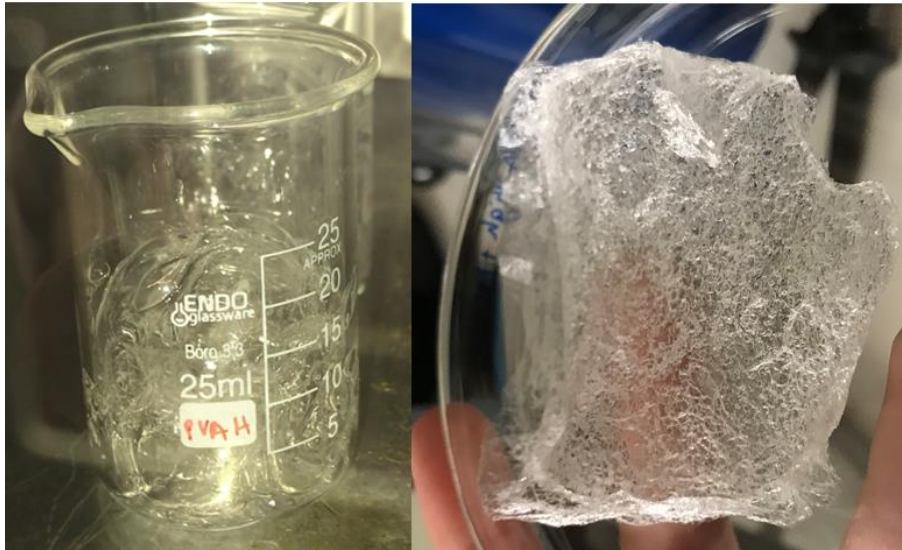


Figure 21: Effects of vacuum on the gelation of PVA.

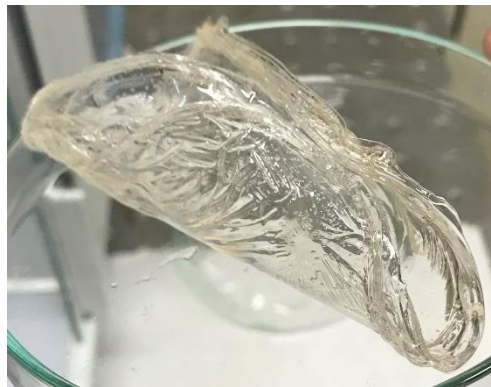


Figure 22. Semi irreversible contracture of thick PVA hydrogels.



Figure 23: Thin PVA hydrogels: up and side views.



Figure 24: Thick PVA hydrogel.

This trial-and-error period culminated in the choice of the 7th iteration of the protocol (Table 6), which is more thoroughly explained in section 3.1.. This specific version of the CD method was deemed the best method for the production of PVA-H for this work because it is faster than FT from the moment of deposition, because it is possible to obtain thin-film like gels (CD gels shrink when the solvent evaporates while FT do not) and because the surface both in thin and thick gels is mostly flat and homogeneous. (Fig. 23 and 24)

It is noteworthy to point out that the preparation of the pre-gel solution itself presented some issues, which was adjusted as new protocols were tested. At a first stage, pre-gel solution was mixed using a magnetic stirrer at 95°C. This method is ineffective because dissolution, although possible, is too time-consuming and the solution is too viscous for a magnetic stirrer.

Concerning the containers, the first strategy involved using flasks, adding the solid solute and making up to volume. This method did not work because the shape of the flask is inadequate for the viscous nature of the solution, and PVA clumps at the bottom. It solidified on the flask walls, being extremely difficult to remove the remainder of the material from its walls. Furthermore, the high temperatures at which the flasks were subjected deform them permanently. So, laboratory falcons were used. Two issues came with their use: formation of air bubbles and loss of solution. The first attempt revealed that when water follows the solid solutes, water is unable to penetrate until the bottom of the container. This resulted in very large, irremovable air bubbles. To counter this issue, a small amount of water was poured first, followed by the solutes and only then, made up to volume. This helped to minimize the formation of air bubbles. Agitation mid-solution also plays a role in the formation of air bubbles. Vortex agitation helps to release bubbles at the bottom. However, strong manual agitation is discouraged because the lid is not air tight and when the solution fully blocks the lid, very large air bubbles form that do not disappear with the vortex. Instead, gentle, slow agitation where the solution has minimal contact

with the lid is preferred. Another measure to minimize air bubbles is to pour a small amount of water before mixing in the solute – this way, water penetrates the PVA powder and there is less tendency for the formation of air pockets.

Loss of solution always occurred. In instances where the falcon lids were sealed as tightly as possible, results were unpredictable and occasionally the lid would burst from internal pressure. Working at 95°C, it naturally follows that part of the solution would evaporate. Posteriorly, the falcons were loosely closed. While the integrity of the lid was no longer compromised, air circulation still made partial evaporation possible (although it improved). This effect was particularly noticeable in more viscous solutions. The inconvenient side effect to his occurrence is that preparing 10mL of solution did not necessarily implicate 10mL of usable solution, not only due to the partial evaporation but due to the intrinsic viscosity. After removing the solution from the oven one must work fast, since it immediately starts to cool down and to solidify. Having to do the deposition step quickly made it extremely challenging to guarantee a consistent thickness in a batch. This was particularly key for mechanical testing, where it was desirable for thickness to be as consistent as possible.

While this protocol was perfectly adequate for thin gels, it does not translate seamlessly to thicker gels. Upon gelation, PVA-H contracts about an axis and the flat shape is not easily restored through swelling, which did not occur in film-like gels. To add to that, there is a lot more variability in the thickness of these gels, with one single gel presenting different thicknesses at separate points. This is partly due to the loss of solution through partial evaporation in the dissolution step, which limits the amount of material available, but it can also be attributed to the viscosity of the solution, as previously mentioned. More viscous hydrogels (PVA H and PVA M) formed striations faster and more often than more fluid ones (PVA L).

Thicker gels are prone to a lot more variation, and small tweaks in temperature and aeration did not produce visible changes. Notwithstanding, the obtained gels produced generally consistent results. While the gels were perfectly usable, the protocol is clearly less reproducible at a larger scale and if a specific 3D architecture eventually becomes necessary, changes should be made in either the composition of hydrogels, the drying temperature or the aeration of the atmosphere in the vicinity.

FT hydrogels are more frequent in the literature than CD hydrogels. Research so far suggests that FT might be the best method for PVA gelation, as the freezing cycle promotes crystallization of the gel and its properties can be attuned as a function of number of FT cycles¹². Even though a few studies suggest the ideal hydrogel combines the advantages of FT and CD^{225,226}, FT PVA gels are generally reported to exhibit better, more customizable properties without compromising biocompatibility with the addition of crosslinkers or other molecules that can introduce toxicity.²²¹ As so, it would be in the best interest of the future course of this project to elaborate a FT protocol to compare its properties with those of CD gels.

It was observed that dissolution occurred in gels at temperatures of 95°C and, consequently, that gels were physically, not chemically, cross-linked. Even though the gel was proven to be stable up until temperatures of 50°C, sterilization is often performed by autoclaving the hydrogel at 120°C^{237,238}, which

would be impossible for these samples. An alternative to autoclaving is ionizing radiation (gamma rays), which has the advantage that gelation and sterilization are achieved in one step, and it can be incorporated into the protocol to tailor the swelling behaviour and the mechanical properties of the gel.^{239–241}

4.2. SAMPLES CHARACTERIZATION

4.2.1. PHYSICAL PROPERTIES

4.2.1.1. SWELLING BEHAVIOUR

Swelling is extremely fast in all samples, denoting the high hydrophilicity of PVA and PVP.²⁴² In 30 minutes, equilibrium swelling is almost reached. In all %SR profiles except for pure PVA samples, the swelling ratio peaks at the 30-minute mark, and stabilizes at a slightly lower value over the course of a week. Initially, water penetrates the samples and the gel network expands. This induces the rearrangement of polymer chains, stimulating the formation of new hydrogen bonds between PVA molecules. The balance between the rates of osmotic diffusion and rearrangement of the chains is a possible explanation for this overshooting phenomenon.²⁴³

A typical %SR profile for a PVA sample of this kind can be found in Figure 25. All the individual %SR of PVA hydrogels can be found in Section 8 (Fig. 45 to 52).

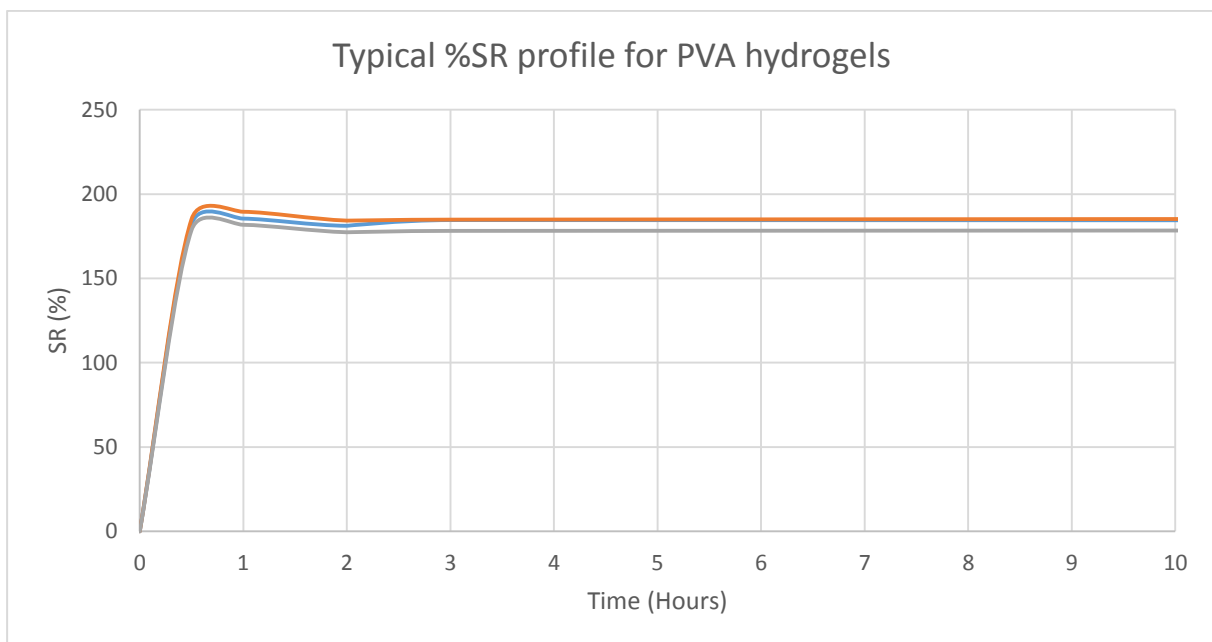


Figure 25: Typical %SR profile for PVA hydrogels displaying an overshooting phenomenon at the 30-minute mark.

The data analysis of %SR and %EWC can be found below in Table 7. A visual representation of this data can be found in Section 8 (Fig 52 and 53).

Table 7: Average Swelling Ratio (%) and Equilibrium Water Content (%) for the tested gels.

Material	%SR	%EWC
Native Cartilage	-	65 - 85
PVA Hydrogels in the literature	FT: 40 – 70 ²⁴⁴ FT: 100 - 150 ²⁴⁵ CD & FT: 260 - 320 ^{246,247}	61 – 70 ^{246,248}
PVA L	195 ± 2	66.1 ± 0.3
PVA L + PVP	238 ± 19	70.4 ± 1.7
PVA L + PVP + G	308 ± 14	75.4 ± 1.5
PVA M	163 ± 2	62.9 ± 0.7
PVA M + PVP	166 ± 11	62.4 ± 1.5
PVA M + PVP + G	184 ± 6	64.8 ± 0.7
PVA H	138 ± 3	58.0 ± 0.6
PVA H + PVP	149 ± 6	59.8 ± 1.0
PVA H + PVP + G	152 ± 8	60.2 ± 1.3

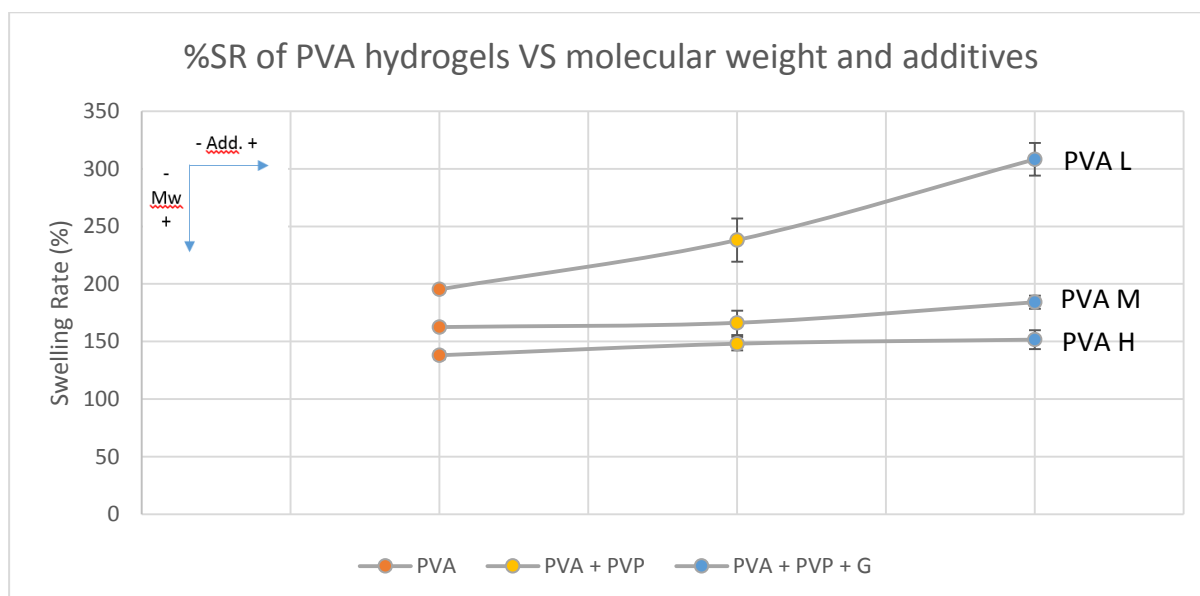


Figure 26: Qualitative summary of the trends of the %SR of PVA as a function of additives and molecular weight.

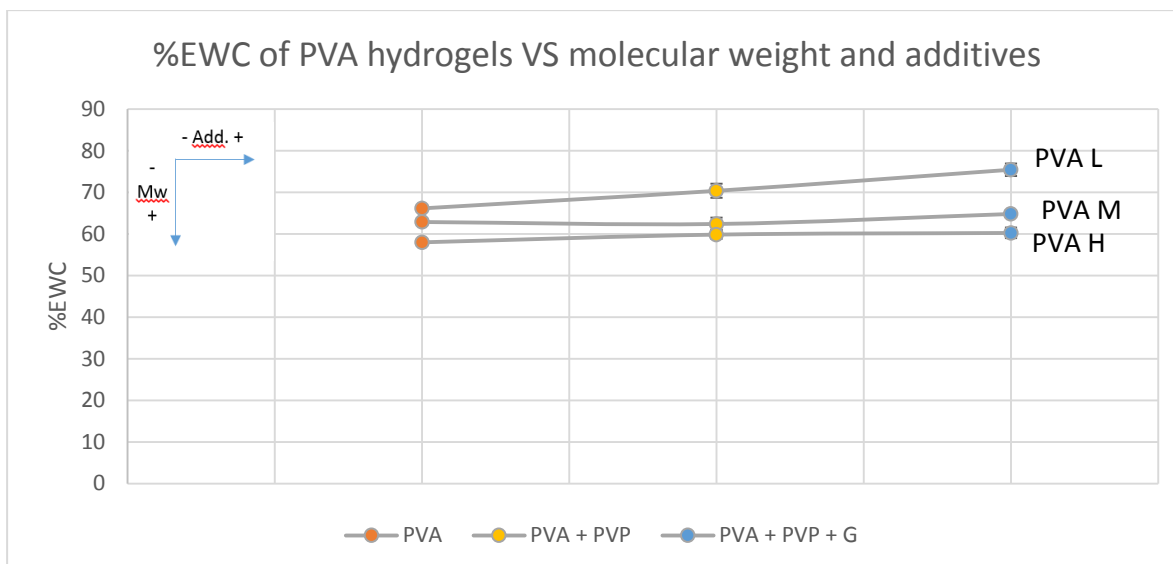


Figure 27: Qualitative summary of the trends of the %EWC of PVA as a function of additives and molecular weight.

The swelling rates varied between 138% and 308% across the board. In terms of water content, the water content in progressively lower as molecular weight increases. This is consistent with the concept that heavier chains form a tighter network of bonds, thus leaving less space in the amorphous region of the gel for water to fill.²⁴⁶

Cartilage is approximately 65% to 85% water¹⁶. All gels seem to be within or very close to the %EWC range found in the human articular cartilage. Moreover, the values obtained are in accordance with values from the literature, including recent research that compares the swelling properties of PVA/PVP hydrogels with the exact same polymer proportions, which showed results for the EWC in a similar range (61% - 70%).^{246,248} These findings are thus not only consistent with comparable work by other authors, but also with the water content in the deep zone (65%), which is responsible for most of the mechanical resistance of cartilage.²⁴⁹

The swelling ratio seems to have gathered less consensus thus far, with very different percentages observed in the literature. One study using the same CD method rendered a SR of around twice as much as the PVA hydrogels testes for this thesis.²⁴⁷ It is noteworthy to point out that in this study, the polymer concentrations were different (up to 5 %wt). In the literature, the swelling ratio is frequently used as a means of relative comparison between test samples only, whilst the water content is usually compared quantitatively to reference data.

Other than in PVA L, the presence or absence of additives did not seem to have a very considerable effect in the swelling behaviour of the samples (Table. 7). Generally speaking, however, it would appear that PVP causes the swelling capacity of the samples to increase. This is possibly due to the chain rearrangements that take place when PVA and PVP crosslink – bulky pyrrolidone rings interrupt PVA crystalline chains and form larger pores.^{242,250} It has also been hypothesized that the high affinity to water in amide groups is a possible explanation to the increased swelling capacity in PVP hydrogels.¹²

Oddly, the presence of glyoxal seemed to have little to no effect on the swelling behaviour of the material. The numbers are ever so slightly above those of PVA + PVP, although the standard deviation is an indicator that in all likelihood, glyoxal was not effecting the PVA gel structure. One of the expected effects of chemical cross-linking of gels is the formation of strong covalent bonds, and as a consequence, the insolubility of the polymer.²⁵¹

It was hypothesized that perhaps chemical crosslinking did not occur. For this reason, there was an attempt to solubilize the hydrogels at two different temperatures. Firstly, the original gel preparation parameters were reversed, i.e., solidified gels were submitted to temperatures of 95°C in an attempt to reverse the gelation process. The gel dissolved and became an aqueous solution again, which reflects the little impact of the small percentage of glyoxal used. As little as 5µL of a 40% glyoxal solution in a 25mL solution has been used by Conte et al²²⁸. The use of glyoxal in this thesis was modeled after this work. However, more than one crosslinking agent is used is the same gel and Conte et al. are not able to quantify the degree of crosslinking induced by each crosslinking agent. Zhang et al²¹⁹, however, have studied the relationship between crosslinking density of PVA as a function of glyoxal concentration. They use only as low as 9% glyoxal content. This concentration of glyoxal resulted in less than 1% crosslinking density when measured in a deuterium oxide environment and was undetectable in DMSO. Thus, the possibility that not enough glyoxal was used cannot be ruled out.

As reported by the literature, the reaction between PVA and glyoxal occurs at a low pH (3.7~4), which is achieved by adding HCl as a catalyst.^{219,229} As a result, in theory, the gels containing glyoxal should have been formed under acidic conditions, which is known to affect crosslinking patterns and, thus, the gel properties, especially mechanical properties.²⁵² As will become apparent in Section 4.2.2., no significant mechanical differences were observed between gels with and without glyoxal. In light of these findings, the author proposes that the quantity of glyoxal was not enough or that the amount of HCl present in the solution was not enough to catalyse the crosslinking reactions.

The normal internal body temperature in humans is around 37°C, although it may vary by 1°C in healthy individuals.²⁵³ A fever of 40°C induces mechanisms of cellular damage, local and systemic effects and, often, irreversible organ injury²⁵⁴. On average, death occurs at a temperature of around 45°C²⁵⁵. Depending on its molecular weight, PVA becomes soluble at temperatures between 70°C to 98°C. Taking this information into consideration, there was a second attempt to reverse the process, at 50°C. The gel structure did not dissolve and seemed to be stable at this temperature. A study performed in similar conditions (15 %wt PVA hydrogels) reports solubility of the gel from 60°C upwards.²⁵⁶ As so, it can be concluded that these cast-dried PVA-H samples are physically (not chemically) crosslinked and stable for temperatures compatible with human life.

The importance of swelling behaviour stems from its connection to the mechanical and tribological properties of the hydrogel, as well as how it impacts the risk of implant failure. In 2007, PVA hydrogels were used for treatment of knee cartilage defects in adult rabbits. Results revealed growth over the implant and implant shrinkage.²⁵⁷ Gels can react to osmotic gradients and swell and de-swell accordingly, even in hydrated conditions. This volume change may induce detachment from the tissue or implant and interfacial debonding. For this reason, this is perhaps one of the most important aspects

to consider when measuring the swelling properties. In this sense, a lower swelling capacity would be desirable, since it would provide a greater stabilization in the contact surface or attachment between the PVA implants and bone or metallic alloys.

4.2.1.2. WETTABILITY

The contact angle obtained for the produced PVA hydrogels is generally low, which indicates high hydrophilicity. The swelling behaviour of these samples, which swell up to 3 times their dry weight, is in line with these results. On average, the contact angle decreases, and thus wettability increases, with the increase of the molecular weight of PVA (Fig.28). A possible explanation would be that the length of the heavier PVA chains may be a limitation in the assembly of tightly packed chains upon gelation, thus forming larger amorphous regions.

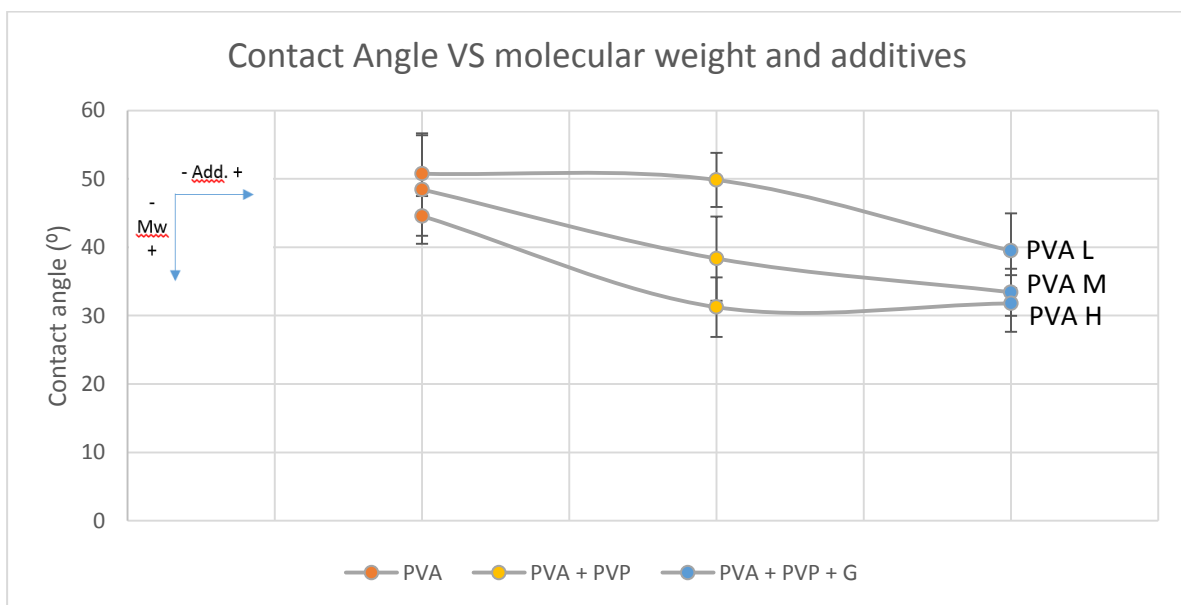


Figure 28: Qualitative summary of the trends of the contact angle of PVA as a function of additives and molecular weight.

It can also be observed that, the addition of PVP and glyoxal increases the wettability of the samples. The concepts that are believed to explain the swelling behaviour of the samples may also be employed for the wetting properties of the material: bulky pyrrolidone rings may prevent the formation of tighter bonds within the PVA and form large pores^{242,250}, and the high affinity between water and amide groups in PVP may further contribute to the hydrophilicity of the gel.¹²

Glyoxal made the samples more hydrophilic, the exception being PVA H + PVP + G. The decrease of the contact angle with the increase of crosslinking agents has been reported before.²⁵⁸ It is possible that the addition of glyoxal hardened localized clusters of high bonding density, giving rise to inhomogeneity in the polymer surface. This interfered with the cohesive bridging flocculation of the polymer, decreasing the contact angle.²⁵⁹

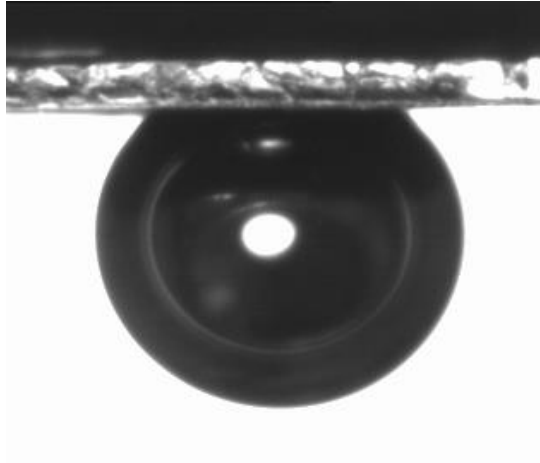


Figure 29: Picture of measured captive air bubble angle.

Table 8: Summary and comparison of measured contact angle in PVA-H VS the literature.^{48,50,55,56}

Tissue	Contact angle (°)	Method
<i>Normal human AC</i>	94 - 105	Sessile Drop
<i>Normal bovine patella</i>	100	
<i>Human knee</i>	80	
<i>Arthritic Knee</i>	63	
<i>Human hip</i>	76	
<i>Arthritic hip</i>	56	
<i>PVA in the literature</i>	37 – 45 ^{260,261}	Captive Bubble
<i>PVA L</i>	50 ± 6	Captive Bubble
<i>PVA L + PVP</i>	50 ± 4	
<i>PVA L + PVP + G</i>	39 ± 5	
<i>PVA M</i>	48 ± 8	
<i>PVA M + PVP</i>	38 ± 6	
<i>PVA M + PVP + G</i>	33 ± 3	
<i>PVA H</i>	45 ± 3	
<i>PVA H + PVP</i>	31 ± 4	
<i>PVA H + PVP + G</i>	32 ± 4	

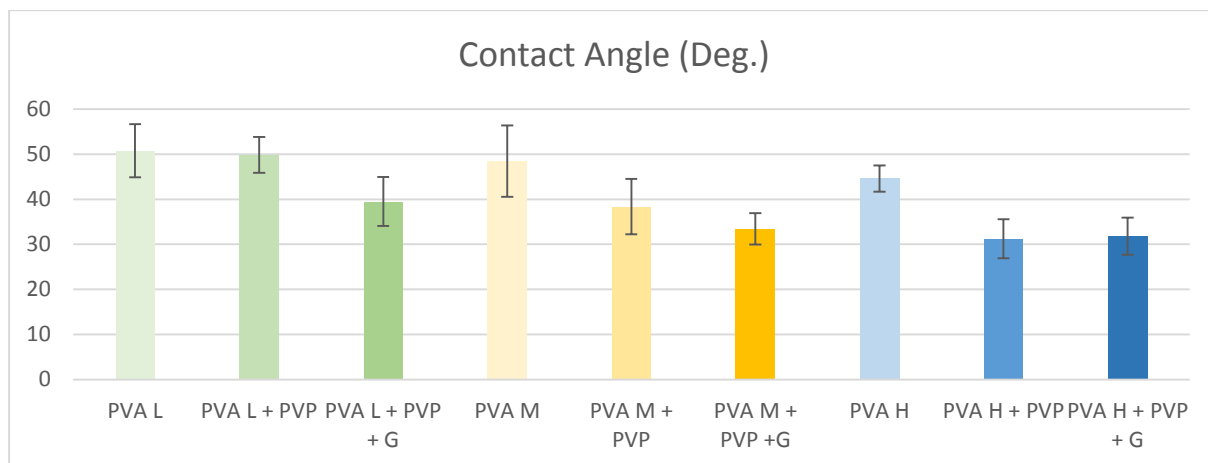


Figure 30: Measurement of the contact angles using the captive bubble method in PVA-H.

The measured angles are drastically different from those seen in the literature for natural cartilage, only coming close to the values observed for osteoarthritic joints (Table 8, Fig 30). One important factor to note, however, is that all the data from the literature was obtained by means of the sessile drop method, as opposed to this work, where the captive bubble method was used. There are important differences between the two methods: in the sessile drop method, the surfaces are dry or partially dry while in the captive bubble, the matrix of the material has reached a swelling equilibrium.

Wetting is also not a static state – there are numerous stable metastates of a droplet of water or air bubble, which explains the variability in the measured contact angles. The sessile drop method is analogous to the maximum end of the spectra, called the advancing contact angle, whilst the captive bubble measures the receding contact angle, at the lower end of the range. The true, Young equilibrium contact angle is seldom reached, due to contact angle hysteresis (the difference between the advancing and the receding contact angles).

According to the literature, contact angle hysteresis is a consequence of heterogeneity and surface roughness.^{262–266} Young's equation considers an ideal, perfectly flat solid surface, where hysteresis does not exist. In reality, most surfaces present surface irregularities that act as barriers to the motion of the contact line, which can alter the macroscopic measurement of contact angles. The surface topography of PVA-based hydrogels has been extensively investigated. Fig. 30 shows two examples of PVA hydrogel surfaces SEM images retrieved from the literature. Thus, it is almost certain that hysteresis exists, and that the values that were measured correspond to the lower end of the range of stable metastates.

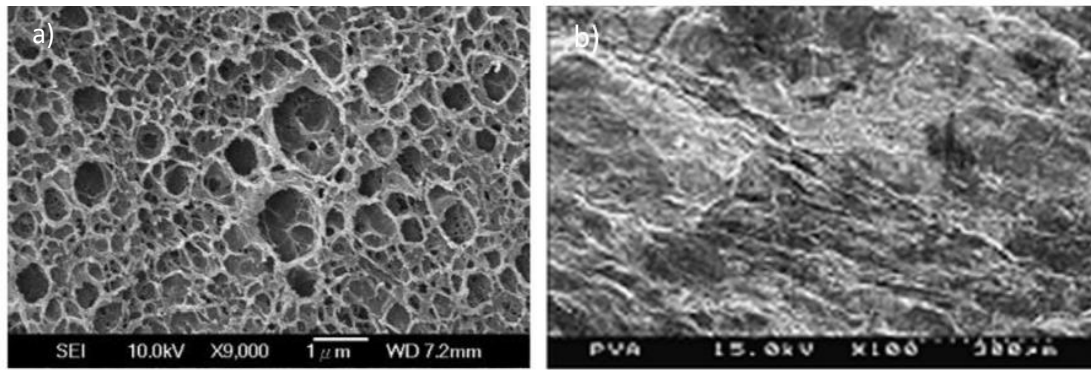


Figure 31: SEM images showing the surface topography of a) a CD irradiated PVA blend hydrogel^[267] b) a FT PVA hydrogel^[268]

No reference values for the captive bubble method have been reported for the natural cartilage. However, cartilage is known to be hydrophilic. The hydrophilicity of these gels means they can absorb high amounts of water, which could potentially more effectively lubricate the surface.²⁶⁹ Compared to other PVA constructs, the range of values obtained for the contact angle is similar to that observed in previous research.

4.2.2. MECHANICAL PROPERTIES

Initially, tensile tests were done with flat, 1mm x 2mm rectangular specimens, no more than 2mm thick. The gels ruptured at the interface of the gels and the grips, which is an indicator that stresses were concentrating at the grips and not evenly distributed along the specimen. The sandpaper on the grips partially compromised the structure of PVA-H, sometimes to the point that they fractured even before the test was conducted, in the case of PVA L. However, without it (and often with it), the hydrated gels are too slippery. The compressive forces at the grip also decreased the cross-sectional area at the tips, creating a weak point. The results were not stable.

A homemade customized punch was made in order to produce specimens with an increased contact area between the serrated grips and the gel and better distribute forces. The goal was to fabricate specimens where tensile forces would focus along a rectangular length and induce rupture in a narrower area in the middle. This technique was rather successful: most gels ruptured along the gage length of the specimen. The protocol for the compression tests, as defined in Section 3.3, was effective and the resulting hydrogels rendered consistent results as well.

From the data obtained, stress-strain curves were plotted, the tensile and compressive YM were calculated, and the UTS, the maximum strain rate, the fracture toughness, and the compression strength were obtained. An overview of the typical stress-strain curves of all the formulations of PVA-H can be seen in Fig. 32 and 33. The individual curves can be seen in Section 8 (Fig. 55 to 64). The thickness of the gels was extremely challenging to control, as mentioned in Section 4.1., but the results obtained were very consistent throughout.

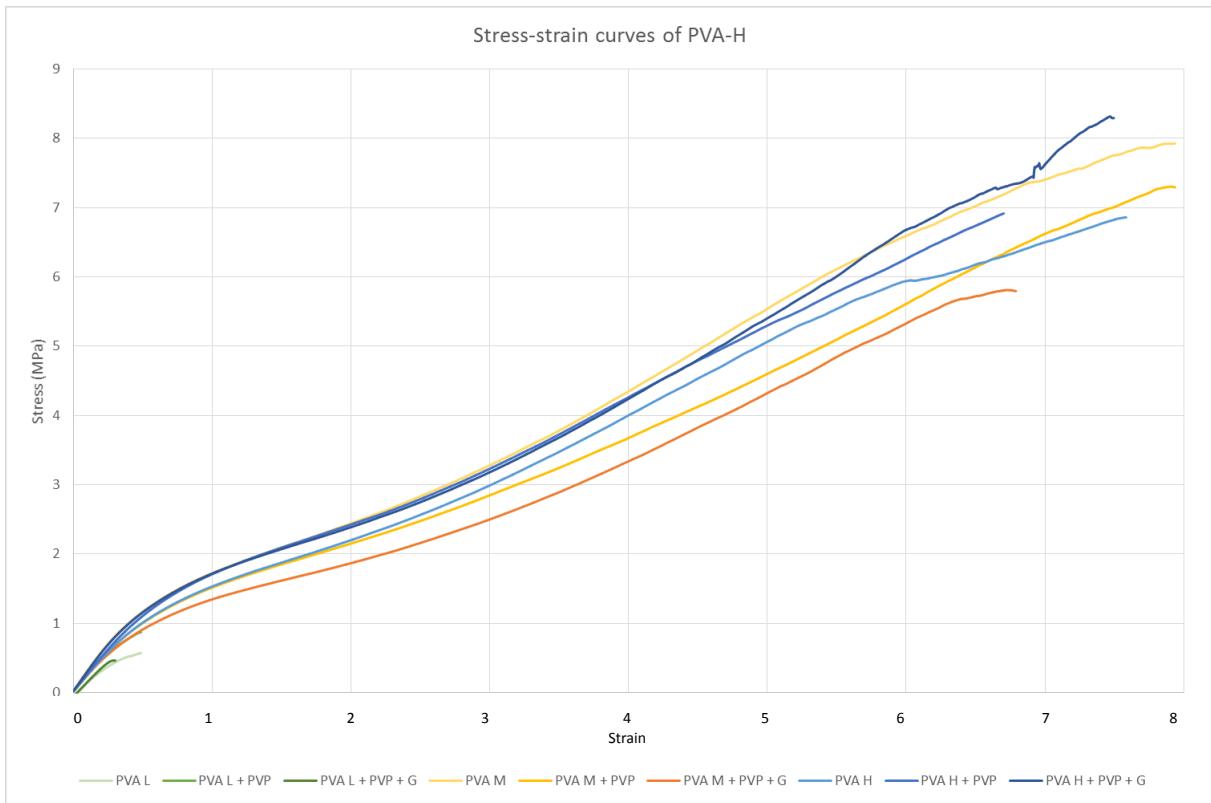


Figure 32: Illustrative example of the tensile stress-strain curves of PVA-H.

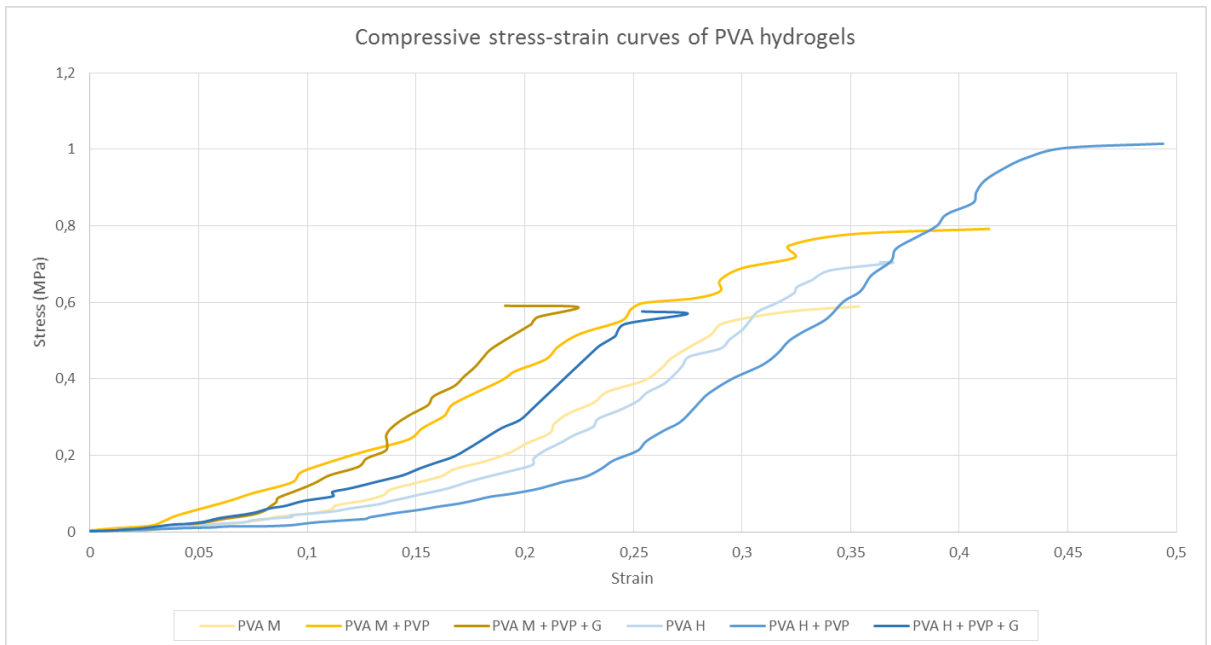


Figure 33: Illustrative example of compressive stress-strain curves of PVA-H.

The stress-strain curves were plotted from the data obtained from these tests (Fig 32 and 33). As mentioned in section 3.3, most materials initially exhibit a linear behaviour. Using Microsoft Excel, a linear trendline was added to the linear portion of the graph only. The reliability of the resulting equation was on average 0.99. The YM is the slope of the adjusted line for both tensile and compressive tests. (Fig. 34 and 35)

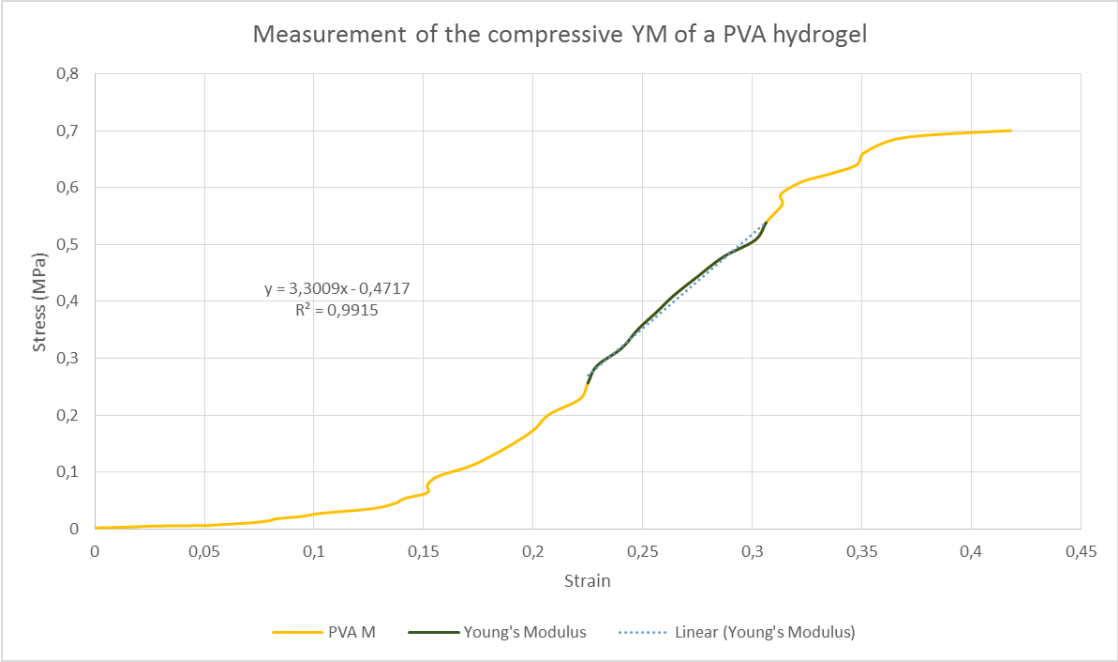


Figure 34: Measurement of the compressive YM of a PVA hydrogel using stress-strain curves. The yellow line represents the measured curve, the green line represents the portion of the curve used to calculate the YM and the dotted line corresponds to its linear adjustment.

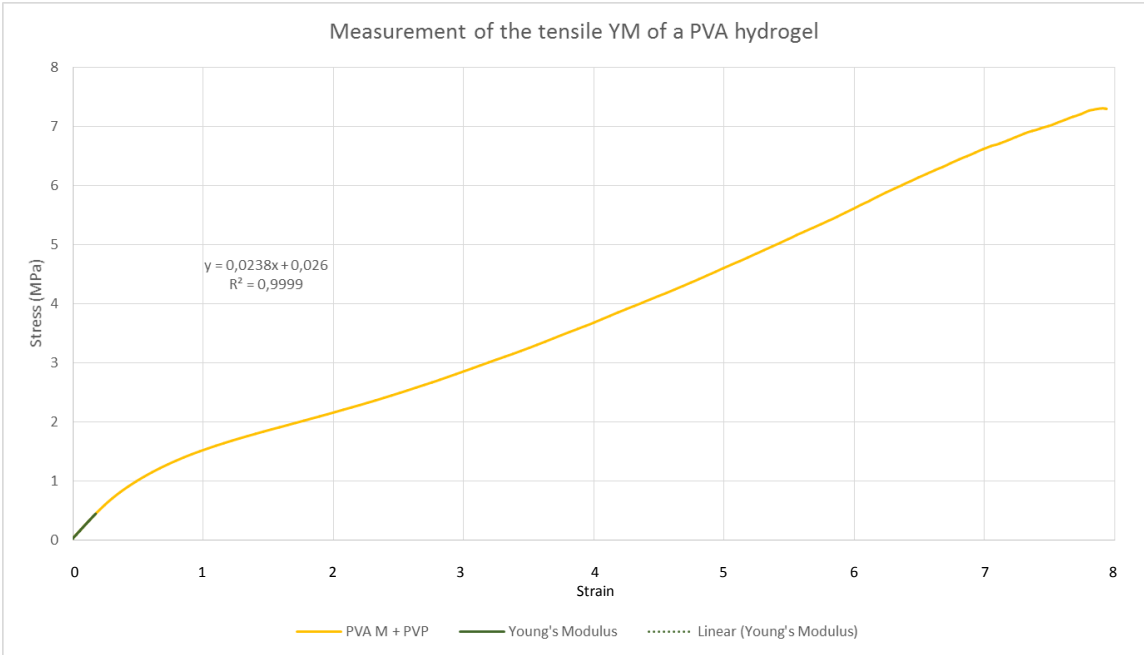


Figure 35: Measurement of the tensile YM of a PVA hydrogel using stress-strain curves. The yellow line represents the measured curve, the green line represents the portion of the curve used to calculate the YM and the dotted line corresponds to its linear adjustment.

The UTS and the maximum strain rate were obtained by direct measurement through the stress-strain curves. The UTS and the maximum strain values are, respectively, the maximum stress the samples withstand, or the maximum strain observed, without breaking. (Fig. 36)

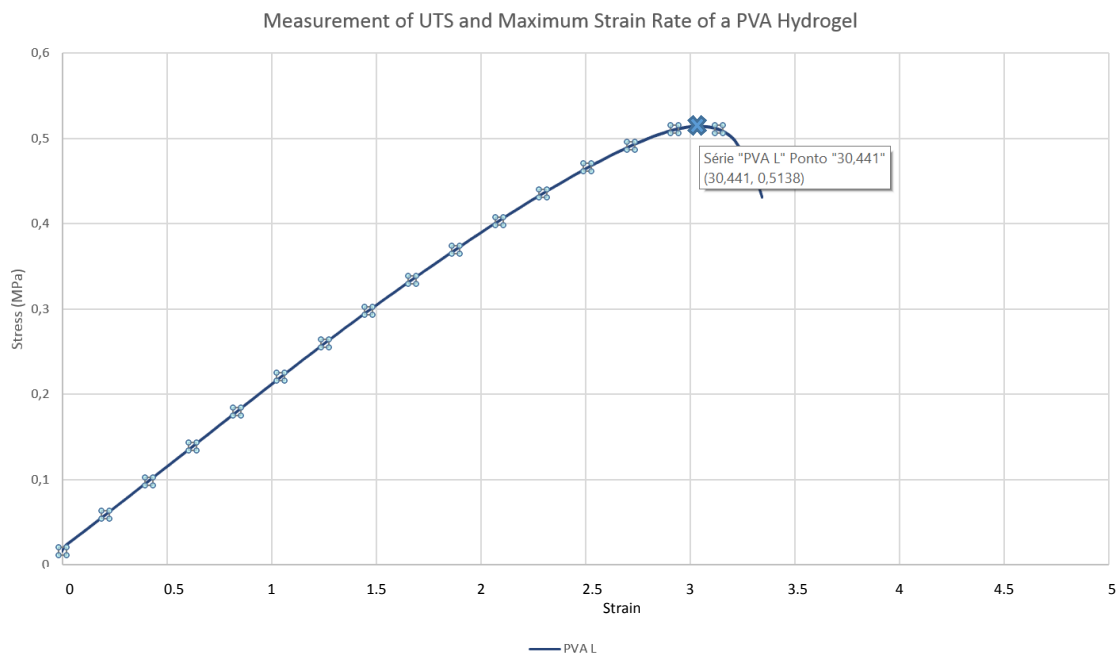


Figure 36: Measurement of UTS and maximum strain rate of a PVA Hydrogel. x-axis: Maximum strain rate (30.441% in this case); y-axis: UTS (0.51 MPa in this case)

The fracture toughness and the compressive strength are the areas under the stress-%strain curves.²⁷⁰ The values obtained for the UTS, MSR and Fracture Toughness were the real values for PVA L, but not for PVA M and PVA H. PVA L consistently ruptured in the middle of the gage length, but the other kinds of PVA hydrogels did not always break, or they did not always rupture evenly. The fracture toughness of PVA M and PVA H was measured up to an strain rate of 3, at which no slippage or breakage was observed in any of the gels. Thus, the values presented for all three of these properties are an underestimation of the real values.

Table 9, below, summarizes the properties that have been measured along with a pertinent reference values. The UTS of PVA L is at the lower end of the range of the UTS in the natural cartilage, and the fracture toughness is significantly lower than articular cartilage and other PVA-H formulations. The fact that PVA M and H form a tighter network of bonds may explain the difference in toughness in regard to PVA L.^{246,271} In the literature, water content has also been inversely related with toughness, which is in line with the results obtained in the swelling tests and toughness for these samples.²⁷² Because of its weak mechanical properties, further analysis of PVA L was not pursued.

Table 9: Summary of the mechanical properties of natural cartilage, PVA in the literature and PVA in the scope of this work. Note: In samples where fractured toughness is defined as a minimum value, the presented value was measured at a strain rate of 3. Compressive toughness was measured at a stress level of 500kPa.

Material	Tensile Young's Modulus (MPa)	Ultimate Tensile Strength (MPa)	Maximum Strain	Fracture Toughness (MPa/mm^{0.5})	Compressive Young's Modulus (MPa)	Compressive Toughness (MPa/mm^{0.5})
<i>Native cartilage</i>	4.3 – 25 ⁷⁹	0.8 – 25 ⁷⁹	-	305 - 391 ⁷⁸	0.24 – 1 ⁷⁹	-
<i>Co-Cr alloy</i>	210*10 ³ 122,123	1085 122,123	-	-	-	-
<i>PE</i>	220*10 ³ 122,123	820 ^{122,123}	-	-	-	-
<i>Allumina</i>	380*10 ³ 122,123	300 ^{122,123}	-	-	-	-
<i>Zirconia</i>	880 ^{122,123}	35 ^{122,123}	-	-	-	-
<i>PVA in the literature</i>	0.19 ²⁷³ 1.4 ²⁷⁴		-		0.07 – 0.24 ²⁴⁴ 2.56 – 3.68 ⁹	-
<i>PVA L</i>	2.1 ± 0.3	0.7	54	18 ± 3	-	-
<i>PVA L + PVP</i>	2.3 ± 0.2	0.9	66	34 ± 6	-	-
<i>PVA L + PVP + G</i>	1.8 ± 0.2	0.5	36	11 ± 1	-	-
<i>PVA M</i>	2.4 ± 0.3	≥ 8	≥ 798	≥ 493 ± 26	3.6 ± 0.4	≥ 48 ± 4
<i>PVA M + PVP</i>	2.5 ± 0.2	≥ 7	≥ 795	≥ 529 ± 37	3.1 ± 0.5	≥ 51 ± 4
<i>PVA M + PVP + G</i>	2.0 ± 0.2	≥ 6	≥ 685	≥ 458 ± 22	4.1 ± 0.5	≥ 43 ± 8
<i>PVA H</i>	2.4 ± 0.4	≥ 7	≥ 812	≥ 543 ± 7	4.5 ± 0.5	≥ 40 ± 4
<i>PVA H + PVP</i>	2.6 ± 0.3	≥ 11	≥ 822	≥ 574 ± 17	3.4 ± 0.6	≥ 52 ± 10
<i>PVA H + PVP + G</i>	2.7 ± 0.3	≥ 8	≥ 755	≥ 592 ± 12	4.05 ± 0.3	≥ 43 ± 4

For the remaining PVA M and PVA H hydrogels, the UTS values presented are well within the limits of articular cartilage, which can go up to 25 MPa. While the values obtained are lower than the upper limit of the UTS of cartilage, as discussed, the UTS for tested hydrogels is an underestimation. Due to slippage, minor misalignments that induce premature breaking or anisotropies in the material, it is plausible to conclude the data obtained does not reflect the apex of the capabilities of the material. The

highest UTS was measured in PVA H + PVP (10.77 MPa) which, in fact, did not rupture (Fig 43). As a result, there is strong evidence that suggests that, under certain circumstances, this material could withstand even higher loads.

The YM was low both in tension and compression. A low YM denotes a flexible material that deforms easily under loads.

The YM is nearly the same in all samples. Depalle et al²⁷¹ measured the effect of cross-linking density in the Young's modulus and concluded that the crosslinking density has no effect on the YM, measured at the elastic region. While the effectiveness of glyoxal in this work is debatable (a more in depth analysis can be found in section 4.2.1.1.), an increase in the YM of PVA-based hydrogels should have been noticeable with the addition of PVP. Namely, the Young's modulus was expected to increase with the addition of PVP, which was not observed in this work.¹²

In theory, tensile and compressive elastic moduli should be equal, which is not observed in the case of cartilage and PVA constructs, both self-made and referenced material. The calculated tensile and compressive YM are slightly different in the case of the tested hydrogels but this has been observed before in the literature.¹² The YM is, in reality, dynamic. While metals and ceramics have YM that can be thought of as constant, the same does not happen with cartilage or polymers, whose properties depend on test conditions such as the type of load (tensile or compressive), time of application of the load, temperature, strain rate and fiber orientation.

Anisotropy and tensile-compressive nonlinearity are two reasons why PVA might behave differently under tensile and compressive stresses and have dissimilar YM.²⁷⁵ The results here presented support the idea that PVA is an anisotropic material, as well as cartilage.

The YM shows that natural cartilage is stiffer when subjected to tensile loads and softer when compressive loads are applied.⁷⁹ Presumably, it is this elastic behaviour upon compression that allows the release of synovial fluid and enables efficient lubrication. In this sense, it is not advantageous that PVA-H seem to be stiffer under compressive loads.

Table 10 represents the tensile and compressive toughness measured on the materials at a stress level of 500KPa, since compression tests did not reach the same stress levels as tensile tests. The data there presented confirms that PVA is tougher under compression.

Table 10: Toughness properties under tension and compression for PVA-H at a stress level of 500kPa.

	Fracture Toughness (MPa/mm^{0.5})	Compressive Toughness (MPa/mm^{0.5})
<i>PVA M</i>	$\geq 5.7 \pm 0.4$	$\geq 48 \pm 4$
<i>PVA M + PVP</i>	$\geq 5.2 \pm 0.4$	$\geq 51 \pm 4$
<i>PVA M + PVP + G</i>	$\geq 6.4 \pm 0.1$	$\geq 43 \pm 8$
<i>PVA H</i>	$\geq 5.6 \pm 0.8$	$\geq 40 \pm 4$
<i>PVA H + PVP</i>	$\geq 5.2 \pm 0.1$	$\geq 52 \pm 10$
<i>PVA H + PVP + G</i>	$\geq 4.5 \pm 0.23$	$\geq 43 \pm 4$

It has previously been mentioned that not all test specimens break. In most cases, this was due to slippage but, in one of the tests, not rupture nor slippage occurred. Fig 37, below, shows this example, which was measured on a PVA H + PVP hydrogel hydrogel, that shows that, in general, PVA H (and most probably M) displays a great capacity to deform under loads, reaching strain levels of approximately 8.2, i.e. it can extend over 9 times its original length without breaking. After unloading, it can be observed that the hydrogel recovers partially by 4.7 (elastic deformation) but plastic deformation also occurs at a strain level of 3.5.

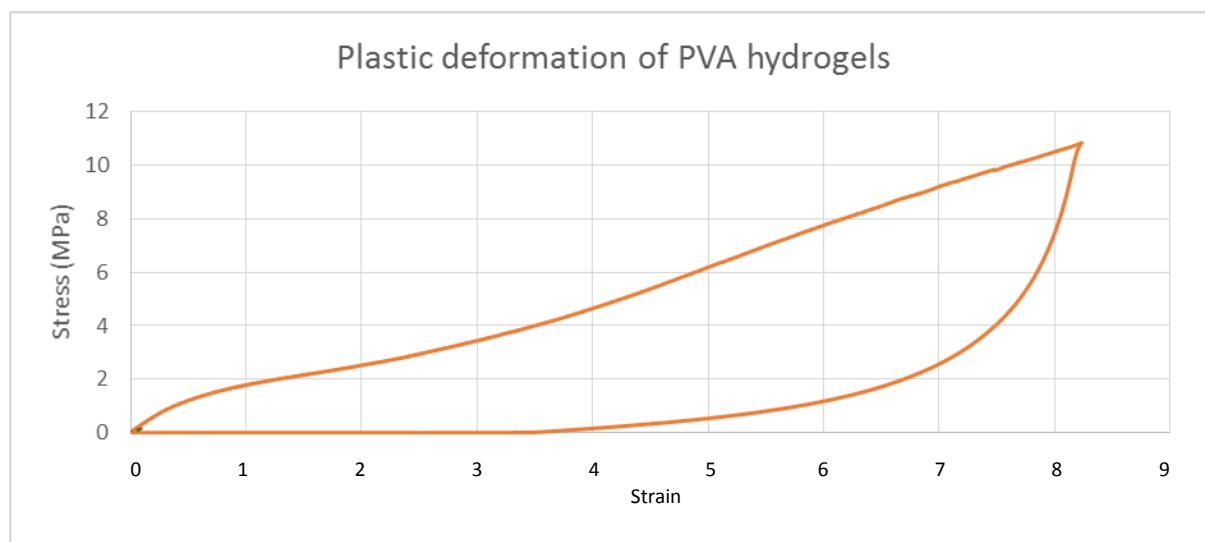


Figure 37: Stress-strain curve of PVA H + PVP hydrogel sample showing plastic deformation upon unloading.

4.2.3. THERMOTROPIC BEHAVIOUR

The thermotropic behaviour of the prepared PVA hydrogels is now described and compared with the literature. Fig. 38, 39 and 40 contain all the data concerning DSC of dry samples, and Table 11

summarizes all the properties extrapolated through this test. It is important to note that these tests were initiated after mechanical testing, at which point the tensile data had already revealed PVA L was not the most fitting material for cartilage replacement applications. As so, at the time of DSC, the decision not to further pursue PVA L studies had already been made, and this section features only PVA M and PVA H hydrogels.

The degree of crystallinity, calculated as described in section 3.2.3., varies from 43% to 49%. This indicated a semi-crystalline material with both crystalline and amorphous regions. The presence of amorphous areas originates disorder, reducing the enthalpy of the system.

The T_m is an important measurement of the degree of purity of the substance. According to the literature, PVA melts at approximately 210 – 215°C²³⁵. Tubbs²⁷⁶ investigated the influence of heating rate on the T_m of PVA and concluded that for a 10°C/min heating rate (the same as that used in this work), the T_m is 225.8°C. The T_m of the hydrogels was very similar to the values found in the literature - around 227-228 °C for PVA M and 229-230°C for PVA H. The enthalpy of fusion of the PVA M and the PVA H samples also did not present significant differences.

The T_g of PVA is usually found at around 85°C²⁷⁷ but could not be identified for any of the samples. The T_g is typically more difficult to locate, especially when the T_m is very pronounced, because it can occur over a very small range of temperatures that make it extremely difficult to identify. On the other hand, glass transition is associated with segmental motility of the amorphous region, which could be impaired due to high density of hydrogen bonds and crosslinking.²⁷⁸ Therefore, it is also entirely possible for a polymer not to exhibit a T_g . However, the degree of crystallinity shows that the amorphous region exists, and it is consistent with the fact that PVA is a semi-crystalline polymer. As so, the hypothesis that a T_g exists but could not be detected is more likely.

Table 11: Thermotropic behaviour (T_m , enthalpy of fusion, degree of crystallinity) of the PVA hydrogels under dry conditions. (* a PVA product by Kuraray)

Dry samples	T_m (°C)	Enthalpy of fusion (J/g)	Degree of Crystallinity (%)
PVA M	227.8 ± 1.0	61.5 ± 3.7	44
PVA M + PVP	227.5 ± 0.9	60.1 ± 0.6	43
PVA M + PVP + G	228.3 ± 0.2	64.6 ± 0.6	47
PVA H	229.8 ± 0.4	67.4 ± 4.5	49
PVA H + PVP	230.9 ± 2.0	68.4 ± 0.5	49
PVA H + PVP + G	230.1 ± 1.2	66.3 ± 2.1	47
PVA in the literature	210 – 215 ^{235,279,280}	-	45 – 46 ²⁴⁶
Elvanol 73 – 125 G*	218 - 219 ²⁰⁹	-	-

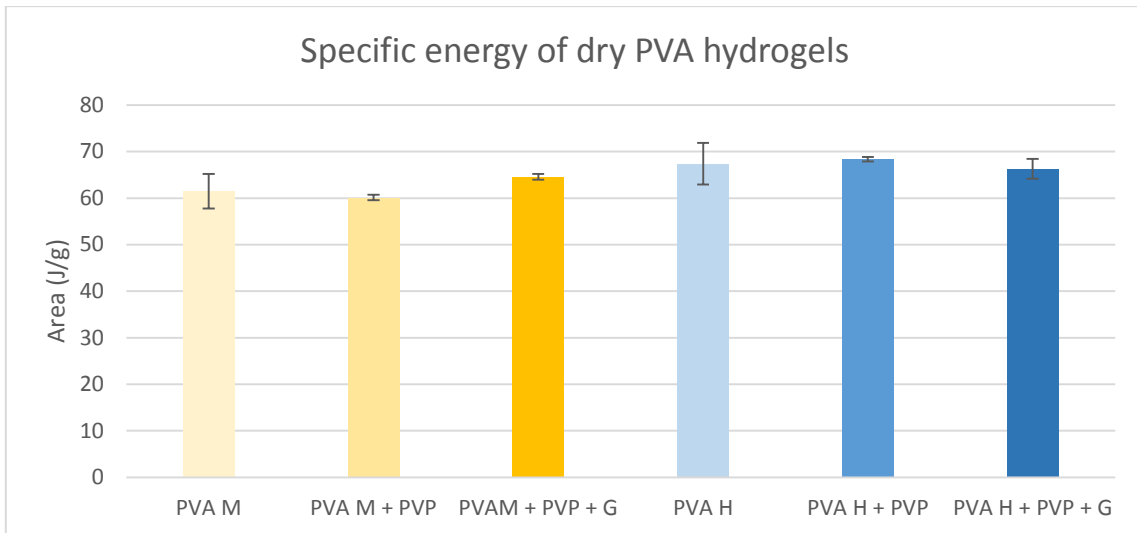


Figure 38: Enthalpy of fusion of PVA hydrogels under dry conditions.

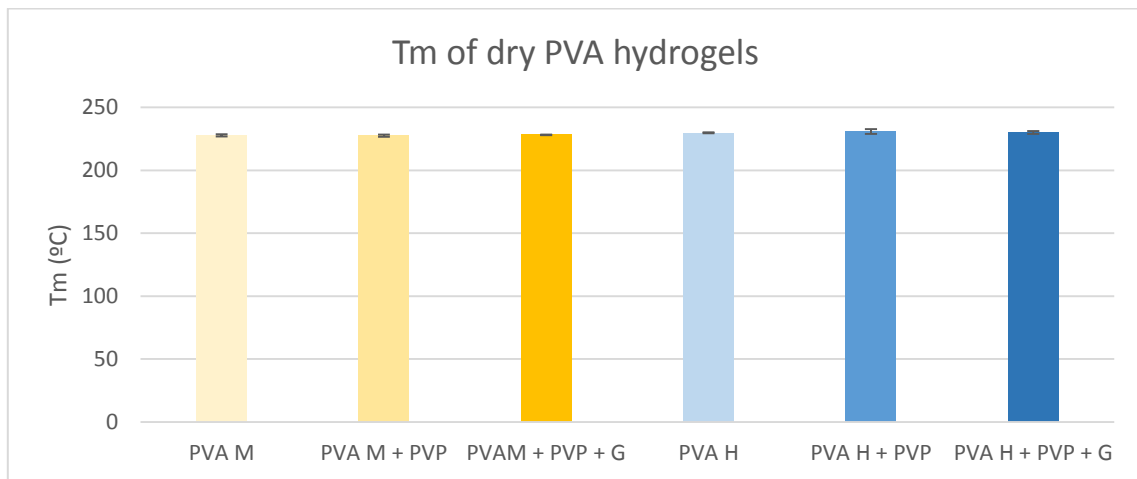


Figure 39: Peak temperature of PVA hydrogels under dry conditions.

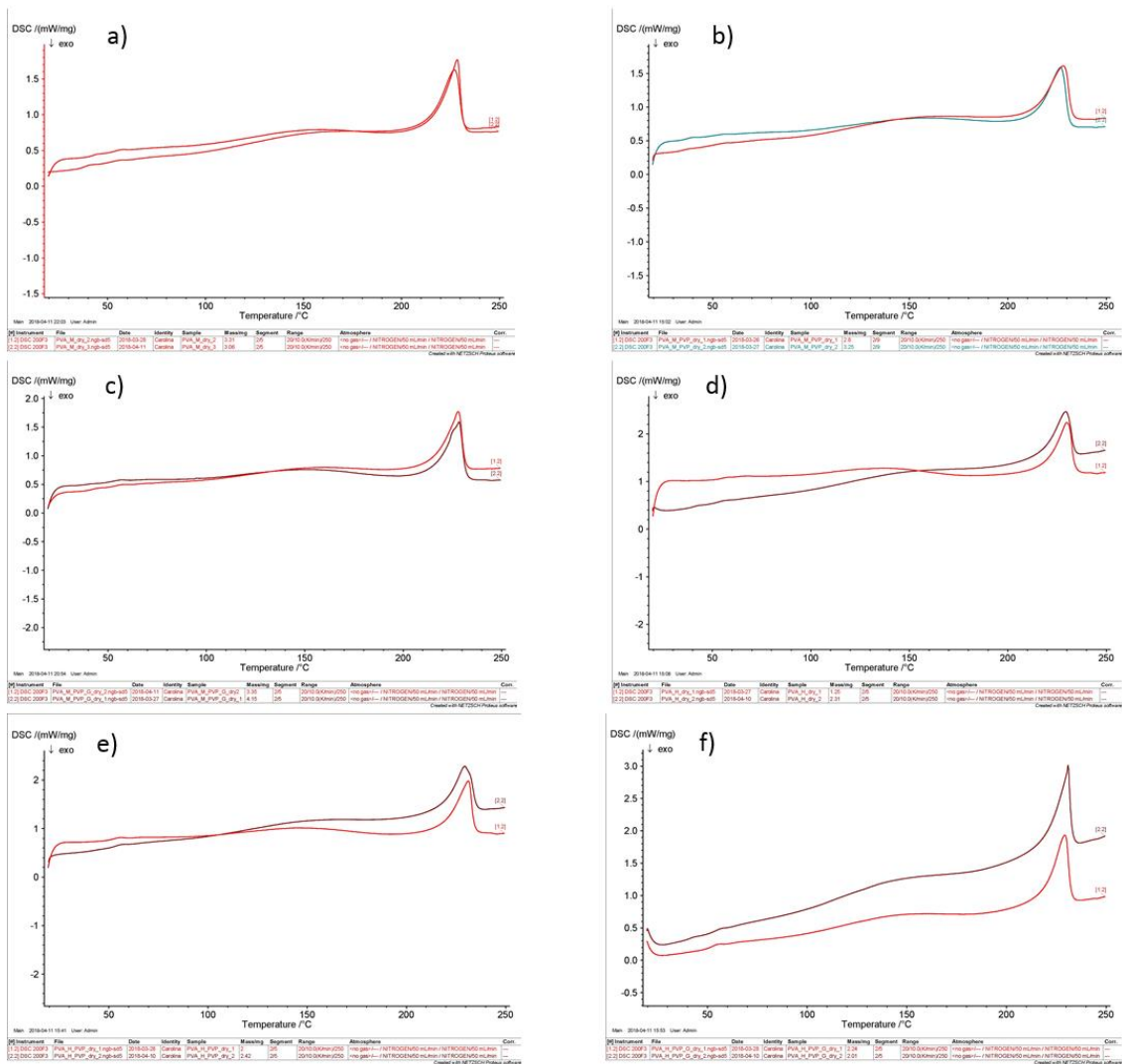


Figure 40: DSC curves of dry samples (each curve represents a different test). a) PVA M; b) PVA M + PVP; c) PVA M + PVP + G; d) PVA H; e) PVA H + PVP; f) PVA H + PVP + G

To evaluate the effect of the presence of water in the samples, the tests were also conducted in the hydrated state (Fig. 41). There can be three types of water in a polymer: tightly bound water, loosely bound water and free water. Tightly bound water is associated with the polymer matrix and cannot be observed in the range of the test that was performed, since it can only be seen for temperatures lower than -10°C .²⁸¹ Loosely bound water, as the name suggests, is loosely bound to the matrix and melts at temperatures slightly lower than those of normal water. Lastly, free water can be detected for its T_m at around 0°C .²⁸²

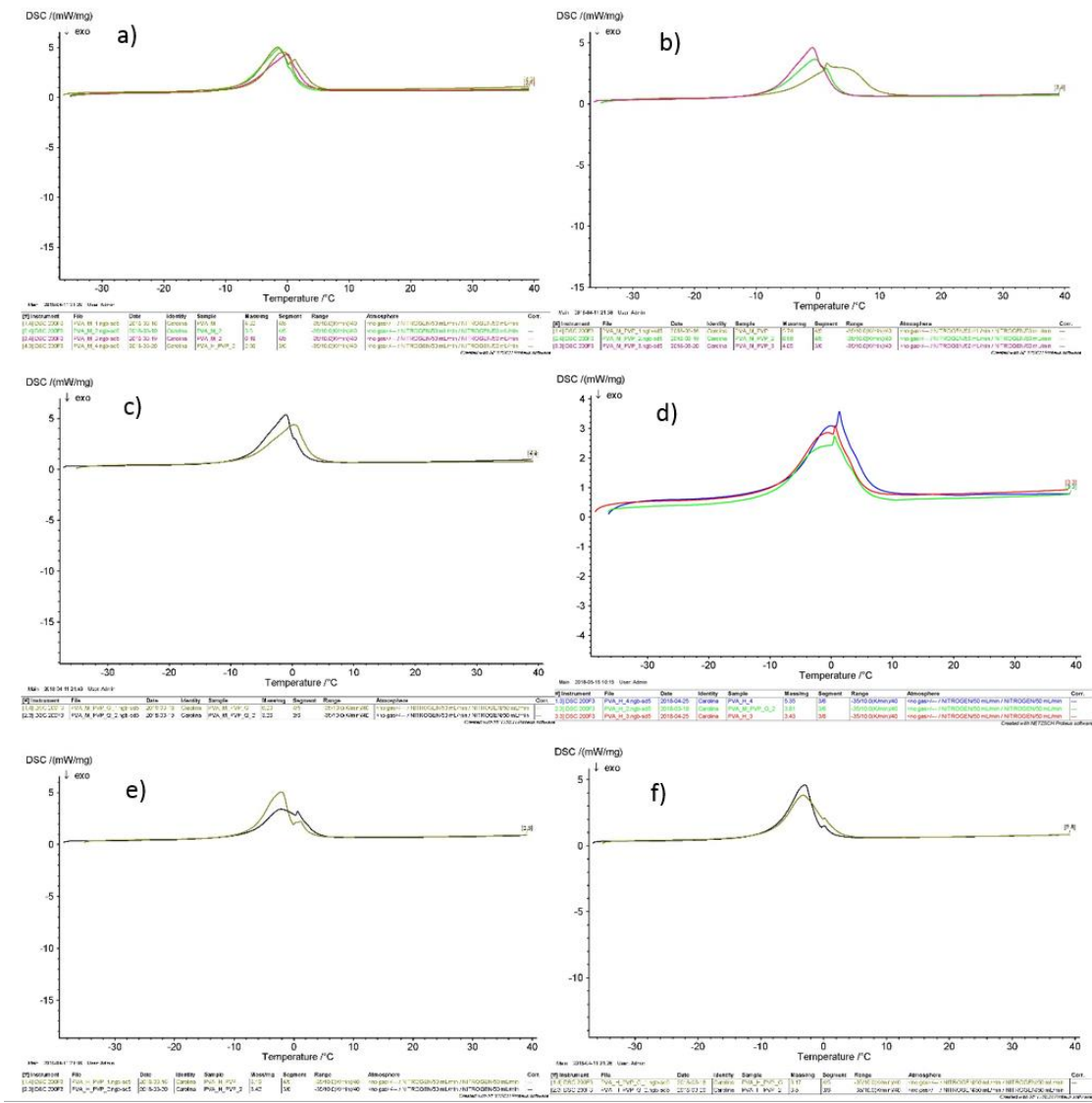


Figure 41: DSC curves of hydrated samples (each curve represents a different test). a) PVA M; b) PVA M + PVP; c) PVA M + PVP + G; d) PVA H; e) PVA H + PVP; f) PVA H + PVP + G

Knowing the WC of the gels, the theoretical enthalpy of water and the experimental enthalpies and weights of each individual sample, the percentage of free and loosely bound water within the samples was calculated as described in Section 3.2.3.. Table. 12 lists the results of this calculation, with values averaging at about 74% for PVA M and 65% for PVA H – these values qualitatively align with those obtained for the swelling behaviour.

In Fig. 41, in most images, two overlapping peaks are distinguishable. The first, occurs at negative temperatures, while the second occurs at around 0°C. The first peak corresponds to loosely bound water and the second, to free water. From the images and the measured peak temperatures, it is apparent that within the free and loosely bound water percentage, a higher amount of that water is loosely bound water on the hydrogels.

Table 12: Thermotropic behaviour (T_m , enthalpy of fusion and percentage of free and loosely bound water) of the PVA hydrogels under hydrated conditions.

Hydrated samples	T_m ($^{\circ}\text{C}$)	Enthalpy of Fusion (J/g)	Free and Loosely Bound Water (%)
PVA M	-0.6 ± 0.9	156 ± 6	74 ± 3
PVA M + PVP	0.6 ± 1.0	153 ± 9	74 ± 4
PVA M + PVP + G	-0.4 ± 0.9	159 ± 6	74 ± 3
PVA H	0.9 ± 0.5	126 ± 7	65 ± 4
PVA H + PVP	-2.1 ± 0.0	146 ± 14	73 ± 7
PVA H + PVP + G	-3.2 ± 0.2	134 ± 0	67 ± 0

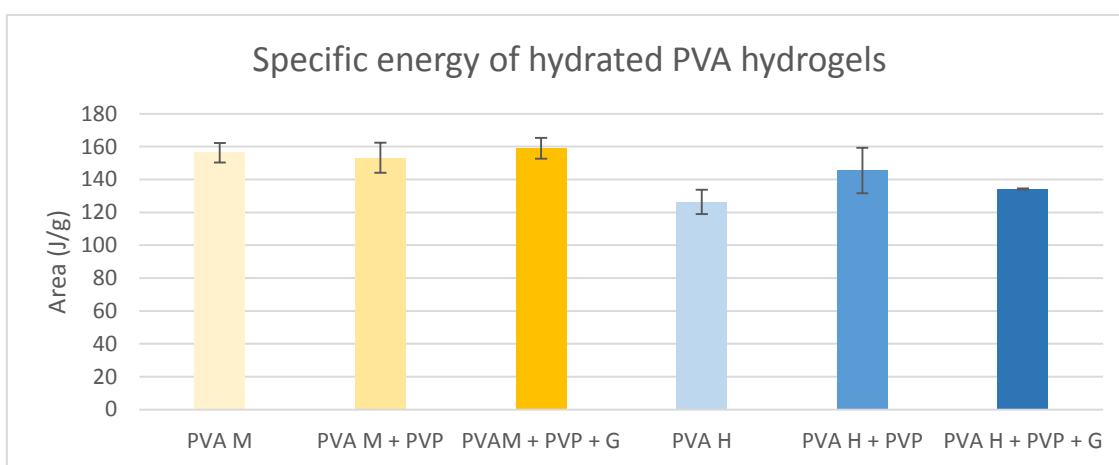


Figure 42: Enthalpy of fusion of PVA hydrogels under hydrated conditions.

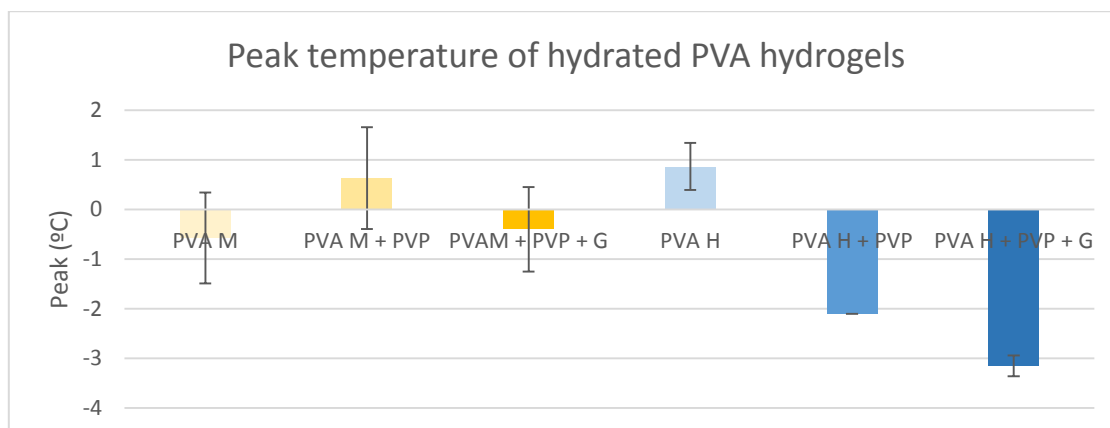


Figure 43: Visual representation of the peak temperature of PVA hydrogels under hydrated conditions.

5. CONCLUSIONS

After several iterations of the protocol, it was possible to create a simple protocol for the production of physically crosslinked, CD PVA hydrogels. The end product consisted of transparent, flat, homogeneous physically crosslinked gels. While the process is not seamlessly upscaled to produce thicker hydrogels, the results were very consistent.

All the different PVA hydrogels that have been studied present a significantly larger water content percentage in their swelled state, with swelling rates varying between 138% and 308% across the board. Regarding their %EWC, all gels seem similar to natural cartilage and other PVA constructs. Generally speaking, all PVA hydrogels swell significantly in the presence of water. %SR and %EWC both increase when the molecular weight of the PVA decreases. This is consistent with the concept that heavier chains form a tighter network of bonds, thus leaving less space for water to fill.

%SR and %EWC also increase as PVP and glyoxal are added to the solution. This might be due to bulky pyrrolidone rings which prevent the formation of tighter bonds and the high affinity to water of PVP.

Glyoxal seems to have little to no effect on the gels.

All PVA hydrogels tested exhibit values that are not far or within the range of natural cartilage, with %EWC ranging from 60% to 75%.

The samples were found to be very hydrophilic, with low contact angles in the interval 32° - 50°. The trends observed are in line with those of the swelling behaviour – the contact angle decreases with 1) the increase of molecular weight; 2) the addition of PVP and glyoxal.

Similar values have been reported in the literature for the captive bubble method (37° - 45°).

Here, a static contact angle has been considered, but the differences in the sessile drop method and the captive bubble test also demonstrate that contact angle hysteresis exists. It is believed that contact angle hysteresis is a consequence of heterogeneity and surface roughness. Most surfaces present surface irregularities that act as barriers to the motion of the contact line, which can alter the macroscopic measurement of contact angles. The existence of surface roughness on PVA hydrogels has also been confirmed by the literature.

As far as the mechanical properties go, the tensile and compressive YM were calculated, and the UTS, the maximum strain, the toughness, and the compressive strength were obtained.

The first conclusion that can be drawn from the stress-strain curves and its derivative properties is that PVA L is rather below the desirable range of values for UTS or fracture toughness. Its UTS sits on the lower limit of the registered values of articular cartilage and the toughness of cartilage is at least 10 times larger than that of PVA L. Very early on into the mechanical testing, PVA L displayed weak mechanical properties and for that reason it was put aside.

The fracture toughness of PVA M and PVA H is already greater than that of the cartilage at just 300% elongation. Some gels have been seen to reach over 800% elongation, which means that the PVA-H hydrogels are, in this instance, superior to cartilage.

UTS values for PVA M and PVA H hydrogels are encompassed in the interval determined for the articular cartilage. The UTS in the literature for the articular cartilage ranges between 0.8 and 25 MPa. The tested PVA-H go from 5.7 to 10.8 MPa. Once again, these measurements should, however, be but an underestimation of the true value, since the anisotropies of the material can sometimes lead to premature failure and, in some cases, slippage of the test specimens occurred.

One of the hydrogels, PVA H + PVP, reached the highest measured UTS value across the board (10.8 MPa) without rupturing. According to this curve, PVA H + PVP displays a great capacity to deform under loads, reaching strain levels of approximately 8.2. Part of this deformation was seen to be elastic (4.7), while a smaller portion of it was plastic (3.5). Overall, this indicates that, under certain circumstances, this material has the capability to go beyond these values.

The anisotropies of the gels are confirmed upon the knowledge that the YM differs in tensile and compressive conditions. Toughness at 500 kPa for both tensile and compressive tests further supports this hypothesis. In fact, from the YM and the toughness of the material in tension and compression, one can conclude that the PVA-H samples are stiffer under compressive loads than under tensile loads. Whereas this trend is in accordance with PVA-H in the literature, it is opposite to the trend seen in articular cartilage.

As for the thermotropic behaviour of PVA, the dry tests should allow for the extrapolation of the T_g, the T_m and the degree of crystallinity. The results regarding the T_m were very comparable to those found in the literature: all the tested PVA hydrogels presented values within the 227-228°C range. The degree of crystallinity varies from 43% to 49%. This is consistent with PVA being a semi-crystalline material. The T_g of PVA could not be identified for any of the samples.

The gels contain about 66% (PVA H) to 74% (PVA M) of free and loosely bound water. Analysis of the DSC curve suggests that most of the water in the gels is loosely bound water.

Table 13 provides a qualitative comparison of PVA hydrogels according to the evaluated properties. As far as swelling behaviour goes, all gels were within or very close to the values observed in cartilage. From this parameter, all materials are adequate or acceptable. In what concerns wettability, no comparable results exist for the cartilage. However, it is known to be highly hydrophilic. The mechanical testing rapidly excluded PVA L as a good candidate for cartilage replacement because of inadequate toughness. All the other gels performed favourably and may be potentially used. As for the thermotropic behaviour, the results were remarkably similar to the reference material both for PVA M and PVA H. All in all, the best materials resulting from this work, according to the data, are PVA M + PVP + G, followed by PVA M, PVA M + PVP, PVA H, PVA H + PVP and PVA H + PVP + G.

Table 13: Qualitative comparison of PVA hydrogels.

Material	Swelling Behaviour	Wettability	Thermotropic Behaviour	YM	UTS	Toughness
<i>PVA L</i>	Dark Grey	Dark Grey	White	Medium Grey	Light Grey	Light Grey
<i>PVA L + PVP</i>	Dark Grey	Dark Grey	White	Medium Grey	Light Grey	Light Grey
<i>PVA L + PVP + G</i>	Dark Grey	Dark Grey	White	Medium Grey	Light Grey	Light Grey
<i>PVA M</i>	Light Grey	Dark Grey	Dark Grey	Medium Grey	Dark Grey	Dark Grey
<i>PVA M + PVP</i>	Light Grey	Dark Grey	Dark Grey	Medium Grey	Dark Grey	Dark Grey
<i>PVA M + PVP + G</i>	Dark Grey	Dark Grey	Dark Grey	Medium Grey	Dark Grey	Dark Grey
<i>PVA H</i>	Light Grey	Dark Grey	Dark Grey	Medium Grey	Dark Grey	Dark Grey
<i>PVA H + PVP</i>	Light Grey	Dark Grey	Dark Grey	Medium Grey	Dark Grey	Dark Grey
<i>PVA H + PVP + G</i>	Light Grey	Dark Grey	Dark Grey	Medium Grey	Dark Grey	Dark Grey

Adequate properties ✓✓	Acceptable properties ✓	Inadequate Properties X	No information
---------------------------	----------------------------	----------------------------	----------------

6. FUTURE WORK

The tribological properties could not be ascertained during the course of this work, due to lack of time. It would be important to complete the data in this thesis with information regarding the coefficient of friction. Water is thought to underestimate the coefficient of friction, so the use of other lubricants, such as hyaluronic acid (present in the synovial fluid), could be advantageous.

Also, the relationship between wettability, surface morphology and coefficient of friction should be studied, since information in the literature suggests these properties influence the tribological behaviour of the samples.

The study of the cell adhesion and protein adsorption properties of PVA-H could be interesting. These have been studied for applications in the replacement of localized defects of the cartilage. While this is not the application initially planned, many studies place importance on cell adhesion for appropriate integration of hydrogels with surrounding tissue.

Moving forward, it might be interesting to explore other gelation methods. Namely, freeze-thawing might be a compelling course of work, since its properties can be tailored by changing the number FT cycles.

Still regarding alternative gelation processes, ionizing radiation is another pertinent suggestion. PVA must be sterilized for this type of biomedical applications. Methods that resort to heat are not adequate for CD PVA hydrogels, for example, since the heat compromises the integrity of the gel. Ionizing radiation is the most frequently reported sterilization method for hydrogels, along with autoclaving. However, ionizing radiation induces gelation and sterilizes in one step. Surely, introducing gamma rays as a variable in the protocol could generate very interesting results.

Furthermore, the environment surrounding these gels in their intended application would be very fragile as a result of inflammation. Following up on the possibility of embedding the polymer matrix with therapeutic drugs and achieving their controlled release would be key.

Lastly, extending this study to other materials, such as alginate, chitosan, PEG and others might be an asset.

7. REFERENCES

1. Ledingham J, Snowden N, Ide Z. Diagnosis and early management of inflammatory arthritis. *BMJ*. 2017;j3248. doi:10.1136/bmj.j3248
2. Centers for Disease Control and Prevention. Arthritis-Related Statistics. https://www.cdc.gov/arthritis/data_statistics/arthritis-related-stats.htm. Accessed April 30, 2018.
3. Woolf AD. The bone and joint decade. strategies to reduce the burden of disease: the Bone and Joint Monitor Project. *J Rheumatol Suppl.* 2003;67:6-9. <http://www.ncbi.nlm.nih.gov/pubmed/12926644>.
4. Scuderi GR, Insall JN, Windsor R., Moran MC. Survivorship of Cemented Knee Replacements. *J Bone Jt Surg.* 1978:798-803.
5. Ranawat CS, Padgett DE, Ohashi Y. Total knee arthroplasty for patients younger than 55 years. *Clin Orthop Relat Res.* 1989;(248):27-33.
6. Dalury DF, Ewald FC, Christie MJ, Scott RD. Total knee arthroplasty in a group of patients less than 45 years of age. *J Arthroplasty.* 1995;10(5):598-602.
7. Schai PA, Scott RD, Thornhill TS. Total knee arthroplasty with posterior cruciate retention in patients with rheumatoid arthritis. *Clin Orthop Relat Res.* 1999;(367):96-106.
8. Kim KT, Lee S, Ko DO, Seo BS, Jung WS, Chang BK. Causes of Failure after Total Knee Arthroplasty in Osteoarthritis Patients 55 Years of Age or Younger. *Knee Surg Relat Res.* 2014;26(1):13-19. doi:10.5792/ksrr.2014.26.1.13
9. Baker MI, Walsh SP, Schwartz Z, Boyan BD. A review of polyvinyl alcohol and its uses in cartilage and orthopedic applications. *J Biomed Mater Res - Part B Appl Biomater.* 2012;100 B(5):1451-1457. doi:10.1002/jbm.b.32694
10. Sasada T, Takahashi M, Watanabe M, Mabuchi K, Tsukamoto Y, Nanbu M. Frictional behaviour of a total hip prosthesis containing artificial articular cartilage. *J Jpn Soc Biomater.* 1985;(3):151-157.
11. Świążzkowski W, Ku DN, Bersee HEN, Kurzydłowski KJ. An elastic material for cartilage replacement in an arthritic shoulder joint. *Biomaterials.* 2006;27(8):1534-1541. doi:10.1016/j.biomaterials.2005.08.032
12. Ma R, Xiong D, Miao F, Zhang J, Peng Y. Novel PVP/PVA hydrogels for articular cartilage replacement. *Mater Sci Eng C.* 2009;29(6):1979-1983. doi:10.1016/j.msec.2009.03.010
13. Fathi E, Atyabi N, Imani M, Alinejad Z. Physically crosslinked polyvinyl alcohol-dextran blend xerogels: Morphology and thermal behavior. *Carbohydr Polym.* 2011;84(1):145-152. doi:10.1016/j.carbpol.2010.11.018
14. Bichara DA, Zhao X, Hwang NS, et al. Porous poly(vinyl alcohol)-alginate gel hybrid construct for neocartilage formation using human nasoseptal cells. *J Surg Res.* 2010;163(2):331-336. doi:10.1016/j.jss.2010.03.070
15. Maroudas a. Physicochemical properties of cartilage in the light of ion exchange theory. *Biophys J.* 1968;8(5):575-595. doi:10.1016/S0006-3495(68)86509-9
16. BUCKWALTER JA, MANKIN HJ. Instructional Course Lectures, The American Academy of Orthopaedic Surgeons - Articular Cartilage. Part I: Tissue Design and Chondrocyte-Matrix Interactions*†. *J Bone Jt Surg Am.* 1997;79(4):600-611. doi:http://dx.doi.org/
17. Torzilli PA. Influence of cartilage conformation on its equilibrium water partition. *J Orthop Res.* 1985;3(4):473-483. doi:10.1002/jor.1100030410
18. Maroudas A, Wachtel E, Grushko G, Katz EP, Weinberg P. The effect of osmotic and mechanical pressures on water partitioning in articular cartilage. *BBA - Gen Subj.* 1991;1073(2):285-294. doi:10.1016/0304-4165(91)90133-2

19. Mow VC, Kuei SC, Lai WM, Armstrong CG. Biphasic Creep and Stress Relaxation of Articular Cartilage in Compression: Theory and Experiments. *J Biomech Eng.* 1980;102(1):73. doi:10.1115/1.3138202
20. Mow VC, Ratcliffe A, Robin Poole A. Cartilage and diarthrodial joints as paradigms for hierarchical materials and structures. *Biomaterials.* 1992;13(2):67-97. doi:10.1016/0142-9612(92)90001-5
21. Oatis CA, Mansour J. *Kinesiology The Mechanics & Pathomechanics of Human Movement.* Vol 1.; 2009. doi:10.1017/CBO9781107415324.004
22. Eyre D. Collagen of articular cartilage. *Arthritis Res.* 2002;4(1):30-35. doi:10.1186/ar380
23. Maroudas A. Physiochemical properties of articular cartilage. In: *Adult Articular Cartilage.* Kent, United Kingdom: Cambridge University Press; 1979.
24. Brittberg M, Lindahl A. Tissue Engineering of Cartilage. In: *Tissue Engineering of Cartilage.* New York: Academic Press; 2008:533-557. doi:https://doi.org/10.1016/B978-0-12-370869-4.00018-5
25. Buckwalter J, Rosenberg L, Hunziker EB. *Articular Cartilage and Knee Joint Function: Basic Science and Arthroscopy.* New York: Raven Press; 1990.
26. Sophia Fox AJ, Bedi A, Rodeo SA. The basic science of articular cartilage: Structure, composition, and function. *Sports Health.* 2009;1(6):461-468. doi:10.1177/1941738109350438
27. Hunziker EB, Quinn TM, Häuselmann HJ. Quantitative structural organization of normal adult human articular cartilage. *Osteoarthr Cartil.* 2002;10(7):564-572. doi:10.1053/joca.2002.0814
28. Buckwalter J, Hunziker EB, Rosenberg L. Articular cartilage: composition and structure. In: *Injury and Repair of the Musculoskeletal Soft Tissues.* Park Ridge, IL: American Academy of Orthopaedic Surgeons; 1988:405-425.
29. Poole AR, Kojima T, Yasuda T, Mwale F, Kobayashi M, Lavery S. Composition and structure of articular cartilage: a template for tissue repair. *Clin Orthop Relat Res.* 2001;1(391 Suppl):S26-S33. doi:11603710
30. Woodfield TBF, Blitterswijk CA Van, Wijn J De, Sims TJ, Hollander AP, Riesle J. Polymer Scaffolds Fabricated with Pore-Size Gradients as a Model for Studying the Zonal Organization within Tissue-Engineered Cartilage Constructs. *Tissue Eng.* 2005;11(9-10):1297-1311. doi:10.1089/ten.2005.11.1297
31. Roth V, Mow VC. The intrinsic tensile behavior of the matrix of bovine articular cartilage and its variation with age. *J Bone Joint Surg Am.* 1980;62(7):1102-1117. <http://europepmc.org/abstract/MED/7430196%5Cnhttp://www.ncbi.nlm.nih.gov/pubmed/7430196>.
32. Schinagl RM, Gurskis D, Chen AC, Sah RL. Depth-dependent confined compression modulus of full-thickness bovine articular cartilage. *J Orthop Res.* 1997;15(4):499-506. doi:10.1002/jor.1100150404
33. Egli PS, Herrmann W, Hunziker EB, Schenk RK. Matrix compartments in the growth plate of the proximal tibia of rats. *Anat Rec.* 1985;211(3):246-257. doi:10.1002/ar.1092110304
34. Mow VC, Guo XE. Mechano-Electrochemical Properties Of Articular Cartilage: Their Inhomogeneities and Anisotropies. *Annu Rev Biomed Eng.* 2002;4(1):175-209. doi:10.1146/annurev.bioeng.4.110701.120309
35. Buckwalter J, Mow V, Ratcliffe A. Restoration of Injured or Degenerated Articular Cartilage. *J Am Acad Orthop Surg.* 1994;2(August 1994):192-201. <http://www.ncbi.nlm.nih.gov/pubmed/10709009>.
36. Buckwalter J, Mankin H. Articular cartilage repair and transplantation. *Arthritis Rheum.* 1998;41(8):1331-1342. doi:10.1002/1529-0131(199808)41:8<1331::AID-ART2>3.0.CO;2-J
37. Poole CA, Flint MH, Beaumont BW. Chondrons in cartilage: Ultrastructural analysis of the pericellular microenvironment in adult human articular cartilages. *J Orthop Res.* 1987;5(4):509-

522. doi:10.1002/jor.1100050406
38. Sympson CJ, Talhouk RS, Bissell MJ, Werb Z. The role of metalloproteinases and their inhibitors in regulating mammary epithelial morphology and function in vivo. *Perspect Drug Discov Des.* 1995;2(3):401-411. doi:10.1007/BF02172033
 39. Heinegård D, Oldberg a. Structure and biology of cartilage and bone matrix noncollagenous macromolecules. *FASEB J.* 1989;3(9):2042-2051. doi:10.1007/SpringerReference_33640
 40. Hardingham TE, Fosang AJ. Proteoglycans: many forms and many functions. *FASEB J.* 1992;6(3):861-870. doi:10.1017/CBO9781107415324.004
 41. Mow VC, Wang CC, Hung CT. The extracellular matrix, interstitial fluid and ions as a mechanical signal transducer in articular cartilage. *Osteoarthr Cartil.* 1999;7(1):41-58. doi:10.1053/joca.1998.0161
 42. Mankin HJ, Thrasher AZ. Water content and binding in normal and osteoarthritic human cartilage. *J Bone Joint Surg Am.* 1975;57(1):76-80.
 43. Ficat C, Maroudas A. Cartilage of the patella. Topographical variation of glycosaminoglycan content in normal and fibrillated tissue. *Ann Rheum Dis.* 1975;34(6):515-519. doi:10.1136/ard.34.6.515
 44. Grushko G, Schneiderman R, Maroudas A. Some biochemical and biophysical parameters for the study of the pathogenesis of osteoarthritis: A comparison between the processes of ageing and degeneration in human hip cartilage. *Connect Tissue Res.* 1989;19(2-4):149-176. doi:10.3109/03008208909043895
 45. Brocklehurst R, Bayliss MT, Maroudas A, et al. The composition of normal and osteoarthritic articular cartilage from human knee joints. *J Bone Joint Surg Am.* 1984;66(1):95-106. <http://www.ncbi.nlm.nih.gov/pubmed/6690447>.
 46. Maroudas A, Venn M. Chemical composition and swelling of normal and osteoarthrotic femoral head cartilage. II. Swelling. *Ann Rheum Dis.* 1977;36(5):399-406. doi:10.1136/ard.36.5.399
 47. Davim JP. *Biomaterials and Medical Tribology: Research and Development.*; 2013. doi:10.1533/9780857092205
 48. Pawlak Z, Petelska AD, Urbaniak W, Yusuf KQ, Oloyede A. Relationship Between Wettability and Lubrication Characteristics of the Surfaces of Contacting Phospholipid-Based Membranes. *Cell Biochem Biophys.* 2013;65(3):335-345. doi:10.1007/s12013-012-9437-z
 49. Pawlak Z, Urbaniak W, Oloyede A. The relationship between friction and wettability in aqueous environment. *Wear.* 2011;271(9-10):1745-1749. doi:10.1016/j.wear.2010.12.084
 50. Hills B a, Monds MK. Deficiency of lubricating surfactant lining the articular surfaces of replaced hips and knees. *Br J Rheumatol.* 1998;37(2):143-147. <http://www.ncbi.nlm.nih.gov/pubmed/9569068>.
 51. Jebens EH, Monk-Jones ME. On the viscosity and pH of synovial fluid and the pH of blood. *J Bone Joint Surg Br.* 1959;41-B(2):388-400.
 52. Pawlak Z, Figaszewski ZA, Gadomski A, Urbaniak W, Oloyede A. The ultra-low friction of the articular surface is pH-dependent and is built on a hydrophobic underlay including a hypothesis on joint lubrication mechanism. *Tribol Int.* 2010;43(9):1719-1725. doi:10.1016/j.triboint.2010.04.002
 53. Chen YLE, Gee ML, Helm CA, Israelachvili JN, McGuiggan PM. Effects of humidity on the structure and adhesion of amphiphilic monolayers on mica. *J Phys Chem.* 1989;93(20):7057-7059. doi:10.1021/j100357a008
 54. Burke SE, Barrett CJ. pH-responsive properties of multilayered poly(L-lysine)/hyaluronic acid surfaces. *Biomacromolecules.* 2003;4(6):1773-1783. doi:10.1021/bm034184w
 55. Chappuis J, Sherman IA, Neumann AW. Surface tension of animal cartilage as it relates to friction in joints. *Ann Biomed Eng.* 1983;11(5):435-449. doi:10.1007/BF02584218

56. Hills BA. Oligolamellar lubrication of joints by surface active phospholipid. *J Rheumatol.* 1989;16(1):82-91.
57. Horkay F. Interactions of cartilage extracellular matrix macromolecules. *J Polym Sci Part B Polym Phys.* 2012;50(24):1699-1705. doi:10.1002/polb.23191
58. Soltz MA, Ateshian GA. Experimental verification and theoretical prediction of cartilage interstitial fluid pressurization at an impermeable contact interface in confined compression. In: *Journal of Biomechanics.* Vol 31. ; 1998:927-934. doi:10.1016/S0021-9290(98)00105-5
59. Soltz MA, Ateshian GA. Interstitial Fluid Pressurization during Confined Compression Cyclical Loading of Articular Cartilage. *Ann Biomed Eng.* 2000;28(2):150-159. doi:10.1114/1.239
60. Setton LA, Zhu W, Mow VC. The biphasic poroviscoelastic behavior of articular cartilage: Role of the surface zone in governing the compressive behavior. *J Biomech.* 1993;26(4-5):581-592. doi:10.1016/0021-9290(93)90019-B
61. Ateshian GA. The role of interstitial fluid pressurization in articular cartilage lubrication. *J Biomech.* 2009;42(9):1163-1176. doi:10.1016/j.jbiomech.2009.04.040
62. Woo SLY, Mow VC, Lai WM. Biomechanical properties of articular cartilage. In: *Handbook of Engineering.* McGraw-Hil. New York; 1987.
63. Mow VC, Zhu W, Ratcliffe A. Structure and function of articular cartilage and meniscus. *Basic Orthop Biomech Raven Press New York.* 1991:143-1998.
64. Setton LA, Mow VC, Howell DS. Mechanical behavior of articular cartilage in shear is altered by transection of the anterior cruciate ligament. *J Orthop Res.* 1995;13(4):473-482. doi:10.1002/jor.1100130402
65. Jurvelin JS, Arokoski JPA, Hunziker EB, Helminen HJ. Topographical variation of the elastic properties of articular cartilage in the canine knee. *J Biomech.* 2000;33(6):669-675. doi:10.1016/S0021-9290(00)00007-5
66. Athanasiou KA, Agarwal A, Dzida FJ. Comparative study of the intrinsic mechanical properties of the human acetabular and femoral head cartilage. *J Orthop Res.* 1994;12(3):340-349. doi:10.1002/jor.1100120306
67. Athanasiou KA, Rosenwasser MP, Buckwalter JA, Malinin TI, Mow VC. Interspecies comparisons of in situ intrinsic mechanical properties of distal femoral cartilage. *J Orthop Res.* 1991;9(3):330-340. doi:10.1002/jor.1100090304
68. Kempson GE. Relationship between the tensile properties of articular cartilage from the human knee and age. *Ann Rheum Dis.* 1982;41(5):508-511. doi:10.1136/ard.41.5.508
69. Kempson GE. Age-related changes in the tensile properties of human articular cartilage: a comparative study between the femoral head of the hip joint and the talus of the ankle joint. *Biochim Biophys Acta.* 1991;1075(3):223-230. doi:10.1016/0304-4165(91)90270-Q
70. Williamson AK, Chen AC, Masuda K, Thonar EJMA, Sah RL. Tensile mechanical properties of bovine articular cartilage: Variations with growth and relationships to collagen network components. *J Orthop Res.* 2003;21(5):872-880. doi:10.1016/S0736-0266(03)00030-5
71. Kempson, G. E., Freeman, M.A.R., Swanson SAV. Tensile properties of AC. 1968;220(December):1127-1128.
72. Woo SLY, Akeson WH, Jemmott GF. Measurements of nonhomogeneous, directional mechanical properties of articular cartilage in tension. *J Biomech.* 1976;9(12):785-791. doi:10.1016/0021-9290(76)90186-X
73. Korhonen RK, Laasanen MS, Töyräs J, et al. Comparison of the equilibrium response of articular cartilage in unconfined compression, confined compression and indentation. *J Biomech.* 2002;35(7):903-909. doi:10.1016/S0021-9290(02)00052-0
74. Chan BP, Fu SC, Qin L, Rolf C, Chan KM. Pyridinoline in relation to ultimate stress of the patellar tendon during healing: An animal study. *J Orthop Res.* 1998;16(5):597-603.

doi:10.1002/jor.1100160512

75. Eleswarapu S V., Responde DJ, Athanasiou KA. Tensile properties, collagen content, and crosslinks in connective tissues of the immature knee joint. *PLoS One*. 2011;6(10). doi:10.1371/journal.pone.0026178
76. Abdurrahmanoglu S, Can V, Okay O. Design of high-toughness polyacrylamide hydrogels by hydrophobic modification. *Polymer (Guildf)*. 2009;50(23):5449-5455. doi:10.1016/j.polymer.2009.09.042
77. Stok K, Oloyede A. Conceptual fracture parameters for articular cartilage. *Clin Biomech*. 2007;22(6):725-735. doi:10.1016/j.clinbiomech.2007.03.005
78. Xiao Y, Rennerfeldt DA, Friis EA, Gehrke SH, Detamore MS. Evaluation of apparent fracture toughness of articular cartilage and hydrogels. *J Tissue Eng Regen Med*. 2017;11(1):121-128. doi:10.1002/term.1892
79. Little CJ, Bawolin NK, Chen X. Mechanical Properties of Natural Cartilage and Tissue-Engineered Constructs. *Tissue Eng Part B Rev*. 2011;17(4):213-227. doi:10.1089/ten.teb.2010.0572
80. Moore AC, Burris DL. Tribological and material properties for cartilage of and throughout the bovine stifle: Support for the altered joint kinematics hypothesis of osteoarthritis. *Osteoarthr Cartil*. 2015;23(1):161-169. doi:10.1016/j.joca.2014.09.021
81. Williamson AK, Masuda K, Thonar EJ-MA, Sah RL. Growth of Immature Articular Cartilage *in Vitro*: Correlated Variation in Tensile Biomechanical and Collagen Network Properties. *Tissue Eng*. 2003;9(4):625-634. doi:10.1089/107632703768247322
82. Mak AF, Lai WM, Mow VC. Biphasic indentation of articular cartilage-I. Theoretical analysis. *J Biomech*. 1987;20(7):703-714. doi:10.1016/0021-9290(87)90036-4
83. Jurvelin JS, Buschmann MD, Hunziker EB. Optical and mechanical determination of Poisson's ratio of adult bovine humeral articular cartilage. *J Biomech*. 1997;30(3):235-241. doi:10.1016/S0021-9290(96)00133-9
84. Armstrong CG, Mow VC. Variations in the intrinsic mechanical properties of human articular cartilage with age, degeneration, and water content. *J Bone Joint Surg Am*. 1982;64(1):88-94. <http://www.ncbi.nlm.nih.gov/pubmed/7054208>.
85. Almarza AJ, Athanasiou KA. Design characteristics for the tissue engineering of cartilaginous tissues. *Ann Biomed Eng*. 2004;32(1):2-17. doi:10.1023/B:ABME.0000007786.37957.65
86. Mansour JM. Biomechanics of cartilage. In: *Kinesiology: The Mechanics and Pathomechanics of Human Movement*. Philadelphia: Lippincott Williams and Wilkins; 2003:66-79.
87. Moroni L, De Wijn JR, Van Blitterswijk CA. 3D fiber-deposited scaffolds for tissue engineering: Influence of pores geometry and architecture on dynamic mechanical properties. *Biomaterials*. 2006;27(7):974-985. doi:10.1016/j.biomaterials.2005.07.023
88. Korhonen RK, Jurvelin JS. Compressive and tensile properties of articular cartilage in axial loading are modulated differently by osmotic environment. *Med Eng Phys*. 2010;32(2):155-160. doi:10.1016/j.medengphy.2009.11.004
89. Spirt AA, Mak AF, Wassell RP. Nonlinear viscoelastic properties of articular cartilage in shear. *J Orthop Res*. 1989;7(1):43-49. doi:10.1002/jor.1100070107
90. LeRoux MA, Guilak F, Setton LA. Compressive and shear properties of alginate gel: Effects of sodium ions and alginate concentration. *J Biomed Mater Res*. 1999;47(1):46-53. doi:10.1002/(SICI)1097-4636(199910)47:1<46::AID-JBM6>3.0.CO;2-N
91. Zhu W, Mow VC, Koob TJ, Eyre DR. Viscoelastic shear properties of articular cartilage and the effects of glycosidase treatments. *J Orthop Res*. 1993;11(6):771-781. doi:10.1002/jor.1100110602
92. Sherrer YS, Bloch DA, Mitchell DM, Young DY, Fries JF. The development of disability in

- rheumatoid arthritis. *Arthritis Rheum.* 1986;29(4):494-500. doi:10.1002/art.1780290406
93. Scott DL, Symmons DP, Coulton BL, Popert AJ. Long-term outcome of treating rheumatoid arthritis: results after 20 years. *Lancet.* 1987;1(8542):1108-1111. doi:S0140-6736(87)91672-2 [pii]
 94. Homik JE. Who's holding up the queue? Delay in treatment of rheumatoid arthritis. *J Rheumatol.* 2011;38(7):1225-1227. doi:10.3899/jrheum.110649
 95. EUMUSC. Musculoskeletal Health in Europe Report v5.0. Eur Musculoskelet Heal Surveill Information Netw [Internet]. 2014:1-13.
 96. Lundkvist J, Kastäng F, Kobelt G. The burden of rheumatoid arthritis and access to treatment: health burden and costs. *Eur J Health Econ.* 2008;8 Suppl 2:S49-60. doi:10.1007/s10198-007-0088-8
 97. By R CT. Services for people with rheumatoid arthritis.
 98. Pincus T, Callahan LF. The "side effects" of rheumatoid arthritis: Joint destruction, disability and early mortality. *Br J Rheumatol.* 1993;32(SUPPL. 1):28-37. <http://ovidsp.ovid.com/ovidweb.cgi?T=JS&CSC=Y&NEWS=N&PAGE=fulltext&D=emed3&AN=1993089038%5Cnhttp://nhs1407223.on.worldcat.org/atoztitles/link?sid=OVID:embase&id=pmid:&id=doi:&issn=0263-7103&isbn=&volume=32&issue=SUPPL.+1&spage=28&pages=28-37&date=1993&tit.>
 99. Green K. Arthritis of The Knee: Types, Symptoms, Diagnosis & Treatment. <https://hlives.com/arthritis-of-the-knee-types-symptoms-diagnosis-treatment/>. Accessed May 9, 2018.
 100. OrthoInfo. Osteoarthritis of the hip. <https://orthoinfo.aaos.org/en/diseases--conditions/osteoarthritis-of-the-hip/>. Accessed May 9, 2018.
 101. World Health Organization. The burden of musculoskeletal conditions at the start of the new millennium. *World Health Organ Tech Rep Ser.* 2003;919(i-x):1-218. doi:10.1093/ije/dyh383
 102. Murphy L, Schwartz TA, Helmick CG, et al. Lifetime risk of symptomatic knee osteoarthritis. *Arthritis Rheum.* 2008;59(9):1207-1213. doi:10.1002/art.24021
 103. Murphy LB, Helmick CG, Schwartz TA, et al. One in four people may develop symptomatic hip osteoarthritis in his or her lifetime. *Osteoarthr Cartil.* 2010;18(11):1372-1379. doi:10.1016/j.joca.2010.08.005
 104. Vos T, Flaxman AD, Naghavi M, et al. Years lived with disability (YLDs) for 1160 sequelae of 289 diseases and injuries 1990-2010: A systematic analysis for the Global Burden of Disease Study 2010. *Lancet.* 2012;380(9859):2163-2196. doi:10.1016/S0140-6736(12)61729-2
 105. Hiligsmann M, Reginster J-Y. The economic weight of osteoarthritis in Europe. *Medicographia.* 2013;35:197-202. <http://www.medicographia.com/2013/10/the-economic-weight-of-osteoarthritis-in-europe/>.
 106. Cross M, Smith E, Hoy D, et al. The global burden of hip and knee osteoarthritis: Estimates from the Global Burden of Disease 2010 study. *Ann Rheum Dis.* 2014;73(7):1323-1330. doi:10.1136/annrheumdis-2013-204763
 107. Palazzo C, Ravaud J-F, Papelard A, Ravaud P, Poiraud S. *The Burden of Musculoskeletal Conditions.*; 2014.
 108. Johnson VL, Hunter DJ. The epidemiology of osteoarthritis. *Best Pract Res Clin Rheumatol.* 2014;28(1):5-15. doi:10.1016/j.berh.2014.01.004
 109. Birtwhistle R, Morkem R, Peat G, et al. Prevalence and management of osteoarthritis in primary care: an epidemiologic cohort study from the Canadian Primary Care Sentinel Surveillance Network. *C Open.* 2015;3(3):E270-E275. doi:10.9778/cmajo.20150018
 110. Prieto-Alhambra D, Judge A, Javaid MK, Cooper C, Diez-Perez A, Arden NK. Incidence and risk factors for clinically diagnosed knee, hip and hand osteoarthritis: Influences of age, gender and

- osteoarthritis affecting other joints. *Ann Rheum Dis.* 2014;73(9):1659-1664. doi:10.1136/annrheumdis-2013-203355
111. King LK, March L, Anandacoomarasamy A. Obesity & osteoarthritis. *Indian J Med Res.* 2013;138(AUG):185-193. doi:IndianJMedRes_2013_138_2_185_117544 [pii]
 112. Maiese K. Picking a bone with WISP1 (CCN4): new strategies against degenerative joint disease. *J Transl Sci.* 2016:83-85.
 113. Slauterbeck JR, Kousa P, Clifton BC, et al. Geographic mapping of meniscus and cartilage lesions associated with anterior cruciate ligament injuries. *J Bone Joint Surg Am.* 2009;91(9):2094-2103. doi:10.2106/JBJS.H.00888
 114. O'Hara J, Rose A, Jacob I, Burke T, Walsh S. The Burden of Rheumatoid Arthritis across Europe: a socioeconomic survey. (BRASS). 2017.
 115. Zhang W, Doherty M, Arden N, et al. EULAR evidence based recommendations for the management of hip osteoarthritis: Report of a task force of the EULAR Standing Committee for International Clinical Studies Including Therapeutics (ESCISIT). *Ann Rheum Dis.* 2005;64(5):669-681. doi:10.1136/ard.2004.028886
 116. Fernandes L, Hagen KB, Bijlsma JWJ, et al. EULAR recommendations for the non-pharmacological core management of hip and knee osteoarthritis. *Ann Rheum Dis.* 2013;72(7):1125-1135. doi:10.1136/annrheumdis-2012-202745
 117. Zhang W, Nuki G, Moskowitz RW, et al. OARSI recommendations for the management of hip and knee osteoarthritis. Part III: Changes in evidence following systematic cumulative update of research published through January 2009. *Osteoarthr Cartil.* 2010;18(4):476-499. doi:10.1016/j.joca.2010.01.013
 118. Conaghan PG, Dickson J, Grant RL. Care and management of osteoarthritis in adults: summary of NICE guidance. *BMJ.* 2008;336(7642):502-503. doi:10.1136/bmj.39490.608009.AD
 119. Phillips CB, Barrett JA, Losina E, et al. Incidence rates of dislocation, pulmonary embolism, and deep infection during the first six months after elective total hip replacement. *J Bone Jt Surg - Ser A.* 2003;85(1):20-26. doi:10.2106/00004623-200301000-00004
 120. Barrett J, Losina E, Baron J a, Mahomed NN, Wright J, Katz JN. Survival following total hip replacement. *J Bone Joint Surg Am.* 2005;87(9):1965-1971. doi:10.2106/JBJS.D.02440
 121. Beddoes CM, Whitehouse MR, Briscoe WH, Su B. Hydrogels as a replacement material for damaged articular hyaline cartilage. *Materials (Basel).* 2016;9(6). doi:10.3390/ma9060443
 122. Black J, Hastings G. *Handbook of Biomaterial Properties.* London, UK: Chapman & Hall; 1998.
 123. Ramakrishna S, Mayer J, Wintermantel E, Leong KW. Biomedical applications of polymer-composite materials: A review. *Compos Sci Technol.* 2001;61(9):1189-1224. doi:10.1016/S0266-3538(00)00241-4
 124. Ridzwan MIZ, Shuib S, Hassan AY, Shokri AA, Mohammad Ibrahim MN. Problem of stress shielding and improvement to the hip implant designs: A review. *J Med Sci.* 2007;7(3):460-467. doi:10.3923/jms.2007.460.467
 125. Bos I, Willmann G. Morphologic characteristics of periprosthetic tissues from hip prostheses with ceramic-ceramic couples: A comparative histologic investigation of 18 revision and 30 autopsy cases. *Acta Orthop Scand.* 2001;72(4):335-342. doi:10.1080/000164701753541970
 126. García-Rey E, García-Cimbrelo E. Polyethylene in total hip arthroplasty: Half a century in the limelight. *J Orthop Traumatol.* 2010;11(2):67-72. doi:10.1007/s10195-010-0091-1
 127. Gudena R, Kuna S, Pradhan N. Aseptic loosening of total hip replacement presenting as an anterior thigh mass. *Musculoskelet Surg.* 2013;97(3):247-249. doi:10.1007/s12306-011-0167-y
 128. Spinarelli A, Patella V, Petrera M, Abate A, Pesce V, Patella S. Heterotopic ossification after total hip arthroplasty: Our experience. *Musculoskelet Surg.* 2011;95(1):1-5. doi:10.1007/s12306-010-0091-6

129. Schaffer a W, Pilger a, Engelhardt C, Zweymueller K, Ruediger HW. Increased blood cobalt and chromium after total hip replacement. *J Toxicol Clin Toxicol.* 1999;37(7):839-844. doi:10630267
130. Dunstan E, Sanghrajka AP, Tilley S, et al. Metal ion levels after metal-on-metal proximal femoral replacements: a 30-year follow-up. *J Bone Joint Surg Br.* 2005;87(5):628-631. doi:10.1302/0301-620X.87B5.15384
131. Jantzen C, Jørgensen HL, Duus BR, Sparring SL, Lauritzen JB. Chromium and cobalt ion concentrations in blood and serum following various types of metal-on-metal hip arthroplasties: A literature overview. *Acta Orthop.* 2013;84(3):229-236. doi:10.3109/17453674.2013.792034
132. De Boeck M, Kirsch-Volders M, Lison D. Cobalt and antimony: Genotoxicity and carcinogenicity. *Mutat Res - Fundam Mol Mech Mutagen.* 2003;533(1-2):135-152. doi:10.1016/j.mrfmmm.2003.07.012
133. Scharf B, Clement CC, Zolla V, et al. Molecular analysis of chromium and cobalt-related toxicity. *Sci Rep.* 2014;4. doi:10.1038/srep05729
134. Cohen D. Medical devices - Out of joint: The story of the ASR. *BMJ.* 2011;342(7807). doi:10.1136/bmj.d2905
135. U.S. Food and Drug Administration. Recalls, Market Withdrawals, & Safety Alerts - Stryker Initiates Voluntary Product Recall of Modular-Neck Stems Action Specific to Rejuvenate and ABG II Modular-Neck Stems. U.S. Department of Health & Human Services. <http://www.fda.gov/safety/recalls/ucm311043.htm>. Published 2012.
136. Bal BS, Garino J, Ries M, Rahaman MN. A review of ceramic bearing materials in total joint arthroplasty. *HIP Int.* 2007;17(1):21-30. doi:10.5301/HIP.2008.3092
137. Langer R, Vacanti J. Tissue engineering. *Science (80-).* 1993;260(5110):815-818. doi:10.1126/science.8493529
138. Zhao W, Jin X, Cong Y, Liu Y, Fu J. Degradable natural polymer hydrogels for articular cartilage tissue engineering. *J Chem Technol Biotechnol.* 2013;88(3):327-339. doi:10.1002/jctb.3970
139. Li H, Hu C, Yu H, Chen C. Chitosan composite scaffolds for articular cartilage defect repair: a review. *RSC Adv.* 2018;8(7):3736-3749. doi:10.1039/C7RA11593H
140. Tran SC, Cooley AJ, Elder SH. Effect of a mechanical stimulation bioreactor on tissue engineered, scaffold-free cartilage. *Biotechnol Bioeng.* 2011;108(6):1421-1429. doi:10.1002/bit.23061
141. Civinini R. Growth factors in the treatment of early osteoarthritis. *Clin Cases Miner Bone Metab.* 2013;10(1):26-29. doi:10.11138/ccmbm/2013.10.1.026
142. Ahmad Z, Howard D, Brooks RA, et al. The role of platelet rich plasma in musculoskeletal science. *JRSM Short Rep.* 2012;3(6):1-9. doi:10.1258/shorts.2011.011148
143. Nöth U, Steinert AF, Tuan RS. Technology Insight: Adult mesenchymal stem cells for osteoarthritis therapy. *Nat Clin Pract Rheumatol.* 2008;4(7):371-380. doi:10.1038/ncprheum0816
144. Rakovsky A, Marbach D, Lotan N, Lanir Y. Poly(ethylene glycol)-based hydrogels as cartilage substitutes: Synthesis and mechanical characteristics. *J Appl Polym Sci.* 2009;112(1):390-401. doi:10.1002/app.29420
145. Scholz B, Kinzelmann C, Benz K, Mollenhauer J, Wurst H, Schlosshauer B. Suppression of adverse angiogenesis in an albumin-based hydrogel for articular cartilage and intervertebral disc regeneration. *Eur Cells Mater.* 2010;20:24-37. doi:10.22203/eCM.v020a03
146. Tan H, Chu CR, Payne KA, Marra KG. Injectable in situ forming biodegradable chitosan-hyaluronic acid based hydrogels for cartilage tissue engineering. *Biomaterials.* 2009;30(13):2499-2506. doi:10.1016/j.biomaterials.2008.12.080
147. Hoemann CD, Sun J, Légaré A, McKee MD, Buschmann MD. Tissue engineering of cartilage

- using an injectable and adhesive chitosan-based cell-delivery vehicle. *Osteoarthr Cartil.* 2005;13(4):318-329. doi:10.1016/j.joca.2004.12.001
148. Park KM, Lee SY, Joung YK, Na JS, Lee MC, Park KD. Thermosensitive chitosan-Pluronic hydrogel as an injectable cell delivery carrier for cartilage regeneration. *Acta Biomater.* 2009;5(6):1956-1965. doi:10.1016/j.actbio.2009.01.040
 149. Hao T, Wen N, Cao JK, et al. The support of matrix accumulation and the promotion of sheep articular cartilage defects repair in vivo by chitosan hydrogels. *Osteoarthr Cartil.* 2010;18(2):257-265. doi:10.1016/j.joca.2009.08.007
 150. Neves SC, Moreira Teixeira LS, Moroni L, et al. Chitosan/Poly(ϵ -caprolactone) blend scaffolds for cartilage repair. *Biomaterials.* 2011;32(4):1068-1079. doi:10.1016/j.biomaterials.2010.09.073
 151. De Mori A, Fernández MP, Blunn G, Tozzi G, Roldo M. 3D printing and electrospinning of composite hydrogels for cartilage and bone tissue engineering. *Polymers (Basel).* 2018;10(3). doi:10.3390/polym10030285
 152. You F, Wu X, Zhu N, Lei M, Eames BF, Chen X. 3D Printing of Porous Cell-Laden Hydrogel Constructs for Potential Applications in Cartilage Tissue Engineering. *ACS Biomater Sci Eng.* 2016;2(7):1200-1210. doi:10.1021/acsbiomaterials.6b00258
 153. Shahin K, Doran PM. Improved seeding of chondrocytes into polyglycolic acid scaffolds using semi-static and alginate loading methods. *Biotechnol Prog.* 2011;27(1):191-200. doi:10.1002/btpr.509
 154. Wan LQ, Jiang J, Miller DE, Guo XE, Mow VC, Lu HH. Matrix Deposition Modulates the Viscoelastic Shear Properties of Hydrogel-Based Cartilage Grafts. *Tissue Eng Part A.* 2011;17(7-8):1111-1122. doi:10.1089/ten.tea.2010.0379
 155. Markstedt K, Mantas A, Tournier I, Martínez Ávila H, Hägg D, Gatenholm P. 3D bioprinting human chondrocytes with nanocellulose-alginate bioink for cartilage tissue engineering applications. *Biomacromolecules.* 2015;16(5):1489-1496. doi:10.1021/acs.biomac.5b00188
 156. Kesti M, Eberhardt C, Pagliccia G, et al. Bioprinting Complex Cartilaginous Structures with Clinically Compliant Biomaterials. *Adv Funct Mater.* 2015;25(48):7406-7417. doi:10.1002/adfm.201503423
 157. Duarte Campos DF, Drescher W, Rath B, Tingart M, Fischer H. Supporting Biomaterials for Articular Cartilage Repair. *Cartilage.* 2012;3(3):205-221. doi:10.1177/1947603512444722
 158. DeKosky BJ, Dormer NH, Ingavle GC, et al. Hierarchically Designed Agarose and Poly(Ethylene Glycol) Interpenetrating Network Hydrogels for Cartilage Tissue Engineering. *Tissue Eng Part C Methods.* 2010;16(6):1533-1542. doi:10.1089/ten.tec.2009.0761
 159. Buckley CT, Thorpe SD, O'Brien FJ, Robinson AJ, Kelly DJ. The effect of concentration, thermal history and cell seeding density on the initial mechanical properties of agarose hydrogels. *J Mech Behav Biomed Mater.* 2009;2(5):512-521. doi:10.1016/j.jmbbm.2008.12.007
 160. Kelly TAN, Ng KW, Ateshian GA, Hung CT. Analysis of radial variations in material properties and matrix composition of chondrocyte-seeded agarose hydrogel constructs. *Osteoarthr Cartil.* 2009;17(1):73-82. doi:10.1016/j.joca.2008.05.019
 161. Ng KW, Ateshian GA, Hung CT. Zonal Chondrocytes Seeded in a Layered Agarose Hydrogel Create Engineered Cartilage with Depth-Dependent Cellular and Mechanical Inhomogeneity. *Tissue Eng Part A.* 2009;15(9):2315-2324. doi:10.1089/ten.tea.2008.0391
 162. Awad HA, Wickham MQ, Leddy HA, Gimble JM, Guilak F. Chondrogenic differentiation of adipose-derived adult stem cells in agarose, alginate, and gelatin scaffolds. *Biomaterials.* 2004;25(16):3211-3222. doi:10.1016/j.biomaterials.2003.10.045
 163. Mouw JK, Case ND, Guldberg RE, Plaas AHK, Levenston ME. Variations in matrix composition and GAG fine structure among scaffolds for cartilage tissue engineering. *Osteoarthr Cartil.* 2005;13(9):828-836. doi:10.1016/j.joca.2005.04.020

164. Tan AR, Dong EY, Ateshian GA, Hung CT. Response of engineered cartilage to mechanical insult depends on construct maturity. *Osteoarthr Cartil.* 2010;18(12):1577-1585. doi:10.1016/j.joca.2010.09.003
165. Moutos FT, Freed LE, Guilak F. A biomimetic three-dimensional woven composite scaffold for functional tissue engineering of cartilage. *Nat Mater.* 2007;6(2):162-167. doi:10.1038/nmat1822
166. Jakab K, Norotte C, Marga F, Murphy K, Vunjak-Novakovic G, Forgacs G. Tissue engineering by self-assembly and bio-printing of living cells. *Biofabrication.* 2010;2(2). doi:10.1088/1758-5082/2/2/022001
167. Yoon DM, Curtiss S, Reddi a H, Fisher JP. Addition of hyaluronic acid to alginate embedded chondrocytes interferes with insulin-like growth factor-1 signaling in vitro and in vivo. *Tissue Eng Part A.* 2009;15(11):3449-3459. doi:10.1089/ten.TEA.2009.0069
168. Cohen DL, Lipton JI, Bonassar LJ, Lipson H. Additive manufacturing for in situ repair of osteochondral defects. *Biofabrication.* 2010;2(3). doi:10.1088/1758-5082/2/3/035004
169. Scholten PM, Ng KW, Joh K, et al. A semi-degradable composite scaffold for articular cartilage defects. *J Biomed Mater Res - Part A.* 2011;97 A(1):8-15. doi:10.1002/jbm.a.33005
170. Abarrategi A, López-Morales Y, Ramos V, et al. Chitosan scaffolds for osteochondral tissue regeneration. *J Biomed Mater Res - Part A.* 2010;95(4):1132-1141. doi:10.1002/jbm.a.32912
171. Chevrier A, Hoemann CD, Sun J, Buschmann MD. Temporal and spatial modulation of chondrogenic foci in subchondral microdrill holes by chitosan-glycerol phosphate/blood implants. *Osteoarthr Cartil.* 2011;19(1):136-144. doi:10.1016/j.joca.2010.10.026
172. Dorotka R, Bindreiter U, Vavken P, Nehrer S. Behavior of Human Articular Chondrocytes Derived from Nonarthritic and Osteoarthritic Cartilage in a Collagen Matrix. *Tissue Eng.* 2005;11(5-6):877-886. doi:10.1089/ten.2005.11.877
173. Lynn AK, Best SM, Cameron RE, et al. Design of a multiphase osteochondral scaffold. I. Control of chemical composition. *J Biomed Mater Res - Part A.* 2010;92(3):1057-1065. doi:10.1002/jbm.a.32415
174. Liu SQ, Tian Q, Hedrick JL, Po Hui JH, Rachel Ee PL, Yang YY. Biomimetic hydrogels for chondrogenic differentiation of human mesenchymal stem cells to neocartilage. *Biomaterials.* 2010;31(28):7298-7307. doi:10.1016/j.biomaterials.2010.06.001
175. Cao Z, Dou C, Dong S. Scaffolding biomaterials for cartilage regeneration. *J Nanomater.* 2014;2014. doi:10.1155/2014/489128
176. Harley BA, Lynn AK, Wissner-Gross Z, Bonfield W, Yannas I V., Gibson LJ. Design of a multiphase osteochondral scaffold. II. Fabrication of a mineralized collagen-glycosaminoglycan scaffold. *J Biomed Mater Res - Part A.* 2010;92(3):1066-1077. doi:10.1002/jbm.a.32361
177. Harley BA, Lynn AK, Wissner-Gross Z, Bonfield W, Yannas I V., Gibson LJ. Design of a multiphase osteochondral scaffold III: Fabrication of layered scaffolds with continuous interfaces. *J Biomed Mater Res - Part A.* 2010;92(3):1078-1093. doi:10.1002/jbm.a.32387
178. Mueller-Rath R, Gavénis K, Andereya S, et al. Condensed cellular seeded collagen gel as an improved biomaterial for tissue engineering of articular cartilage. *Biomed Mater Eng.* 2010;20(6):317-328. doi:10.3233/BME-2010-0645
179. Chen WC, Yao CL, Wei YH, Chu IM. Evaluating osteochondral defect repair potential of autologous rabbit bone marrow cells on type II collagen scaffold. *Cytotechnology.* 2011;63(1):13-23. doi:10.1007/s10616-010-9314-9
180. Chen H, Yang X, Liao Y, et al. MRI and histologic analysis of collagen type II sponge on repairing the cartilage defects of rabbit knee joints. *J Biomed Mater Res - Part B Appl Biomater.* 2011;96 B(2):267-275. doi:10.1002/jbm.b.31762
181. Ebert JR, Robertson WB, Woodhouse J, et al. Clinical and Magnetic Resonance Imaging–Based Outcomes to 5 Years After Matrix-Induced Autologous Chondrocyte Implantation to Address Articular Cartilage Defects in the Knee. *Am J Sports Med.* 2011;39(4):753-763.

doi:10.1177/0363546510390476

182. Kon E, Delcogliano M, Filardo G, Busacca M, Di Martino A, Marcacci M. Novel nano-composite multilayered biomaterial for osteochondral regeneration: A pilot clinical trial. *Am J Sports Med.* 2011;39(6):1180-1190. doi:10.1177/0363546510392711
183. Abedi G, Sotoudeh A, Soleymani M, Shafiee A, Mortazavi P, Aflatoonian MR. A collagen-poly(Vinyl Alcohol) nanofiber scaffold for cartilage repair. *J Biomater Sci Polym Ed.* 2011;22(18):2445-2455. doi:10.1163/092050610X540503
184. Peretti GM, Xu JW, Bonassar LJ, Kirchhoff CH, Yaremchuk MJ, Randolph MA. Review of injectable cartilage engineering using fibrin gel in mice and swine models. *Tissue Eng.* 2006;12(5):1151-1168. doi:10.1089/ten.2006.12.1151 [doi]
185. Haleem AM, Singergy AA EI, Sabry D, et al. The Clinical Use of Human Culture–Expanded Autologous Bone Marrow Mesenchymal Stem Cells Transplanted on Platelet-Rich Fibrin Glue in the Treatment of Articular Cartilage Defects. *Cartilage.* 2010;1(4):253-261. doi:10.1177/1947603510366027
186. Rampichová M, Filová E, Varga F, et al. Fibrin/hyaluronic acid composite hydrogels as appropriate scaffolds for in vivo artificial cartilage implantation. *ASAIO J.* 2010;56(6):563-568. doi:10.1097/MAT.0b013e3181fcb24
187. Lisignoli G, Cristino S, Piacentini A, et al. Cellular and molecular events during chondrogenesis of human mesenchymal stromal cells grown in a three-dimensional hyaluronan based scaffold. *Biomaterials.* 2005;26(28):5677-5686. doi:10.1016/j.biomaterials.2005.02.031
188. Toh WS, Lee EH, Guo XM, et al. Cartilage repair using hyaluronan hydrogel-encapsulated human embryonic stem cell-derived chondrogenic cells. *Biomaterials.* 2010;31(27):6968-6980. doi:10.1016/j.biomaterials.2010.05.064
189. Oliveira JT, Martins L, Picciochi R, et al. Gellan gum: A new biomaterial for cartilage tissue engineering applications. *J Biomed Mater Res - Part A.* 2010;93(3):852-863. doi:10.1002/jbm.a.32574
190. Werkmeister JA, Adhikari R, White JF, et al. Biodegradable and injectable cure-on-demand polyurethane scaffolds for regeneration of articular cartilage. *Acta Biomater.* 2010;6(9):3471-3481. doi:10.1016/j.actbio.2010.02.040
191. Anderson SB, Lin CC, Kuntzler D V., Anseth KS. The performance of human mesenchymal stem cells encapsulated in cell-degradable polymer-peptide hydrogels. *Biomaterials.* 2011;32(14):3564-3574. doi:10.1016/j.biomaterials.2011.01.064
192. Ibusuki S, Iwamoto Y, Matsuda T. System-engineered cartilage using poly(N-isopropylacrylamide)-grafted gelatin as in situ-formable scaffold: in vivo performance. *Tissue Eng.* 2003;9(6):1133-1142. doi:10.1089/10763270360728044
193. Park KH, Lee DH, Na K. Transplantation of poly(N-isopropylacrylamide-co-vinylimidazole) hydrogel constructs composed of rabbit chondrocytes and growth factor-loaded nanoparticles for neocartilage formation. *Biotechnol Lett.* 2009;31(3):337-346. doi:10.1007/s10529-008-9871-6
194. Capito R, Spector M. Scaffold-based articular cartilage repair. *IEEE Eng Med Biol Mag.* 2003;(September/October). http://ieeexplore.ieee.org/xpls/abs_all.jsp?arnumber=1256271.
195. Gentile P, Chiono V, Carmagnola I, Hatton P V. An overview of poly(lactic-co-glycolic) Acid (PLGA)-based biomaterials for bone tissue engineering. *Int J Mol Sci.* 2014;15(3):3640-3659. doi:10.3390/ijms15033640
196. Liu Y, Zhou G, Cao Y. Recent Progress in Cartilage Tissue Engineering—Our Experience and Future Directions. *Engineering.* 2017;3:28-35. doi:10.1016/J.ENG.2017.01.010
197. Charlton DC, Peterson MGE, Spiller K, Lowman A, Torzilli PA, Maher SA. Semi-Degradable Scaffold for Articular Cartilage Replacement. *Tissue Eng Part A.* 2008;14(1):207-213. doi:10.1089/ten.a.2006.0344

198. Tanaka Y, Yamaoka H, Nishizawa S, et al. The optimization of porous polymeric scaffolds for chondrocyte/atelocollagen based tissue-engineered cartilage. *Biomaterials*. 2010;31(16):4506-4516. doi:10.1016/j.biomaterials.2010.02.028
199. Cui W, Wang Q, Chen G, et al. Repair of articular cartilage defects with tissue-engineered osteochondral composites in pigs. *J Biosci Bioeng*. 2011;111(4):493-500. doi:10.1016/j.jbiosc.2010.11.023
200. Pan Z, Ding J. Poly(lactide-co-glycolide) porous scaffolds for tissue engineering and regenerative medicine. *Interface Focus*. 2012;2(3):366-377. doi:10.1098/rsfs.2011.0123
201. Grad S, Kupcsik L, Gorna K, Gogolewski S, Alini M. The use of biodegradable polyurethane scaffolds for cartilage tissue engineering: Potential and limitations. *Biomaterials*. 2003;24(28):5163-5171. doi:10.1016/S0142-9612(03)00462-9
202. Bodugoz-Senturk H, Macias CE, Kung JH, Muratoglu OK. Poly(vinyl alcohol)-acrylamide hydrogels as load-bearing cartilage substitute. *Biomaterials*. 2009;30(4):589-596. doi:10.1016/j.biomaterials.2008.10.010
203. Mohan N, Nair PD, Tabata Y. Growth factor-mediated effects on chondrogenic differentiation of mesenchymal stem cells in 3D semi-IPN poly(vinyl alcohol)-poly(caprolactone) scaffolds. *J Biomed Mater Res - Part A*. 2010;94(1):146-159. doi:10.1002/jbm.a.32680
204. Kobayashi M, Hyu HS. Development and evaluation of polyvinyl alcohol-hydrogels as an artificial articular cartilage for orthopedic implants. *Materials (Basel)*. 2010;3(4):2753-2771. doi:10.3390/ma3042753
205. Razzak MT, Darwis D, Zainuddin, Sukirno. Irradiation of polyvinyl alcohol and polyvinyl pyrrolidone blended hydrogel for wound dressing. *Radiat Phys Chem*. 2001;62(1):107-113. doi:10.1016/S0969-806X(01)00427-3
206. Tubbs RK. Sequence Distribution of Partially Hydrolyzed Poly(vinyl acetate). *J Polym Sci Part A-1 Polym Chem*. 1966;4(3):623-629. doi:10.1002/pol.1966.150040316
207. Jones J. Polyvinyl alcohol. Properties and applications. In: Finch C, ed. *Polymer International*. Chichester: John Wiley; 1973.
208. Peppas NA. *Hydrogels in Medicine and Pharmacy*. Boca Raton: CRC Press; 1989.
209. Bray JC, Merrill EW. Poly(vinyl alcohol) hydrogels for synthetic articular cartilage material. *J Biomed Mater Res*. 1973;7(5):431-443. doi:10.1002/jbm.820070506
210. Thomas BH, Craig Fryman J, Liu K, Mason J. Hydrophilic-hydrophobic hydrogels for cartilage replacement. *J Mech Behav Biomed Mater*. 2009;2(6):588-595. doi:10.1016/j.jmbbm.2008.08.001
211. Katta JK, Marcolongo M, Lowman A, Mansmann KA. Friction and wear behavior of poly(vinyl alcohol)/poly(vinyl pyrrolidone) hydrogels for articular cartilage replacement. *J Biomed Mater Res - Part A*. 2007;83(2):471-479. doi:10.1002/jbm.a.31238
212. Holloway JL, Lowman AM, Palmese GR. The role of crystallization and phase separation in the formation of physically cross-linked PVA hydrogels. *Soft Matter*. 2013;9(3):826-833. doi:10.1039/C2SM26763B
213. Yaping Hou, Junli Hu HP and ML. *J Biomed Mater Res A. Growth (Lakeland)*. 2012;100(1):1-7. doi:doi:10.1002/jbm.a.34031
214. Zabska M, Jaskiewicz K, Kiersnowski A, Szustakiewicz K, Rathgeber S, Piglowski J. Spontaneous exfoliation and self-assembly phenomena in polyvinylpyrrolidone/synthetic layered silicate nanocomposites. *Radiat Phys Chem*. 2011;80(10):1125-1128. doi:10.1016/j.radphyschem.2011.02.019
215. Schmalz G, Arenholt-Bindslev D. *Biocompatibility of Dental Materials*.; 2009. doi:10.1007/978-3-540-77782-3
216. Heris HK, Latifi N, Vali H, Li N, Mongeau L. Investigation of Chitosan-glycol/glyoxal as an

- injectable biomaterial for vocal fold tissue engineering. In: *Procedia Engineering*. Vol 110. ; 2015:143-150. doi:10.1016/j.proeng.2015.07.022
217. Wang L, Stegemann JP. Glyoxal crosslinking of cell-seeded chitosan/collagen hydrogels for bone regeneration. *Acta Biomater*. 2011;7(6):2410-2417. doi:10.1016/j.actbio.2011.02.029
 218. Duong H Van, Chau TTL, Dang NTT, et al. Biocompatible Chitosan-Functionalized Upconverting Nanocomposites. *ACS Omega*. 2018;3(1):86-95. doi:10.1021/acsomega.7b01355
 219. Zhang Y, Zhu PC, Edgren D. Crosslinking reaction of poly(vinyl alcohol) with glyoxal. *J Polym Res*. 2010;17(5):725-730. doi:10.1007/s10965-009-9362-z
 220. Stammen JA, Williams S, Ku DN, Gulberg RE. Mechanical properties of a novel PVA hydrogel in shear and unconfined compression. *Biomaterials*. 2001;22(8):799-806. doi:10.1016/S0142-9612(00)00242-8
 221. Ku D, Braddon L, Wootton D. Poly(vinyl alcohol) cryogel. 1999.
 222. Cartiva FAQ. www.cartiva.com. Accessed May 2, 2018.
 223. Cartiva: Other Indications. <https://www.cartiva.net/Home/OtherIndications>. Accessed May 2, 2018.
 224. Sciarretta F V. 5 to 8 years follow-up of knee chondral defects treated by PVA-H hydrogel implants. *Eur Rev Med Pharmacol Sci*. 2013;17(22):3031-3038.
 225. Sasaki S, Murakami T, Suzuki A. Frictional properties of physically cross-linked PVA hydrogels as artificial cartilage. *Biosurface and Biotribology*. 2016;2(1):11-17. doi:10.1016/j.bsbt.2016.02.002
 226. Yarimitsu S, Sasaki S, Murakami T, Suzuki A. Evaluation of lubrication properties of hydrogel artificial cartilage materials for joint prosthesis. *Biosurface and Biotribology*. 2016;2(1):40-47. doi:10.1016/j.bsbt.2016.02.005
 227. Omata S, Sawae Y, Murakami T. Effect of poly(vinyl alcohol) (PVA) wear particles generated in water lubricant on immune response of macrophage. *Biosurface and Biotribology*. 2015;1(1):71-79. doi:10.1016/j.bsbt.2015.02.003
 228. Conte A, Buonocore GG, Bevilacqua A, Sinigaglia M, Del Nobile MA. Immobilization of lysozyme on polyvinylalcohol films for active packaging applications. *J Food Prot*. 2006;69(4):866-870. doi:10.4315/0362-028X-69.4.866
 229. Mandal A, Chakrabarty D. Synthesis and characterization of nanocellulose reinforced full-interpenetrating polymer network based on poly(vinyl alcohol) and polyacrylamide (both crosslinked) composite films. *Polym Compos*. 2017;38(8):1720-1731. doi:10.1002/pc.23742
 230. Sasaki S, Suzuki A. A Novel Method to Control the Elution Behavior of PVA Cast Gels. In: *Macromolecular Symposia*. Vol 358. ; 2015:170-175. doi:10.1002/masy.201500058
 231. Kruss. Captive Bubble Method. <https://www.kruss-scientific.com/services/education-theory/glossary/captive-bubble-method/>. Accessed May 9, 2018.
 232. Guirguis OW, Moselhey MTH. Thermal and structural studies of poly (vinyl alcohol) and hydroxypropyl cellulose blends. *Nat Sci*. 2012;04(01):57-67. doi:10.4236/ns.2012.41009
 233. Kenawy ER, Kamoun EA, Mohy Eldin MS, El-Meligy MA. Physically crosslinked poly(vinyl alcohol)-hydroxyethyl starch blend hydrogel membranes: Synthesis and characterization for biomedical applications. *Arab J Chem*. 2014;7(3):372-380. doi:10.1016/j.arabjc.2013.05.026
 234. Peng Z, Kong LX. A thermal degradation mechanism of polyvinyl alcohol/silica nanocomposites. *Polym Degrad Stab*. 2007;92(6):1061-1071. doi:10.1016/j.polymdegradstab.2007.02.012
 235. Peppas NA, Merrill EW. Differential scanning calorimetry of crystallized PVA hydrogels. *J Appl Polym Sci*. 1976;20(6):1457-1465. doi:10.1002/app.1976.070200604
 236. Xu J, Hammouda B, Cao F, Yang B. Experimental study of thermophysical properties and

- nanostructure of self-assembled water/polyalphaolefin nanoemulsion fluids. *Adv Mech Eng.* 2015;7(4):1-8. doi:10.1177/1687814015581269
237. Crispim EG, Piai JF, Fajardo AR, et al. Hydrogels based on chemically modified poly(vinyl alcohol) (PVA-GMA) and PVA-GMA/chondroitin sulfate: Preparation and characterization. *Express Polym Lett.* 2012;6(5):383-395. doi:10.3144/expresspolymlett.2012.41
 238. Darwis D, Yoshii F, Makuuchi K, Razzak MT. Improvement of hot water resistance of poly(vinyl alcohol) hydrogel by acetalization and irradiation techniques. *J Appl Polym Sci.* 1995;55(12):1619-1625. doi:10.1002/app.1995.070551202
 239. Caló E, Barros JMS de, Fernández-Gutiérrez M, San Román J, Ballamy L, Khutoryanskiy V V. Antimicrobial hydrogels based on autoclaved poly(vinyl alcohol) and poly(methyl vinyl ether-alt-maleic anhydride) mixtures for wound care applications. *RSC Adv.* 2016;6(60):55211-55219. doi:10.1039/C6RA08234C
 240. Shi Y, Xiong D, Zhang J. Effect of irradiation dose on mechanical and biotribological properties of PVA/PVP hydrogels as articular cartilage. *Tribol Int.* 2014;78:60-67. doi:10.1016/j.triboint.2014.05.001
 241. Varshney L. Role of natural polysaccharides in radiation formation of PVA-hydrogel wound dressing. *Nucl Instruments Methods Phys Res Sect B Beam Interact with Mater Atoms.* 2007;255(2):343-349. doi:10.1016/j.nimb.2006.11.101
 242. Miranda LF, Lugão AB, Machado LDB, Ramanathan L V. Crosslinking and degradation of PVP hydrogels as a function of dose and PVP concentration. In: *Radiation Physics and Chemistry.* Vol 55. ; 1999:709-712. doi:10.1016/S0969-806X(99)00216-9
 243. Hill DJT, Lim MCH, Whittaker AK. Water diffusion in hydroxyethyl methacrylate (HEMA)-based hydrogels formed by gamma-radiolysis. *Polym Int.* 1999;48(10):1046-1052. doi:10.1002/(SICI)1097-0126(199910)48:10<1046::AID-PI267>3.0.CO;2-W
 244. Holloway JL, Spiller KL, Lowman AM, Palmese GR. Analysis of the in vitro swelling behavior of poly(vinyl alcohol) hydrogels in osmotic pressure solution for soft tissue replacement. *Acta Biomater.* 2011;7(6):2477-2482. doi:10.1016/j.actbio.2011.02.016
 245. He G, Zheng H, Xiong F. Preparation and swelling behavior of physically crosslinked hydrogels composed of poly(vinyl alcohol) and chitosan. *J Wuhan Univ Technol Mater Sci Ed.* 2008;23(6):816-820. doi:10.1007/s11595-007-6816-1
 246. Shi Y, Xiong D, Liu Y, Wang N, Zhao X. Swelling, mechanical and friction properties of PVA/PVP hydrogels after swelling in osmotic pressure solution. *Mater Sci Eng C.* 2016;65:172-180. doi:10.1016/j.msec.2016.04.042
 247. Kim SJ, Yoon SG, Lee YM, Kim HC, Kim SI. Electrical behavior of polymer hydrogel composed of poly(vinyl alcohol)-hyaluronic acid in solution. *Biosens Bioelectron.* 2004;19(6):531-536. doi:10.1016/S0956-5663(03)00277-X
 248. Cha W-I, Hyon S-H, Oka M, Ikada Y. Mechanical and wear properties of poly(vinyl alcohol) hydrogels. In: *Macromol. Symp.* ; 1996:115-126.
 249. Bhosale AM, Richardson JB. Articular cartilage: Structure, injuries and review of management. *Br Med Bull.* 2008;87(1):77-95. doi:10.1093/bmb/ldn025
 250. Thomas J, Lowman A, Marcolongo M. Novel associated hydrogels for nucleus pulposus replacement. *J Biomed Mater Res.* 2003;67A(4):1329-1337. doi:10.1002/jbm.a.10119
 251. Maitra J, Shukla VK. Cross-linking in Hydrogels - A Review. *Am J Polym Sci.* 2014;4(2):25-31. doi:10.5923/j.ajps.20140402.01
 252. Xu H, Matysiak S. Effect of pH on chitosan hydrogel polymer network structure. *Chem Commun Chem Commun.* 2017;53(53):7373-7376. doi:10.1039/c7cc01826f
 253. O'Grady NP, Barie PS, Bartlett JG, et al. Guidelines for evaluation of new fever in critically ill adult patients: 2008 Update from the American College of Critical Care Medicine and the Infectious Diseases Society of America. *Crit Care Med.* 2008;36(4):1330-1349.

doi:10.1097/CCM.0b013e318169eda9

254. Walter EJ, Hanna-Jumma S, Carraretto M, Forni L. The pathophysiological basis and consequences of fever. *Crit Care*. 2016;20(1). doi:10.1186/s13054-016-1375-5
255. Keane NP, Ellis FR. Malignant Hyperpyrexia. *Br Med J*. 1971;4(5778):49. doi:10.1136/bmj.4.5778.49-a
256. Hassan CM, Trakampan P, Peppas NA. Water solubility characteristic of poly(vinyl alcohol) and gels prepared by freezing/thawing processes. In: *Water Soluble Polymers*. Boston, MA: Springer; 2002:31-40. doi:https://doi.org/10.1007/0-306-46915-4_3
257. Maher SA, Doty SB, Torzilli PA, et al. Nondegradable hydrogels for the treatment of focal cartilage defects. *J Biomed Mater Res - Part A*. 2007;83(1):145-155. doi:10.1002/jbm.a.31255
258. Lilge I. *Polymer Brush Films with Varied Grafting and Cross-Linking Density via SI-ATRP*. Springer Spektrum; 2017. doi:10.1007/978-3-658-19595-3
259. Lilge I, Schönherr H. Covalently cross-linked poly(acrylamide) brushes on gold with tunable mechanical properties via surface-initiated atom transfer radical polymerization. In: *European Polymer Journal*. Vol 49. ; 2013:1943-1951. doi:10.1016/j.eurpolymj.2013.02.023
260. Vidović E, Klee D, Höcker H. Biodegradable hydrogels based on poly(vinyl alcohol)-graft-[poly(D, L-lactide)/poly(D, L-lactide-co-glycolide)].
261. Wu J, Wei W, Zhao S, Sun M, Wang J. Fabrication of highly underwater oleophobic textiles through poly(vinyl alcohol) crosslinking for oil/water separation: the effect of surface wettability and textile type. *J Mater Sci*. 2017;52(2):1194-1202. doi:10.1007/s10853-016-0415-5
262. R, Jonhson , Dettre H. Contact Angle Hysteresis. 111. Study of an Idealized Heterogeneous Surface. *Contact Angle Hysteresis*. 1963;107(43):1744-1750.
263. Schwartz LW, Garoff S. Contact angle hysteresis on heterogeneous surfaces. *Langmuir*. 1985;1(2):219-230. doi:10.1021/la00062a007
264. Joanny JF, De Gennes PG. A model for contact angle hysteresis. *J Chem Phys*. 1984;81(1):552-562. doi:10.1063/1.447337
265. Krumpfer JW, McCarthy TJ. Contact angle hysteresis: a different view and a trivial recipe for low hysteresis hydrophobic surfaces. *Faraday Discuss*. 2010;146:103. doi:10.1039/b925045j
266. Gao L, McCarthy TJ. Contact angle hysteresis explained. *Langmuir*. 2006;22(14):6234-6237. doi:10.1021/la060254j
267. Nguyen NT, Liu JH. Fabrication and characterization of poly(vinyl alcohol)/chitosan hydrogel thin films via UV irradiation. *Eur Polym J*. 2013;49(12):4201-4211. doi:10.1016/j.eurpolymj.2013.09.032
268. Hwang M-R, Kim JO, Lee JH, et al. Gentamicin-Loaded Wound Dressing With Polyvinyl Alcohol/Dextran Hydrogel: Gel Characterization and In Vivo Healing Evaluation. *AAPS PharmSciTech*. 2010;11(3):1092-1103. doi:10.1208/s12249-010-9474-0
269. Ling D, Bodugoz-Senturk H, Nanda S, Braithwaite G, Muratoglu OK. Quantifying the lubricity of mechanically tough polyvinyl alcohol hydrogels for cartilage repair. *Proc Inst Mech Eng Part H J Eng Med*. 2015;229(12):845-852. doi:10.1177/0954411915599016
270. Novotny PM. Toughness Index for alloy comparisons. *Adv Mater Process*. 2007.
271. Depalle B, Qin Z, Shefelbine SJ, Buehler MJ. Influence of cross-link structure, density and mechanical properties in the mesoscale deformation mechanisms of collagen fibrils. *J Mech Behav Biomed Mater*. 2015;52:1-13. doi:10.1016/j.jmbbm.2014.07.008
272. Lakshmikantha MR, Prat PC, Tapia J, Ledesma A. Effect of moisture content on tensile strength and fracture toughness of a silty soil. In: *Unsaturated Soils: Advances in Geo-Engineering - Proceedings of the 1st European Conference on Unsaturated Soils, E-UNSAT 2008*. ; 2008:405-409.

273. Ohshima H. *Encyclopedia of Biocolloid and Biointerface Science, 2 Volume Set*. Wiley; 2016.
274. Sasaki S, Murakami T, Suzuki A. Frictional properties of physically cross-linked PVA hydrogels as artificial cartilage. *Biosurface and Biotribology*. 2016.
275. Li J, Wang Q, Zhongmin J, Williams S, Fisher J, Wilcox R. The Importance of Tension-Compression Nonlinearity in a Biphasic Hip Model: A Comparison to Experiment. *ORS 2014 Annu Meet*. 2014.
276. Tubbs RK. Melting point and heat of fusion of poly(vinyl alcohol). *J Polym Sci Part A-1 Polym Chem*. 1965;3:4181-4189.
277. Wilkes CE. *PVC Handbook*. Hanser Verlag; 2005.
278. Stavropoulou A, Papadokostaki KG, Sanopoulou M. Thermal properties of poly(vinyl alcohol)-solute blends studied by TMDSC. *J Appl Polym Sci*. 2004;93(3):1151-1156. doi:10.1002/app.20559
279. Gupta S, Pramanik AK, Kailath A, et al. Composition dependent structural modulations in transparent poly(vinyl alcohol) hydrogels. *Colloids Surfaces B Biointerfaces*. 2009;74(1):186-190. doi:10.1016/j.colsurfb.2009.07.015
280. Schanuel FS, Raggio Santos KS, Monte-Alto-Costa A, de Oliveira MG. Combined nitric oxide-releasing poly(vinyl alcohol) film/F127 hydrogel for accelerating wound healing. *Colloids Surfaces B Biointerfaces*. 2015;130:182-191. doi:10.1016/j.colsurfb.2015.04.007
281. Ezhari S, Aserin A, Garti N. Investigation of amphiphilic systems by sub-zero temperature differential scanning calorimetry. In: Mittal K, Shah DO, eds. *Adsorption and Aggregation of Surfactants in Solution*. ; 2002.
282. Instruments T. Thermal Analysis to Determine Various Forms of Water Present in Hydrogels. <http://www.tainstruments.com/pdf/literature/TA384.pdf>. Accessed May 4, 2018.

8. ANNEXES

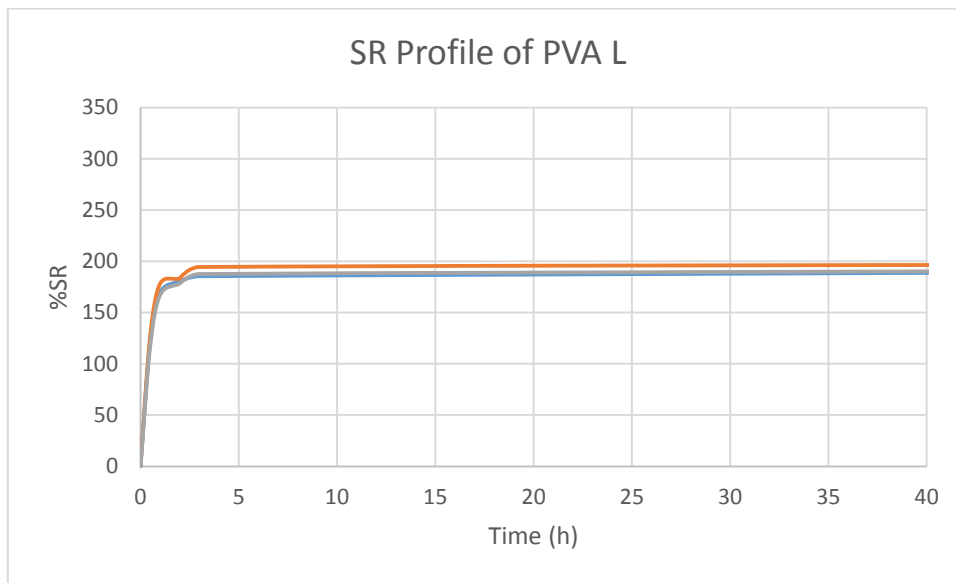


Figure 44: SR Profile of PVA L.

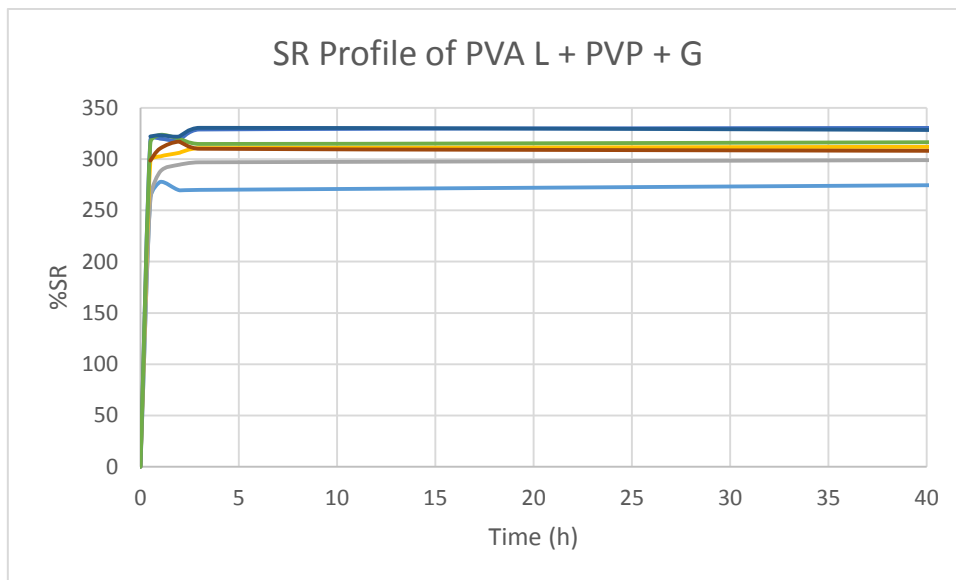


Figure 45: SR Profile of PVA L + PVP.

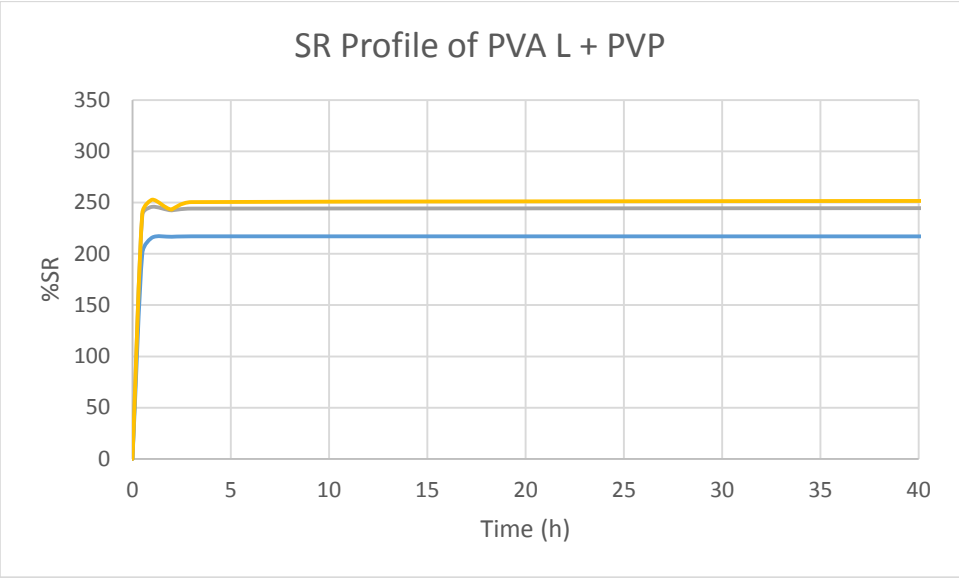


Figure 46: SR Profile of PVA L + PVP + G.

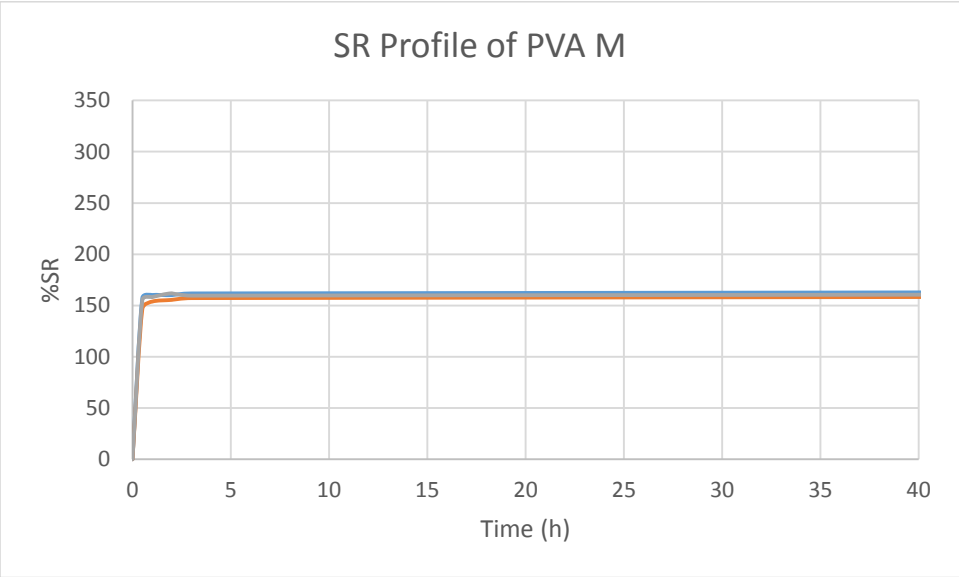


Figure 47: SR Profile of PVA M.

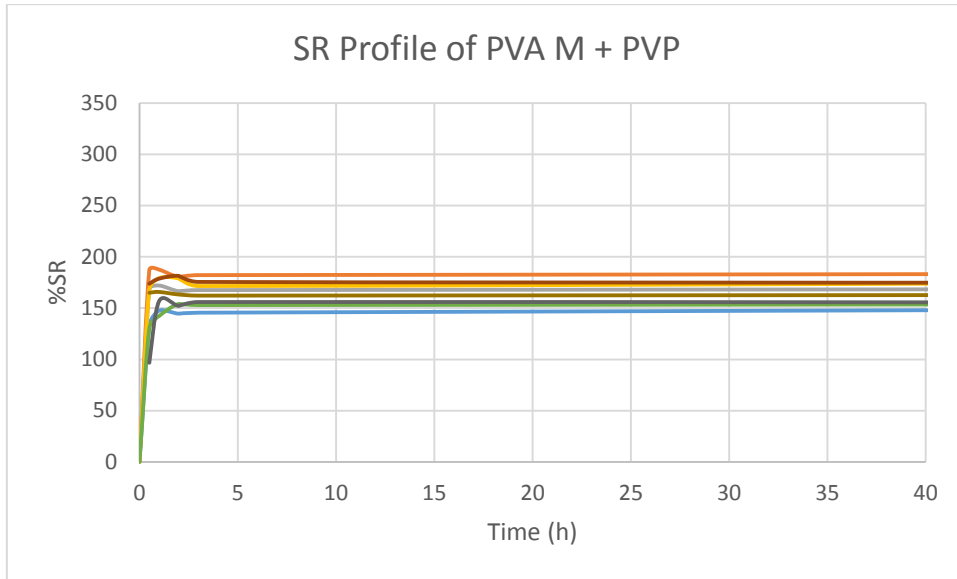


Figure 48: SR Profile of PVA M + PVP.

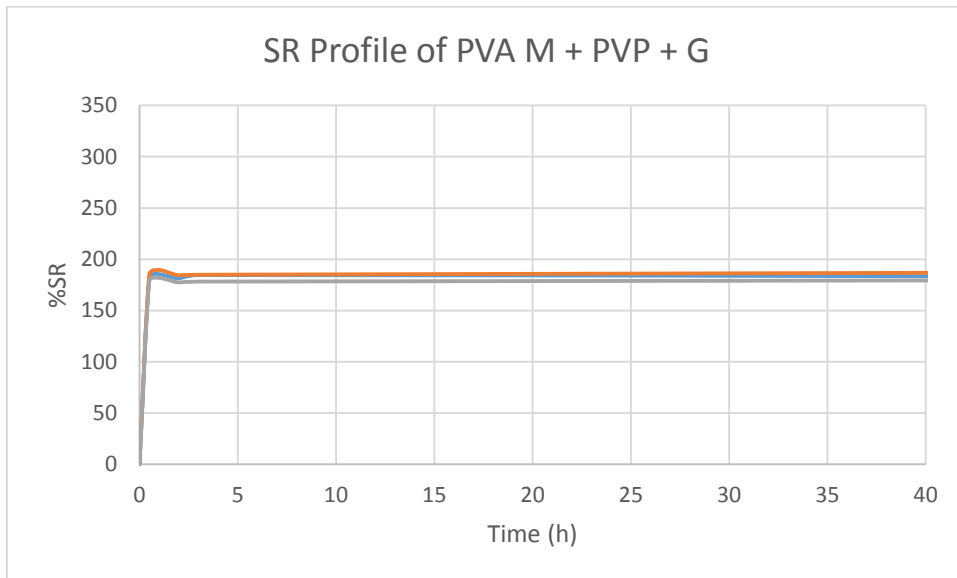


Figure 49: SR Profile of PVA M + PVP + G.

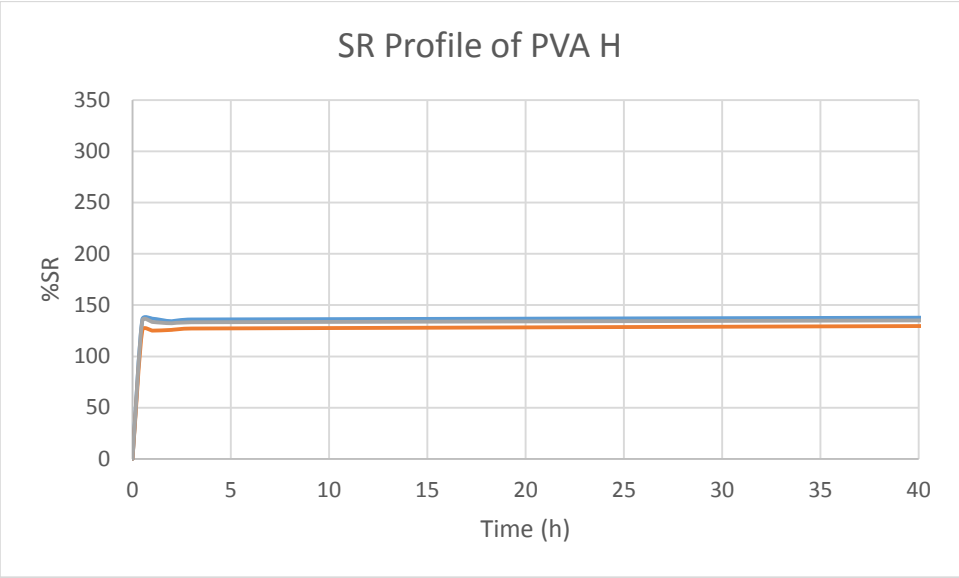


Figure 50: SR Profile of PVA H.

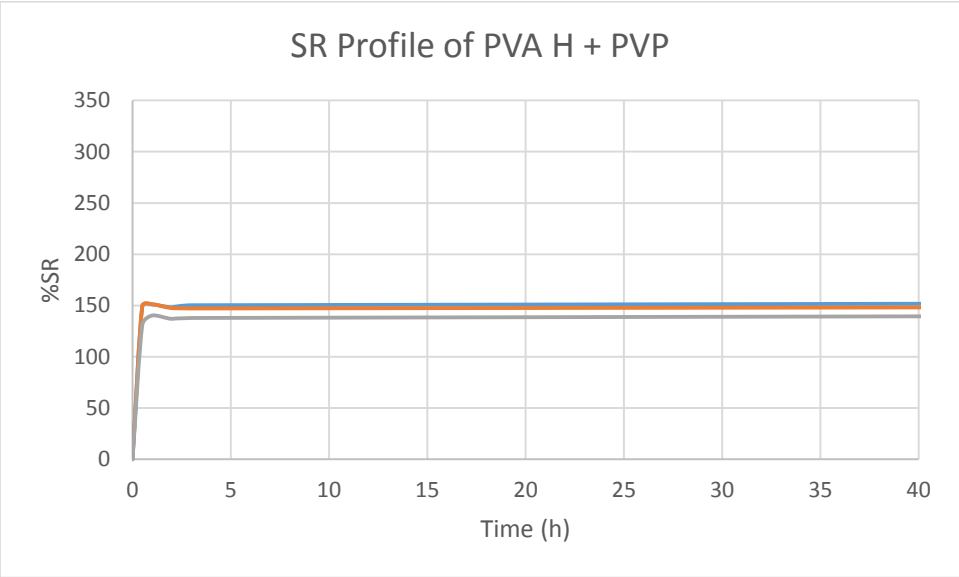


Figure 51: SR Profile of PVA H + PVP.

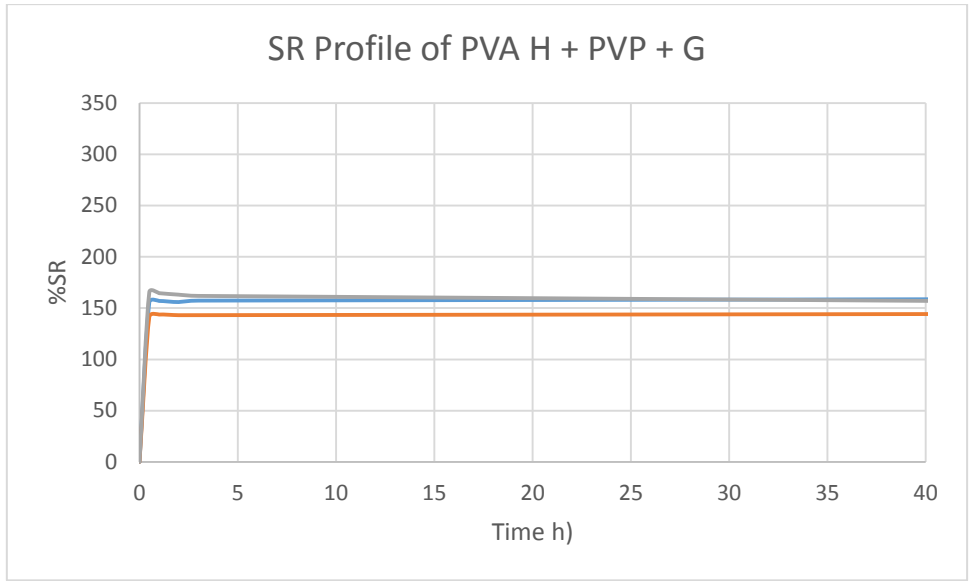


Figure 52: SR Profile of PVA H + PVP + G.

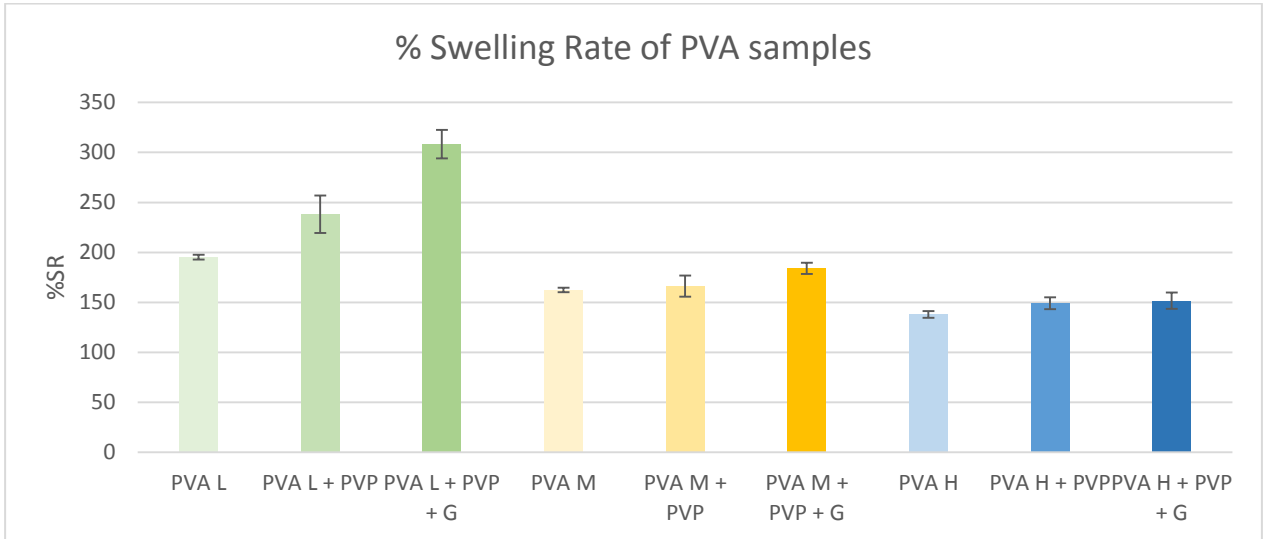


Figure 53: Visual representation of the average %SR of PVA hydrogels.

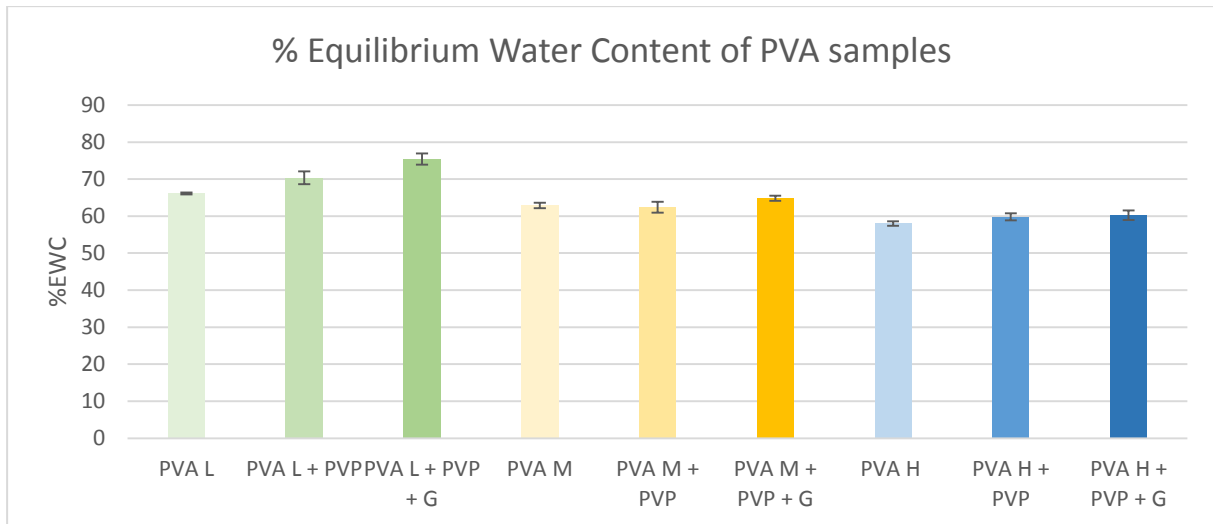


Figure 54: Visual representation of the average %EWC of PVA hydrogels.

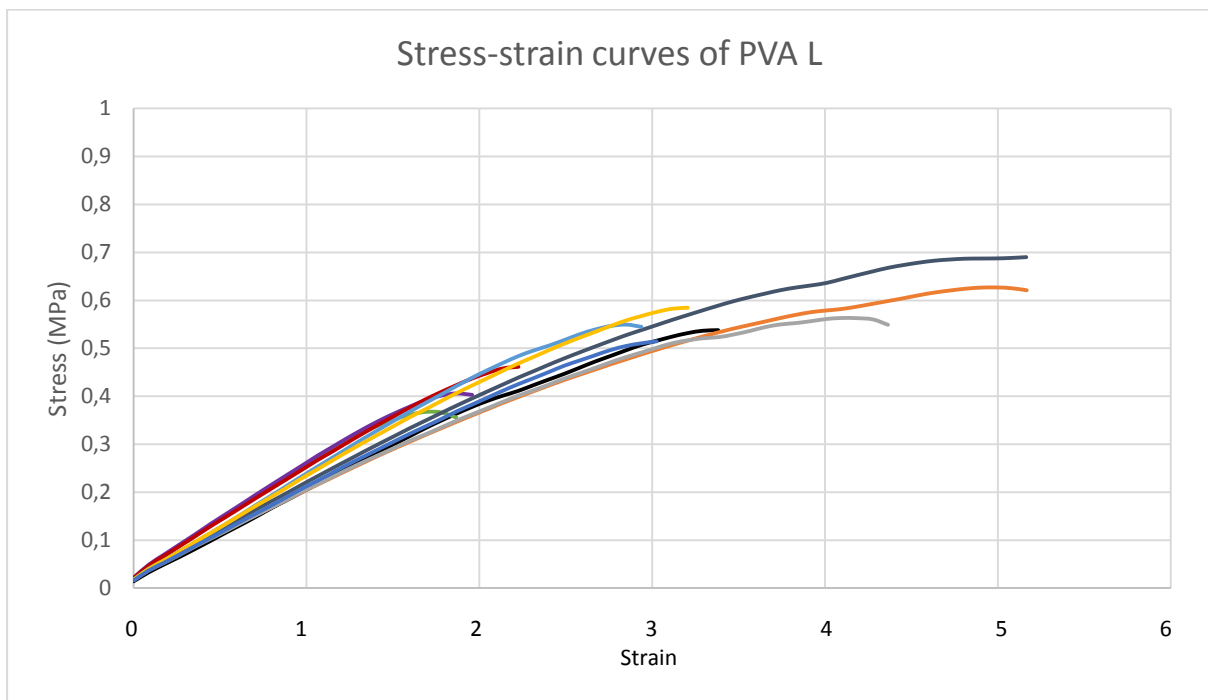


Figure 55: Tensile stress-strain curves of PVA L.

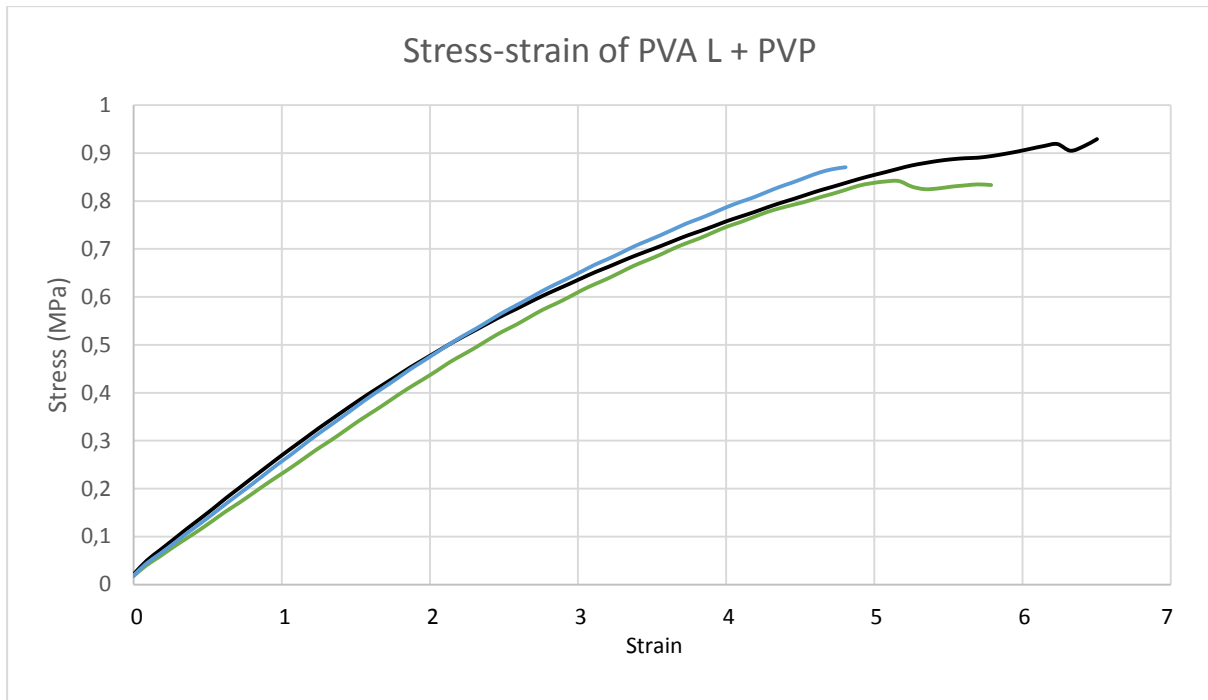


Figure 56: Tensile stress-strain curves of PVA L + PVP.

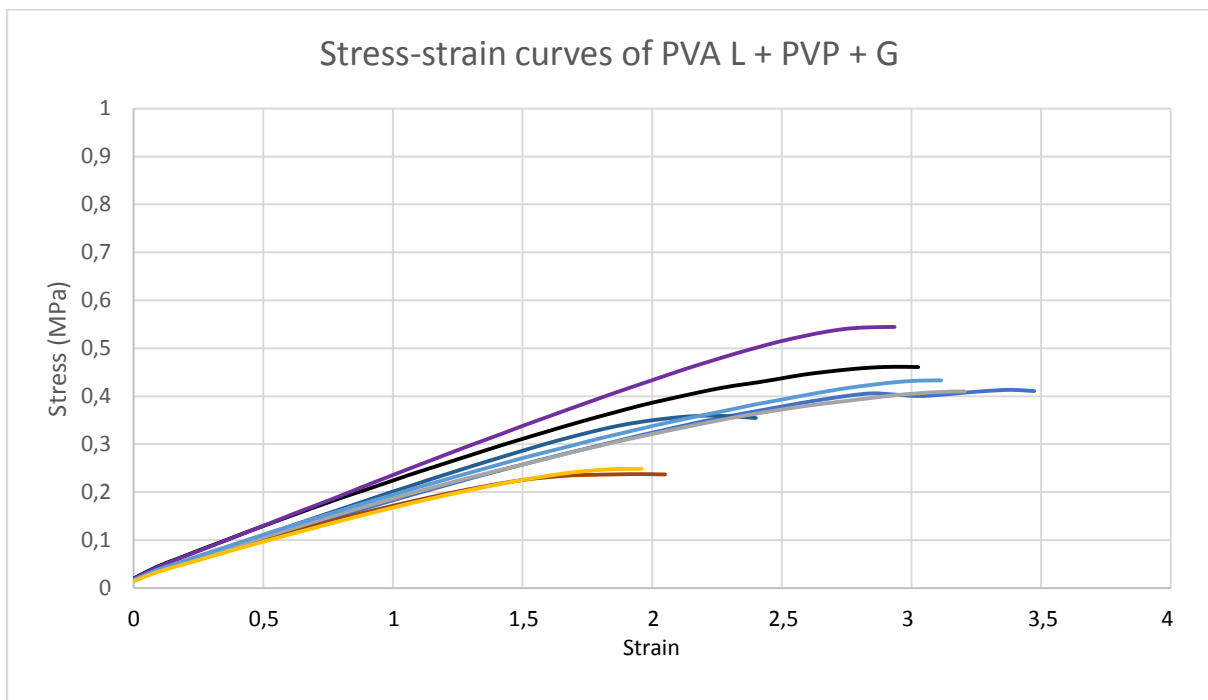


Figure 57: Tensile stress-strain curves of PVA L + PVP + G.

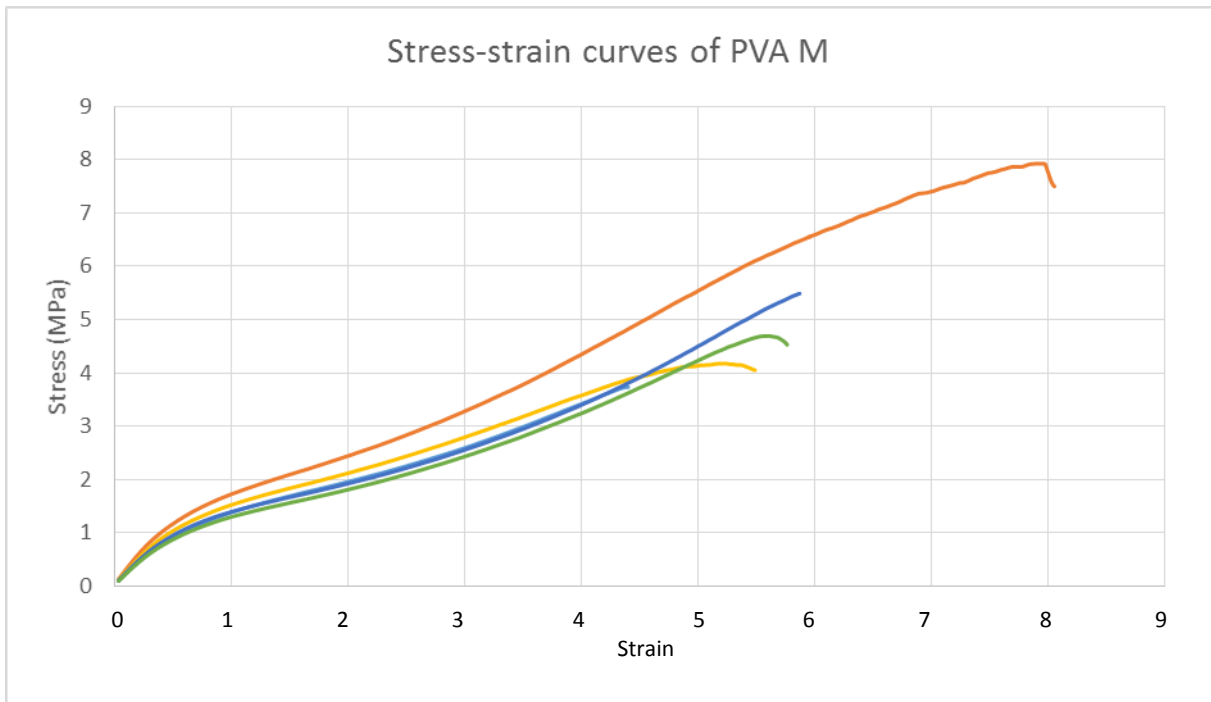


Figure 58: Tensile stress-strain curves of PVA M.

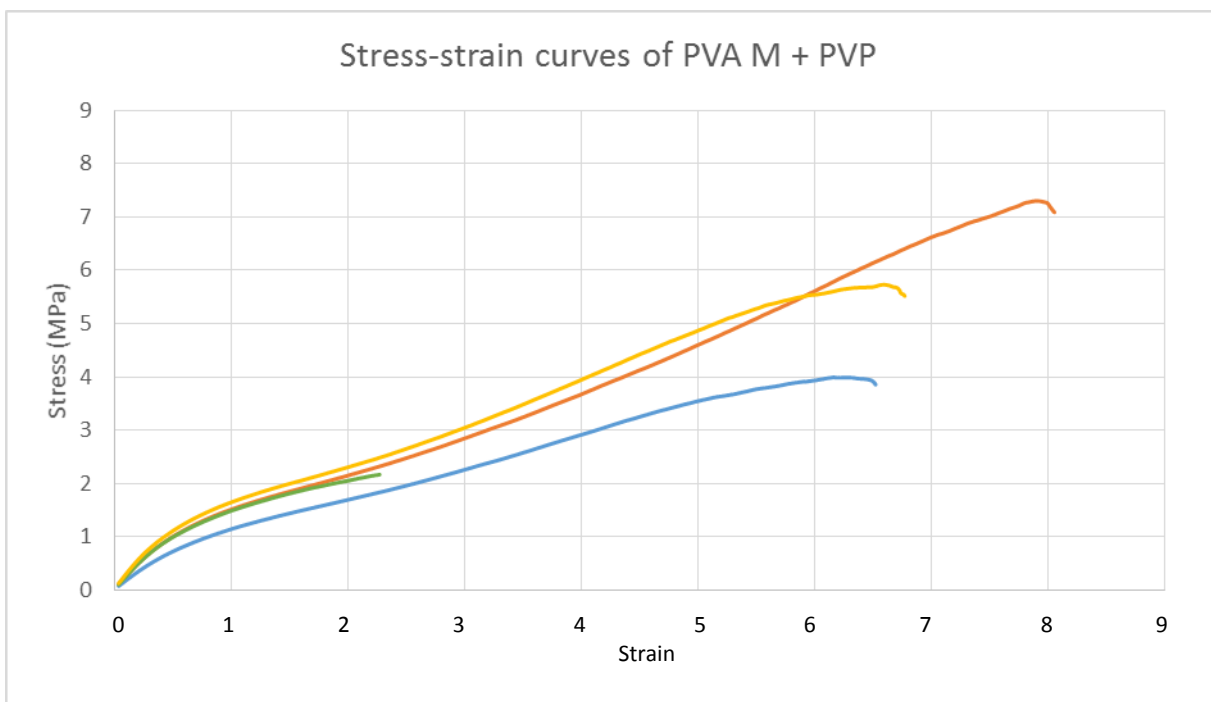


Figure 59: Tensile stress-strain curves of PVA M + PVP.

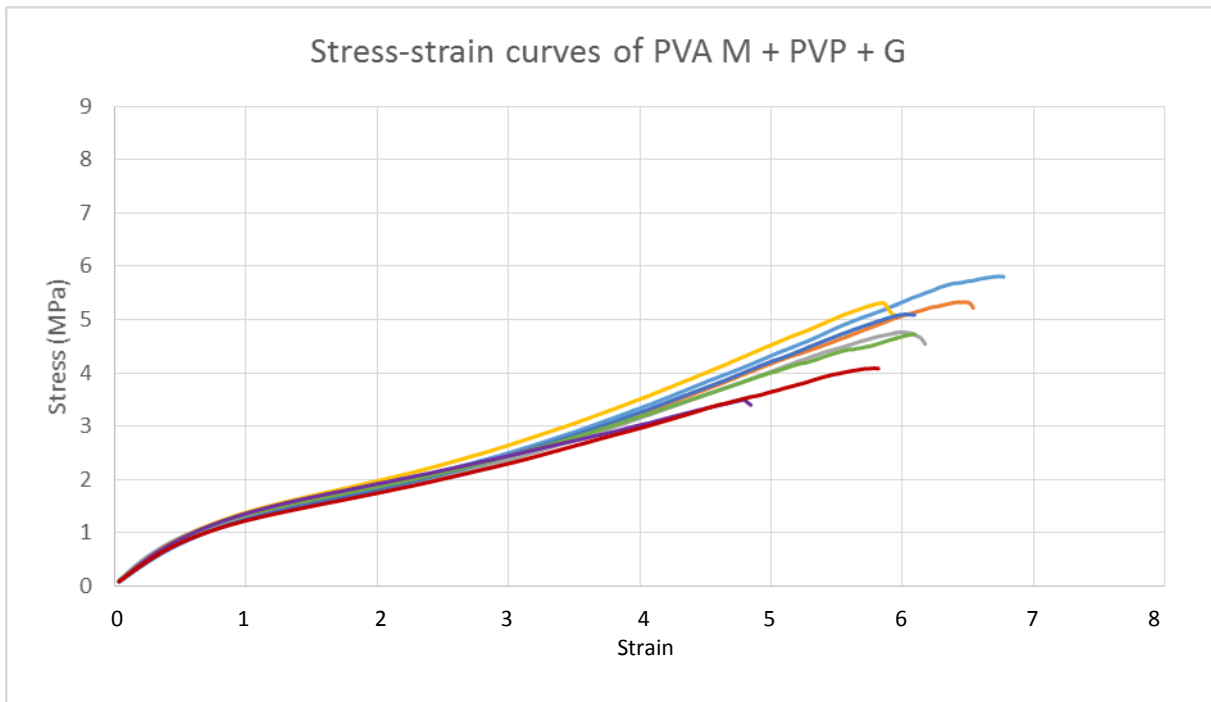


Figure 60: Tensile stress-strain curves of PVA M + PVP + G.

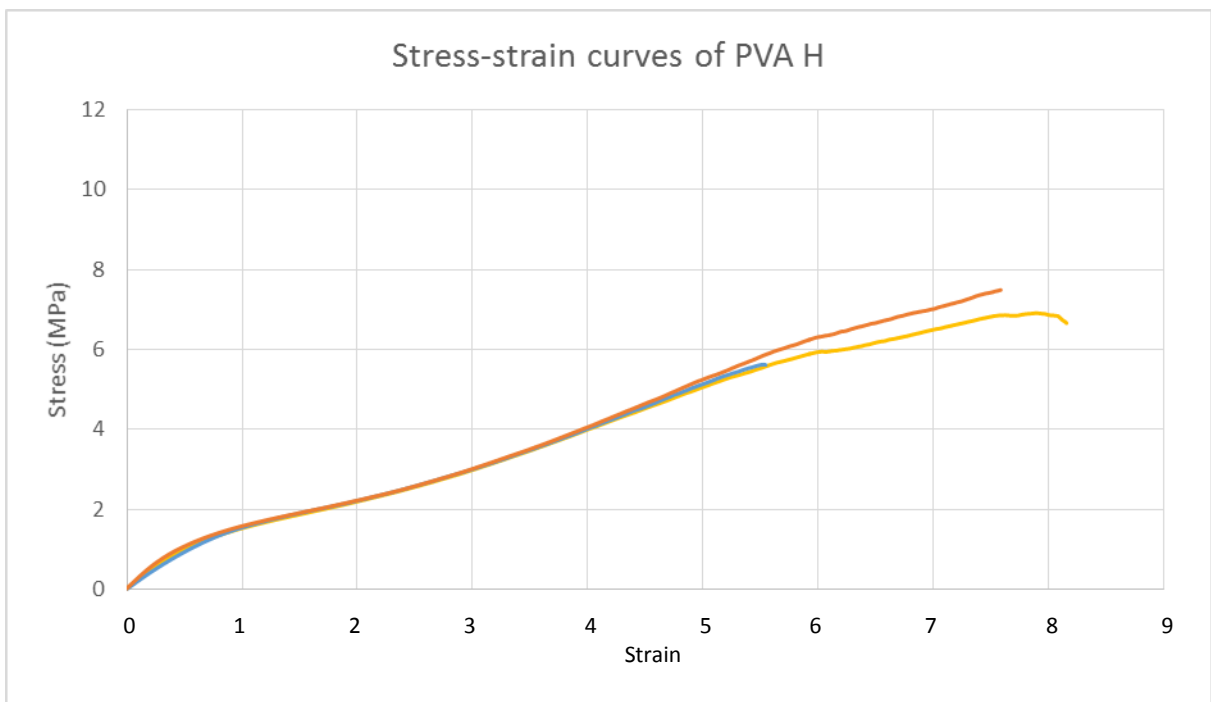


Figure 61: Tensile stress-strain curves of PVA H.

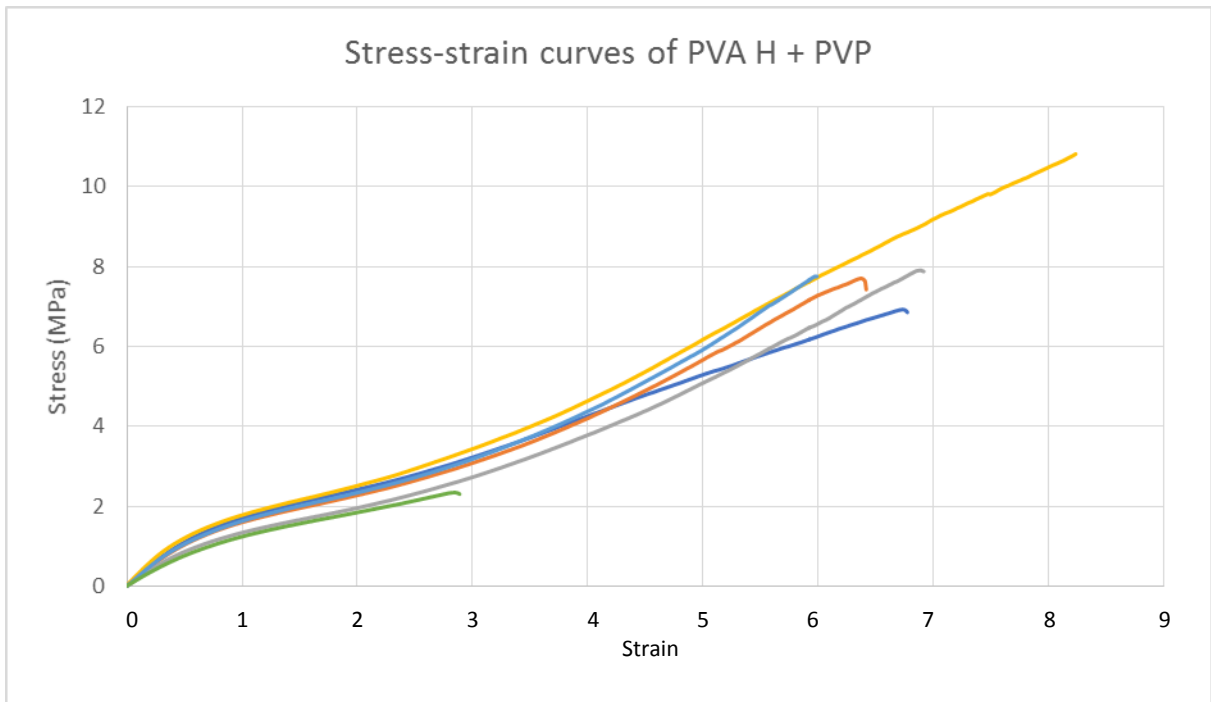


Figure 62: Tensile stress-strain curves of PVA H + PVP.

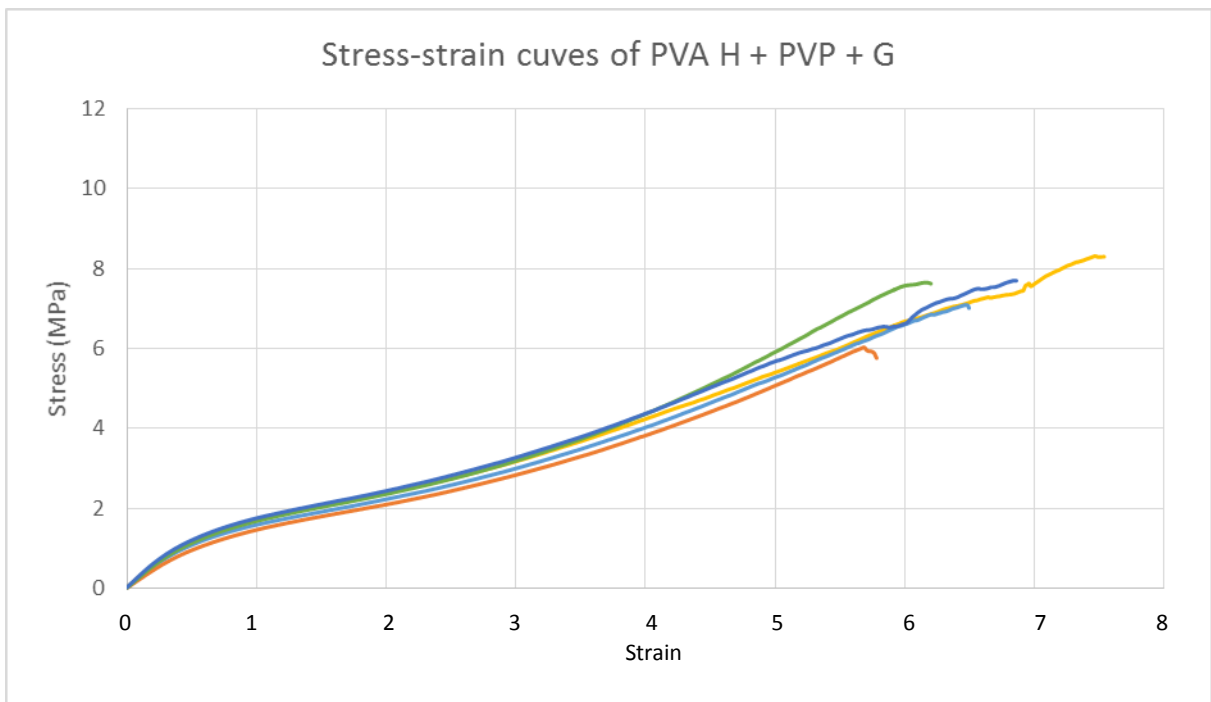


Figure 63: Tensile stress-strain curves of PVA H + PVP + G.

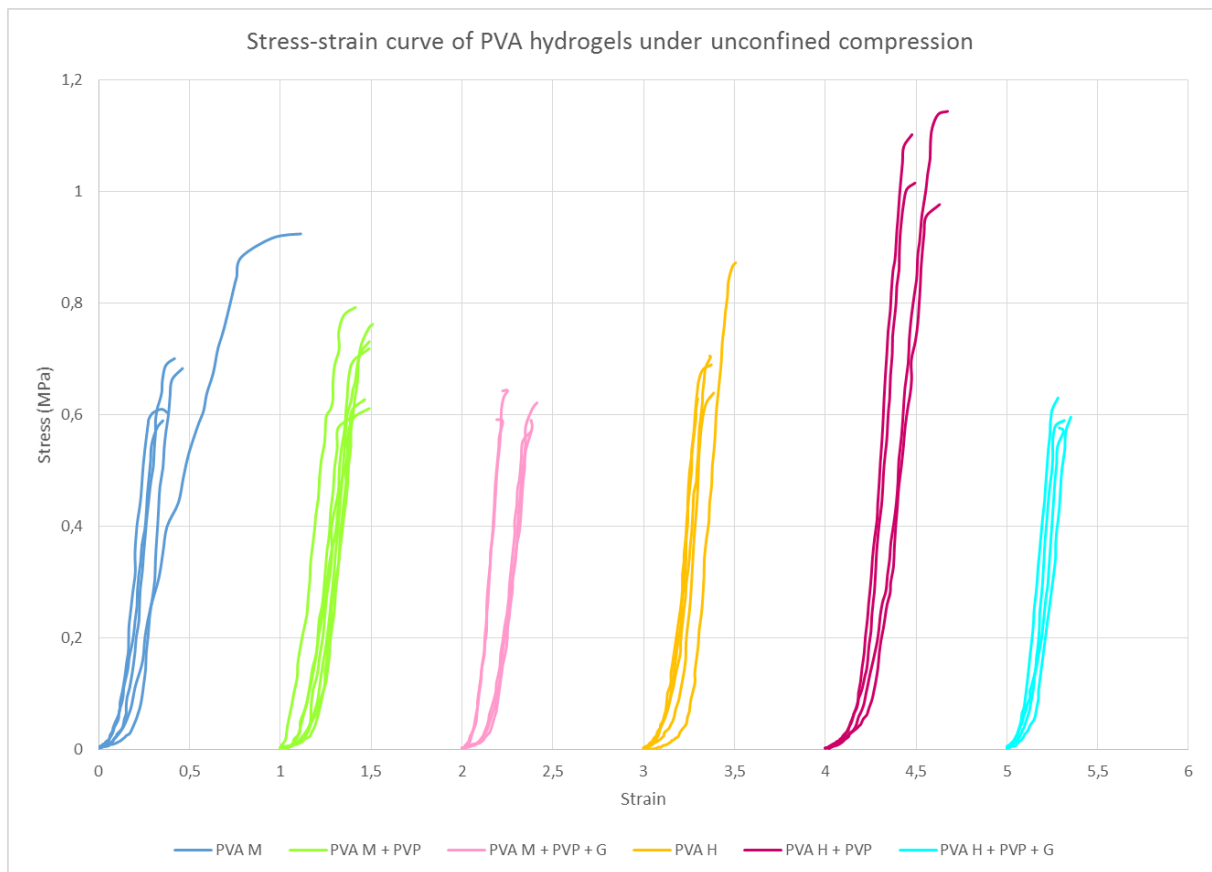


Figure 64: Compressive (unconfined) stress-strain curves of PVA hydrogels. The starting point of the curves has been altered to make it easier to compare repetitions of the same formulation.